# Matrix-bound Nanovesicles as an Extracellular Source of Lysyl Oxidase

by

**Yoojin Cadence Lee**

Bachelor of Science in Physics, Emory University, 2013

Submitted to the Graduate Faculty of the

Swanson School of Engineering in partial fulfillment

of the requirements for the degree of

Doctor of Philosophy

University of Pittsburgh

2020

UNIVERSITY OF PITTSBURGH

SWANSON SCHOOL OF ENGINEERING

This dissertation was presented

by

**Yoojin Cadence Lee**

It was defended on

July 14, 2020

and approved by

Dr. Lance Davidson, Ph.D. Professor
Department of Bioengineering

Dr. George Hussey, Ph.D., Research Assistant Professor
Department of Surgery

Dr. Savio L-Y. Woo, Ph.D., D.Sc., D.Eng. Distinguished University Professor Emeritus
Department of Bioengineering

Dr. Urszula Zdanowicz, M.D., Carolina Medical Center, Warsaw, Poland

Dissertation Director: Dr. Stephen F. Badylak, D.V.M., Ph.D., M.D., Professor
Departments of Surgery and Bioengineering

**Matrix-bound Nanovesicles as an Extracellular Source of Lysyl Oxidase**

Yoojin Cadence Lee, Ph.D.

University of Pittsburgh, 2020

Biologic scaffolds produced from extracellular matrix (ECM) have been commonly implemented as inductive templates for constructive tissue remodeling in multiple musculoskeletal sites. The discovery of matrix-bound nanovesicles (MBV), a unique subpopulation of extracellular vesicles embedded within the ECM, has prompted the further study of MBV structure, internal cargo, and overall function. MBV are more specifically defined as lipid-bound extracellular vesicles that possess the ability to modulate cell behavior as a function of their internal cargo of biologically active signaling molecules (e.g., microRNAs, proteins, lipids, cytokines). The lipid membrane of MBV is decorated with a variety of surface proteins that are unique to the local function and anatomic location from which MBV are harvested.

Lysyl oxidase (LOX) is an enzyme responsible for catalyzing collagen cross-linking and serves an essential role in tissue stabilization. In this dissertation, LOX is investigated because of its function of regulating cross-linking of collagen in tissues and its potential to be implemented as a therapy in damaged or healing tissues that lack sufficient cross-linking. There are substantial challenges associated with isolating and purifying LOX in high quantities, which limits full characterization and understanding of the protein. Herein, MBV is isolated from multiple tissue types in abundance and is presented as a promising method of isolating LOX.

The objectives of the present dissertation were to isolate MBV-associated LOX from ECM bioscaffolds and to determine its effects on the development of collagen fibrils *in vitro*. ECM bioscaffolds were solubilized using enzymatic digestion with collagenase and elastase, and incubation in a high salt solution. Results show that MBV-associated LOX in the ECM is present

in its 52 kDa pro-peptide form and that it is enzymatically active when isolated with elastase digestion. MBV-associated LOX activity significantly decreases when treated with LOX inhibitor β-aminopropionitrile (BAPN) or when proteinase K is utilized to remove surface proteins. Furthermore, MBV-associated LOX enhances the formation of cross-linked collagen and the strength collagen constructs *in vitro*. MBV offer an attractive method to deliver surface-associated LOX, which through its direct role in collagen cross-linking and matrix regulation for enhancing the biomechanics of remodeled tissue, specifically its strength.

## Table of Contents

## List of Tables

## List of Figures

## Preface

My research career has been an indescribable journey filled with exceptional mentors, collaborators, and friends. My doctoral training has specifically been the highlight of my research journey and it has provided me with countless experiences and skills that have furthered my development as a scientist. This work would not have been possible without the exceptional mentorship of my thesis advisory committee. Thank you to Dr. Stephen F. Badylak, Dr. Lance Davidson, Dr. George Hussey, Dr. Savio L-Y. Woo, and Dr. Urszula Zdanowicz. I am forever grateful for your feedback, support, and encouragement along the way.

I want to specifically thank Dr. Stephen F. Badylak for being my advisor during my Ph.D studies. I feel exceptionally fortunate to have been given the opportunity to work in his highly prestigious laboratory. He has challenged me to think more critically and to perform research from a variety of perspectives, ranging from molecular biology, immunology, pathology, engineering, and clinically translational studies. The training I received under his advisement was truly transformative and an opportunity I feel fortunate to have been given. I thank him for challenging me to continually progress in my scientific knowledge and for his patience while guiding me through my doctoral studies.

Special thanks to Dr. George Hussey, who has been my mentor since I first joined the lab. He has instilled not only essential scientific practices, but also valuable life lessons that have impacted me throughout my graduate career. I thank Dr. Hussey for his truly earnest mentorship and his constant encouragement.

The Badylak lab would not be what it is without its members Scott Johnson, Dr. Neill Turner, Li Zhang, and Janet Reing. They were a constant source of knowledge for any question or

problem I encountered in the lab. The former and current members of the Badylak lab make the lab an incredible working and collaborative environment. They have become invaluable friends that I will never forget. Thank you to Dr. Lindsey Saldin, Dr. Catalina Pineda Molina, Dr. Lina Quijano, Dr. Arthi Shridhar, Dr. William D'Angelo, Dr. Joseph Bartolacci, Dr. Luai Huleihel, Dr. Juan Diego Naranjo, Dr. Michelle Scaritt, Dr. Xue Li, Dr. Jonas Eriksson, Dr. Timothy Keane, Dr. Nazia Mehrban, Madeline Cramer, Salma El-Mossier, Mark Murdock, Raphael Crum, Jordan Chang, Lori Walton, and Julia Hart. An equally vital side of the lab is comprised of the administrative members that keep everything organized. This would not be possible without Rachel Thomas, Emily Henderson, and Nicole Wenturine.

I want to acknowledge the undergraduate students that I had the opportunity to mentor throughout my graduate career. They have made me grow as a mentor but have also contributed to my work. Thank you, Jordan Birkhimer, Serena Fisher, Karapet Mkrtchyan, and Andres Castillo. I hope that I have influenced you all to become greater scientists.

Financial support from the Biomechanics in Regenerative Medicine (BiRM) fellowship program, the Bioengineering Department, and Provost's Development Fund from the University of Pittsburgh was provided to complete this work. Thank you for the assistance.

This dissertation is dedicated to my parents, Byeong Lee and Seong Lee. They are the hardest workers I know and have always been my truest inspiration. I am forever grateful for their support and for everything they sacrificed when moving to the United States for me to have the best education opportunity. Thank you for teaching me life values and surrounding me with unconditional love.

I also want to thank my sisters, Jina Lee and Kyung Lee, for life-long support and motivation. I can always count on them to listen when I encounter any problems.

Among many and countless friends, special thanks to Dr. Chris Reyes, Dr. Liza Bruk, and Jorge Jimenez for the incredible friendship. You all have made me feel less alone in graduate school and I am proud to call each other “fam.”

Finally, I am thankful for my fiancé, Dr. Chandler Fountain. Thank you for being silly when I’m serious, patient when I’m haste, and optimistic when I’m discouraged. Your love and support have been essential throughout these years.

# 1.0 Introduction

## 1.1 Cross-Linking of Collagen for Tissue Integrity and Stabilization

Collagen is the most abundant insoluble protein in the extracellular matrix (ECM) and in connective tissues. The network of collagen is formed largely by cell-mediated self-assembly of small collagen molecules and is essential in providing strength to tissues where mechanical function is essential (e.g., skin, cartilage, tendon). The synthesis of collagen begins primarily in fibroblast cells that facilitate the process of transcription and translation of the collagen genes. Collagen chains, known as procollagen, are transported to the endoplasmic reticulum (ER) for post-translational modifications including hydroxylation, glycosylation, and formation of disulfide bonds [1]. Once in the triple helical formation, the procollagen molecules are sorted in the Golgi apparatus, assembled into secretary vesicles, and released into the extracellular space. The procollagen molecules are then cleaved by peptidases and collagen monomers to form stacking units, also known as collagen fibrils [2, 3].

The assembly of collagen fibrils in the extracellular space is an orchestrated process that dictates the stability of the covalently bonded supramolecules. Collagen fibrils are stabilized by cross-links that are driven most notably by the enzyme lysyl oxidase (LOX) [4]. LOX is essential in catalyzing the reaction that forms the covalent bonds between triple helical collagen fibers, which subsequently stabilize the ECM. The dynamic microenvironment of the ECM influences various cellular processes such as proliferation, differentiation, adhesion, and migration; these processes in turn contribute to maintaining tissue and organ homeostasis [5]. Collagen cross-links are also important in the mechanical properties of tissues during development [6]. The strength

and biomechanical properties of the ECM are dependent on proper formation of such intermolecular collagen cross-links, which when gone awry, can dictate the onset or progression of pathologies associated with connective tissues.

## 1.2 Lysyl Oxidase and its Role in the ECM

### 1.2.1 The Enzymatic Role and Function of LOX

Numerous studies have reported the role of LOX in the ECM during remodeling events and fibrillogenesis in various tissues [7, 8]. Although LOX has been classically characterized as an extracellular enzyme, emerging studies also show that LOX has intracellular biological roles [9, 10]. LOX has been reported to be involved in development [11], tissue remodeling [12], fibrosis [13, 14], and neoplasia [15-17], which all elucidate the importance of LOX as a key player in a variety of biological events. The present dissertation focuses on the extracellular role in of LOX and its essential function of mediating collagen cross-linking in the ECM.

LOX is dependent on $Cu^{2+}$ molecules to enzymatically catalyze the cross-linking of collagen and elastin that is essential for the structural integrity and function of connective tissues [18]. The covalent cross-links are formed by oxidative deamination of lysine and hydroxylysine residues to form allysines in the telopeptide domains of collagen molecules [19]. Malfunction and dysregulation of LOX proteins can lead to diseases associated with abnormal collagen fibrils and disruption in fibrillogenesis. Such diseases include lathrysm from the inhibition of LOX [20], Ehlers Danlos syndrome [7], and dilated cardiomyopathy [21]. LOX is essential in reinforcing

and stabilizing collagen fibers and can affect the tensile strength of connective tissues including tendon, bone, and skin, and the ECM.

In mammals, LOX exists in a family of proteins that includes 5 isoforms: LOX, and LOX-like 1-4 (LOXL1-4). These isoforms have >50% sequence homology within their catalytic domain in the carboxy terminus [22], which consists of a cytokine receptor-like (CRL) domain, copper-binding motif, and a lysyl-tyrosyl-quinone (LTQ) cofactor [23, 24]. The amine terminus of the LOX isoforms is more variable and likely important for protein-protein interactions, substrate specificity, and function. Of the five isoforms, LOX and LOXL1 are often paired together for their similar protein structure and presence of pro-domains, which enable their secretion as proenzymes and extracellular processing by procollagen C-proteinases [25]. Such processing has been shown to require the pro-domains of LOX and LOXL1, which allows for substrate recognition for directing the enzymes to elastic fibers that interact with tropoelastin [26]. On the other hand, LOXL2, LOXL3, and LOXL4 contain four scavenger receptor cysteine-rich (SRCR) domains that are not present in the other isoforms. The functions of the SRCR domains are not clear, but may be important for protein-protein interactions [27]. The differences of the LOX isoforms may account for their biological functions and mechanism of associating with ECM. The present dissertation focuses on LOX among the five isoforms, specifically its role and function in the ECM.

## 2.0 The ECM and its Use as a Biologic Scaffold

The ECM is a complex, tissue-specific three-dimensional network defined by the structural and functional components secreted by all cells of tissues [28]. Such secreted products include proteins, polysaccharides, enzymes, and carbohydrates, which all work to form the intricate network of the ECM. The ECM consists primarily of collagens but also contains growth factors, glycoproteins (laminin, fibronectin), proteoglycans, and glycosaminoglycans (GAGs) that are unique to each tissue type and enable tissue-specific roles and functions. The microenvironment of the ECM is highly dynamic, and the maintenance of normal physiology and function is largely dependent on the interaction between the ECM and cells. This concept of bidirectional cross-talk between cells and the surrounding ECM has been described as dynamic reciprocity [29], where the ECM can dictate and influence cell behavior and phenotype [30], which in turn influences the cellular responses to environmental stressors and remodeling events of the ECM.

Understanding the full complex composition and diverse functions of the ECM is an ongoing investigation by researchers today. One of the primary uses of ECM in the field of tissue engineering and regenerative medicine is as a biologic scaffold material. Since the 1940s, scientists have investigated the application of ECM as a biologic scaffold by decellularization. Because the ECM is designed and manufactured by resident cells, it is not only biocompatible but provides the ideal environment when used as a biologic scaffold [31].

The first report of a crude decellularization process was in 1948 by William E. Poel, where muscle tissue was completely pulverized at -70°C [32]. Decellularization strategies and techniques have evolved since Poel's study and have allowed for the beneficial use of the ECM as bioscaffolds. Biologic scaffolds derived from mammalian ECM have been used successfully as

templates of inductive functional tissue remodeling in multiple anatomic sites including urinary bladder [33], ventral hernia [34], musculoskeletal tissues [35], dura mater [36], and tendon [37] to name a few. Advantageously, ECM bioscaffolds are not chemically cross-linked or highly cellularized, which leads to their rapid degradation and replacement with well-organized, site-appropriate host tissue, in contrast to the innate mammalian wound healing response of scar tissue formation [31, 38]. The favorable outcomes of constructive remodeling associated with ECM bioscaffolds are due to scaffold degradation and release or exposure of matricryptic peptides [38], endogenous or stem cell recruitment [39], modulation of macrophage phenotype [40], as well as the exposure to matrix-bound nanovesicles (MBV) [41]. Such properties make ECM bioscaffolds and their molecular components an attractive tool for functional tissue repair and regenerative medicine applications.

### 2.1 Matrix-Bound Nanovesicles in the ECM

Extracellular vesicles (EVs), of which MBV are a unique type, are important mediators of cell-cell communication, sharing biological signals and transmitting information that influence biological processes [42]. The first identification of EVs was in 1967 by Peter Wolf, where he observed EVs as subcellular coagulant material and named them “platelet dust” [43]. It is now clear that EVs are nano-packages of information that all cells release as a form of paracellular communication [44, 45]. The functions of EVs are incredibly diverse, playing different roles in regulating physiological and pathological functions including immune suppression, antigen presentation, tumor suppression, and transfer of signaling molecules to name a few [46-49].

The heterogeneity and variable composition of EVs make defining types of EVs challenging, but EVs can be classified in 3 major subgroups based on their size. The largest group includes apoptotic bodies that are a result of extensive membrane budding during apoptosis and range from 1 to 5 μm in diameter [50]. Microvesicles, released from the plasma membrane, are slightly smaller and range from 150 to 1,000 nm in diameter [51]. The smallest members of EVs, exosomes range from 30 to 100 nm in diameter [46]. Exosomes contain a cargo of cytosolic products including microRNA (miRNA), cytokines, and chemokines that can be internalized by cells and influence various physiologic and pathologic processes [52]. Despite their classification in the subgroups, all EVs are key players in paracellular communication and intercellular transfer of cargo.

Matrix-bound nanovesicles (MBV) are a unique type of EVs, discovered firmly embedded within the ECM in contrast to liquid-phase EVs [41, 53]. EVs are secreted by most cell types into the extracellular space and are typically found in cell culture supernatants, blood, saliva, plasma, and cerebrospinal fluid [51, 54]. MBV are secreted by tissue-resident cells and integrated within the ECM, which delineates their biological roles as uniquely different from EVs found in biological fluids. It has been previously shown that MBV isolated from ECM bioscaffolds have not only unique differential miRNA signatures based on their anatomical tissue source [41], but also distinct phospholipid profiles [53]. MBV have been shown to modulate cell behavior as a function of their cargo of biologically active signaling molecules (e.g., miRNAs, proteins, lipids, cytokines), influence neuron differentiation, and promote a pro-remodeling macrophage phenotype [55-57]. More research is necessary to fully understand the mechanisms of biogenesis and integration of MBV into the fibrillar network of the ECM. One particular interest of study may be associated to the lipid membrane of the vesicles.

## 2.2 MBV-Associated Lysyl Oxidase

As described above in chapter 1.2.1, lysyl oxidase (LOX) is a copper-dependent enzyme that catalyzes the cross-linking of the molecular units of collagen and elastin, which is an essential post-translational modification occurring in the biogenesis of collagenous connective tissues [18]. However, full characterization and understanding of LOX's catalytic activity remain unknown due to its highly insoluble properties and difficulties in obtaining large quantities of LOX [58]. In addition, procedures to isolate LOX from tissue involve high concentrations of urea and extensive buffer changes [59, 60], which ultimately limits the quantity of LOX able to be isolated. Despite these obstacles, it has been demonstrated that LOX is essential for proper ECM development and stabilization of tissues [8, 61, 62].

Previously, studies have used LOX as a targeting approach to treating fibrosis by inhibiting its activity [63, 64]. However, methods of inhibiting LOX have associated adverse impacts. For example, the use of β-aminopropionitrile (BAPN), an irreversible inhibitor of LOX, has the potential of producing toxic byproducts by interacting with other amine oxidases [65]. A copper chelator tetrathiomolybdate has also been utilized to inhibit LOX activity [66, 67], but its use is associated with potential toxicity from the inherent decrease of copper availability for normal physiologic processes [68, 69]. Therapeutic approaches using LOX has been explored but has been limited due to such challenges. MBV-associated LOX is a novel direction to implement the function of LOX as a cross-linking enzyme to strengthen and promote organized healing in musculoskeletal tissues.

LOX has been identified in several proteomic analyses studies of ECM including Matrigel [70], synovium-derived stem cells [71], and ovine forestomach matrix [72]. It is well-established that biologic scaffolds composed of ECM promote constructive tissue remodeling and at least

partial restoration of function. Therefore, it is proposed that LOX, specifically when present in ECM, plays a positive role in tissue remodeling. The present dissertation reports an extracellular source of LOX associated to the ECM, specifically by MBV.

## 2.3 Future Perspectives

Much of the research today on EVs is largely focused on their potential as biomarkers of disease [73-75]. LOX antibodies for targeting disease have been reported in preclinical studies but lack sufficient data showing effectiveness in the extracellular environment [76]. More extensive research is necessary to implement LOX in clinical trials for therapeutic applications. Herein, LOX was discovered on the surface of MBV, which distinguishes its therapeutic potential from prior studies that are directed at targeting LOX's activity, specifically. MBV-associated LOX can be obtained from tissue ECM and provides a novel approach to isolate LOX. Future studies are necessary to implement MBV-associated LOX for the therapeutic purpose of enhance the cross-linking of damaged tissues, such as during overuse injuries like tendinopathy.

## 3.0 Objectives

Extracellular vesicles (EVs) have been under intensive research in the past decade as a natural system for cellular communication and intracellular transfer of molecular cargo. Matrix-bound nanovesicles (MBV) have been a recent biological discovery in the field of EVs. MBV exist embedded within extracellular matrix (ECM) bioscaffolds rather than fluid-based systems. MBV are similar to exosomes, a type of EV, in their nanometer size and containment of molecular cargo, but MBV are different in that they lack common exosomal surface markers including CD63, CD81, CD9, and HSP70 [41]. Rather, one of the early identified surface proteins identified with MBV is lysyl oxidase (LOX). MBV-associated LOX is easily isolated by solubilization of the ECM and ultracentrifugation, avoiding lengthy procedures of isolating LOX proteins, and it offers therapeutic potential in applications where cross-linking of the ECM is dysregulated. However, given that MBV are a relatively new finding, more research is required to understand the physiological roles as well as biogenesis of the vesicle and its associated proteins.

**The objectives of the present dissertation were to determine how LOX is associated with MBV and evaluate the biologic activity of MBV-associated LOX.** MBV-associated LOX was identified in urinary bladder matrix ECM (UBM-ECM), small intestinal submucosa ECM (SIS-ECM), dermal ECM (dECM), and tendon ECM (tECM). MBV-associated LOX was identified on the surface of MBV by immunoprecipitation and immunolabeling experiments. MBV-associated LOX is in its 52 kDa pro-peptide form as assessed by Western blot analyses. In addition, MBV-associated LOX activity significantly decreases when treated with LOX inhibitor β-aminopropionitrile (BAPN) or when proteinase K is utilized to remove MBV surface proteins. Furthermore, MBV-associated LOX enhances the formation of cross-linked collagen and the

strength of *in vitro* collagen constructs. The discovery and investigation of MBV-associated LOX provide insights to the role of MBV in ECM regulation and offers an alternative pathway through which LOX is secreted into the extracellular space.

The long-term goal of the present dissertation is to provide a feasible method of utilizing MBV-associated LOX as a therapeutic by taking advantage of LOX's enzymatic function of cross-linking collagen to strengthen and stabilize tissues. Such therapy could be implemented in musculotendinous tissues that are subject to overuse injuries and where the innate healing process is slow and inefficient. Herein, MBV-associated LOX was determined to be enzymatically active and have biologic effects by enhancing the development of *in vitro* collagen constructs. MBV-associated LOX may be used to strengthen tendons and ligaments where the integrity of the ECM is compromised in the case overuse injuries. In addition, the therapeutic use of MBV-associated LOX can be further applied to other tissue diseases such as aortic aneurysms, pelvic organ prolapses, and cutaneous wounds.

## 4.0 Central Hypothesis and Specific Aims

***Central Hypothesis:*** Matrix-bound nanovesicles (MBV) are an extracellular source of LOX and can be used to implement the enzymatic function of lysyl oxidase (LOX) in regulation of collagen and the ECM.

**Specific Aim 1:** Identification and characterization of LOX isoforms in MBV isolated from ECM bioscaffolds

**Subaim 1.1.** Determine the amount of LOX in MBV isolated from urinary bladder matrix ECM (UBM-ECM), small intestinal submucosa ECM (SIS-ECM), dermis ECM (dECM), and tendon ECM (tECM) by Western blot and nanoparticle tracking analyses (NTA).

**Subaim 1.2.** Quantification of LOX isolated from various ECM scaffolds by ELISA

*Corollary Hypothesis:* MBV isolated from different ECM will have varying amounts of LOX due to source tissue specificity and function, which can be implemented for specific biologic applications.

Corollary Rationale: Previous work has shown that MBV isolated from various ECM bioscaffolds have unique protein cargo signatures, surface markers, and phospholipid signatures [41, 53]. Given that the ECM is an architecture of complex mixture of proteins, proteoglycans, and glycosaminoglycans, it is plausible that MBV isolated from ECM bioscaffolds derived from anatomically distinct source tissue will have varying amounts of LOX associated to the surface of the vesicles.

**Specific Aim 2:** Determine the biologic activity of MBV-associated LOX

**Subaim 2.1.** Determine how LOX is associated with the surface of MBV

*Corollary Hypothesis:* The extracellular processing of MBV-associated LOX, by BMP-1 and other binding partners, is required to proteolytically activate LOX on the surface of MBV, in which MBV then can be utilized to regulate collagen cross-linking to strengthen tissues.

Corollary Rationale: Previous studies have shown that after LOX is secreted to the extracellular space, it is processed and activated by pro-collagen C-proteinase bone morphogenic protein-1 (BMP-1) [77]. However, the full activation mechanism of LOX according to tissue specificity is not fully understood. Other proteins have recently been identified to be associated and play a role in the mechanism of activating LOX (i.e., fibronectin [78], periostin [79], and fibromodulin [80] to name a few, which may be important in getting MBV-associated LOX to activate and function. Identifying and understanding the proteolytic activation mechanism of MBV-associated LOX will guide to identifying cellular binding partners of LOX and analyzing for the presence or absence of the catalytic cross-linking activity.

**Specific Aim 3:** Determine the effect of MBV isolated ECM on the mechanical properties of a grown collagen construct *in vitro* by measurement of mechanical strength

*Corollary Hypothesis:* MBV treatment during *in vitro* tendon development can alter LOX activity, thereby changing mechanical properties and microstructural arrangement of fibers in the matrix by enhancing LOX-mediated collagen cross-linking.

Corollary Rationale: It is important to determine if MBV can enhance the formation and strength of an grown collagen construct *in vitro* to implement the potential therapeutic uses of MBV-associated LOX.

# 5.0 Solubilization of ECM by Various Enzymes and High Salt Solution to Isolate MBV

## 5.1 Introduction

In the past decade, extracellular vesicles (EVs) have become of increasing of interest for their important roles in physiology as well as intracellular communication. EVs affect other cells by transfer of cargo containing biologically active molecules (e.g., miRNA, mRNA, proteins) and through surface receptors that influence processes including homeostasis, angiogenesis, and tumor metastasis. [81-85]. EVs are heterogeneous in size, ranging from 40-5000 nm in diameter, and they are secreted by all cell types into the local microenvironment [86]. EVs have been successfully isolated from a variety of fluids including cell culture medium, plasma, serum, saliva, breast milk, and urine [54, 87-89]. The most commonly used method to isolate EVs is differential centrifugation, which is comprised of numerous successive centrifugation and ultracentrifugation steps [90]. This technique allows particles heavier than the solvent to sediment after each centrifugation step. EVs remain in the supernatant after initial, relatively lower speed centrifugation, and is then able to be isolated with subsequent centrifugation with increased forces (ultracentrifugation) and longer duration.

Matrix-bound nanovesicles (MBV) have been identified in ECM scaffolds and are a unique type of EV distinctly different from those found in biological fluids. After disruption of the ECM by enzymatic digestion using proteinase K, collagenase, or pepsin; MBV are isolated by successive centrifugation and ultracentrifugation [41]. Results from prior studies showed that the different enzymatic digestions affect the amount of extractable nucleic acids from ECM bioscaffolds, and

possibly alter the surface markers of MBV. Unlike the isolation of EVs from biological fluids, the separation of MBV from the ECM requires a disruption of the ECM fibrillar network by enzymatic digestion to release the MBV. This step alludes to the highly dynamic nature of the ECM, which is constantly undergoing remodeling processes. ECM degrading and remodeling enzymes are regulated in homeostasis and disease progression, which may be when MBV are being released for nearby cellular internalization and function.

The present study compares the use of collagenase, elastase, and sodium chloride (NaCl) solution to solubilize the ECM for isolating MBV from urinary bladder matrix ECM (UBM-ECM). Herein, the effect of various enzymes or inorganic NaCl solution on the presence of lysyl oxidase (LOX) as a surface protein was investigated. LOX plays an integral role in ECM remodeling and ultimately determines the extent of intermolecular cross-linking between collagens and elastin. The presence or absence of LOX associated to the surface of MBV uncovers more information about how MBV are integrated within the matrix and how they function differently than EVs found in biological fluids.

## 5.2 Methods

### 5.2.1 Experimental Design Overview

The objective of the present study was to investigate different solubilization methods of ECM for isolation of MBV. In addition, the presence of LOX associated to MBV was investigated. UBM-ECM was used to compare the different solubilization methods. The experimental design is

summarized in Figure 1. Table 1 lists the different experimental techniques used with UBM-ECM, SIS-ECM, or both for all the methods described below.

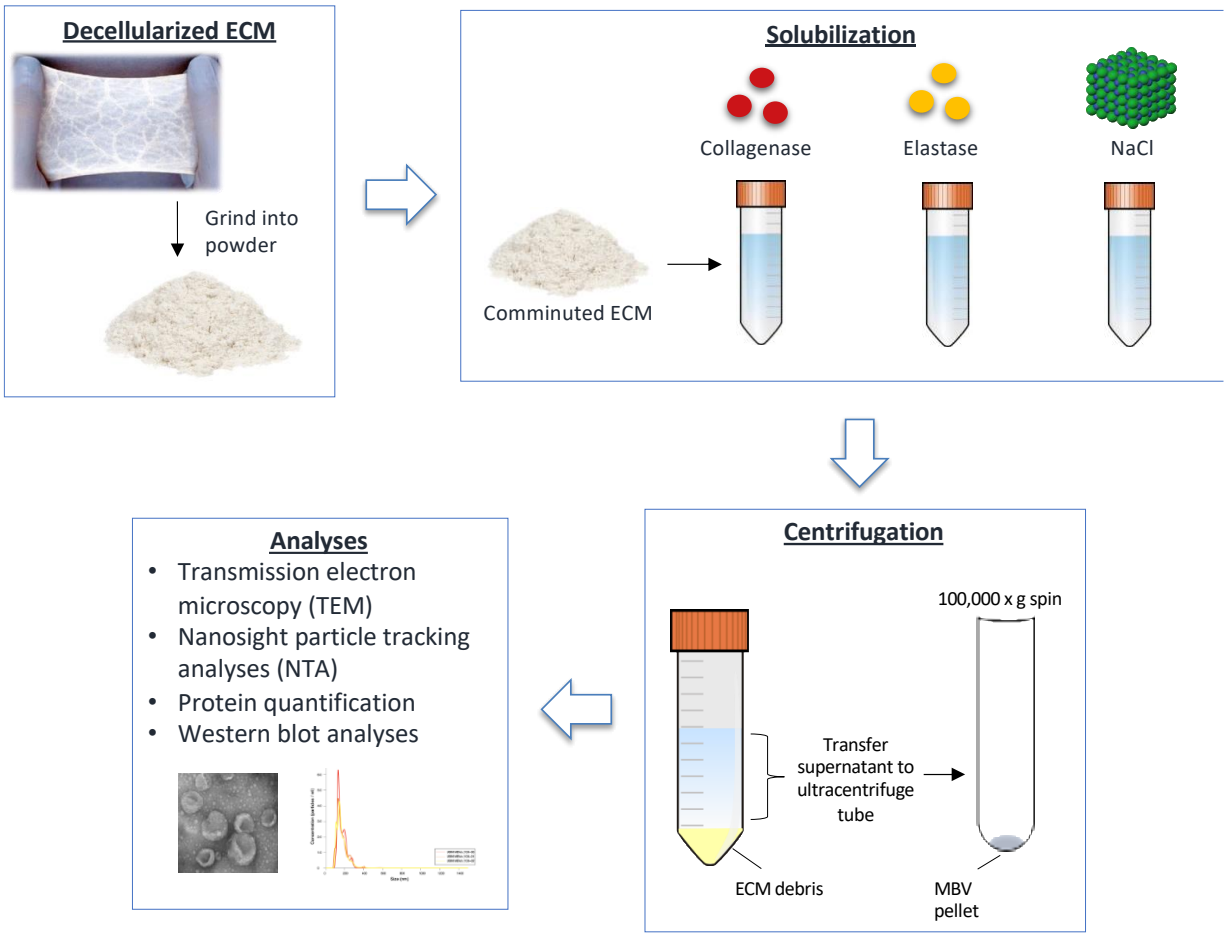


**Figure 1. Experimental design overview.** Decellularized ECM is lyophilized and comminuted into a powder. The ECM is then solubilized by either enzymatic digestion by collagenase or elastase, or incubated in NaCl solution. Then, the solution goes through centrifugation steps to form a pellet of MBV. Analyses of MBV include TEM, determination of vesicle and protein concentration, and Western blot.

**Table 1. Description of experimental goals and techniques used for each type of ECM**

| ECM sources | Goals | Experiments |
|---|---|---|
| UBM-ECM | To investigate different solubilization methods of ECM to isolate MBV-associated LOX | Enzymatic digestion by collagenase or elastase, or incubation in high NaCl solution; Western blot analyses; immunolabeling |
| UBM-ECM, SIS-ECM | To determine if LOX is associated on the surface or in the lumen of MBV | Enzymatic digestion by elastase; immunoprecipitation |

### 5.2.2 Preparation of Urinary Bladder Matrix ECM (UBM-ECM) and Small Intestinal Submucosa ECM (SIS-ECM)

Urinary bladder matrix ECM (UBM-ECM) was prepared as previously described [91], which involved mechanically removing the tunica serosa, tunica muscularis externa, tunica submucosa, and tunica muscularis mucosa from porcine urinary bladders. The remaining tissue consisting of the basement membrane and subjacent lamina propria of the tunica mucosa were decellularized by washing in 0.1% peracetic acid with 4% ethanol for 2 hours at 300 rpm. The tissue was then extensively rinsed with PBS and sterile $H_2O$. UBM was then lyophilized and milled into particulate using a Wiley Mill with a #60 mesh screen.

Small intestinal submucosa ECM (SIS-ECM) was used in comparison with UBM-ECM for immunoprecipitation studies. SIS-ECM was prepared as previously described [92, 93], which involved mechanically removing the superficial layers of the tunica mucosa, the tunica serosa, and tunica muscularis externa. The remaining tissue includes the stratum compactum layer of the tunica mucosa, the tunica muscularis mucosa, and the tunica submucosa [94]. SIS was decellularized and disinfected by washing in 0.1% peracetic acid with 4% ethanol for 2 hours at 300 rpm. The tissue was then extensively rinsed with PBS and sterile $H_2O$. SIS was then lyophilized and milled into particulate using a Wiley Mill with a #60 mesh screen.

### 5.2.3 Solubilization of UBM-ECM

Briefly, 400 mg of lyophilized powdered UBM-ECM was enzymatically digested with either 0.1 mg/ml collagenase from *clostridium histolyticum* (Sigma, C0130) in buffer (20 mM Tris pH 7.5, 150 mM NaCl, 5 mM $CaCl_2$), or 4 μg/ml elastase (Elastin Products Company, SE563) in buffer (20 mM Tris pH 7.5, 150 mM NaCl), or incubated in 0.5 M NaCl for 20 hours at 37°C on an orbital rocker (Table 2).

**Table 2. Solubilization methods of UBM-ECM for MBV isolation**

| Solubilization method | Buffer | Concentration |
|---|---|---|
| Collagenase | 20 mM Tris pH 7.5, 150 mM NaCl, 5 mM $CaCl_2$ | 0.1 mg/ml |
| Elastase | 20 mM Tris pH 7.5, 150 mM NaCl | 4 μg/ml |
| NaCl solution | NaCl dissolved in Type I $H_2O$ | 0.5 M |

### 5.2.4 Isolation of MBV

MBV were isolated from ECM by ultracentrifugation as previously described with minor modifications [41]. The solubilized UBM-ECM was then subjected to centrifugation at 10,000 xg for 30 minutes to remove insoluble ECM remnants, and the supernatant passed through a 0.22 μm filter (Millipore). The clarified supernatant containing the liberated MBV was then centrifuged at 100,000 xg (Beckman Coulter Optima L-90K Ultracentrifuge) at 4°C for 70 minutes to pellet the MBV. The MBV pellet was then resuspended in 1X PBS and the total protein concentration determined using the bicinchoninic acid (BCA) assay quantification kit (Pierce Chemical). Particle size and concentration were determined using Nanoparticle Tracking Analyses (NTA) [54]. Samples were evaluated in triplicate.

### 5.2.5 Transmission Electron Microscopy (TEM)

MBV size and morphology was determined by transmission electron microscopy (TEM). Briefly, suspended MBV were placed on formvar-coated grids with 1% uranyl acetate for negative staining. Grids were imaged at 80 kV with a JEOL 1400 transmission electron microscope (JEOL Peabody, MA) with a side mount AMT 2k digital camera (Advanced Microscopy Techniques, Danvers, MA). Size of MBV was determined from representative images using JEOL TEM software.

### 5.2.6 Western Blot Analysis

MBV were isolated by the different solubilization methods and ultracentrifugation as described in the previous sections. 1 x $10^9$ particles/ml of MBV were resuspended in Laemmli buffer containing 5% β-mercaptoethanol (Sigma-Aldrich). Samples were loaded in triplicate for each solubilization method. Samples were resolved by sodium dodecyl sulfate polyacrylamide gel electrophoresis (SDS-PAGE) in 4-20% Mini-PROTEAN® TGX™ Stain-Free polyacrylamide gels (Bio-Rad). Gels were run at 150 V in running buffer (25 mM Tris, 190 mM glycine, 0.1% SDS) and transferred on to a PVDF membrane for 3 hours at 150 mA in transfer buffer (25 mM Tris, 190 mM glycine, 20% methanol). Membranes were analyzed by immunoblot (Western blot) using 1:1000 dilution of LOX antibody (LS-Bio, LS-C141072) in blocking buffer (5% non-fat milk in TBS) overnight at 4°C. Membranes were washed thoroughly in 0.1% Tween-20 in TBS and incubated with 1:2000 dilution of horseradish peroxidase secondary antibody (Dako) in blocking buffer for 1 hour at room temperature. Bio-Rad Western ECL solution (Bio-Rad, Hercules, MA) was applied to each membrane for 5 minutes before imaging.

### 5.2.7 Immunolabeling

MBV (2.5 x $10^9$ particles/ml) were loaded on formvar-coated grids and decanted with filter paper after 60 seconds. Grids containing samples were fixed in 2% paraformaldehyde for 10 minutes at room temperature, followed by successive washes in 1X PBS and BSA. All wash solutions were filtered through 0.45 µm filter. Samples were exposed to normal goat serum for 30 minutes before addition of biotin conjugated primary antibody to LOX (20 µg/ml, LSBio, LS-C141072) for 1 hour at room temperature. Grids were then washed in BSA before the addition of

Alexa Fluor 488 colloidal gold conjugate (ThermoFisher, A32361). Grids were thoroughly washed with BSA and 1X PBS before fixing in 2.5% glutaraldehyde. Samples were rinsed with deionized $H_2O$ before and between negative staining with 2% neutral uranyl acetate for 7 minutes, then 4% uranyl acetate for 2 minutes. Samples were dried with filter paper before imaging with TEM. For all samples, primary delete samples confirmed the absence of positive labeling of the secondary antibody.

### 5.2.8 Immunoprecipitation

MBV were isolated from UBM-ECM and SIS-ECM by the elastase digestion method and immunoprecipitation (IP) using magnetic Dynabeads coupled to Protein G (ThermoFisher Scientific). The magnetic beads were immunolabeled with anti-LOX (LifeSpan BioSciences, aa305-320) and immunoglobulin G (IgG) (ThermoFisher Scientific, A16110) as a negative control. Samples were imaged by TEM for presence of MBV and characterization of their morphology at 80,000X magnification.

## 5.3 Results

### 5.3.1 MBV can be Isolated from ECM by Various Solubilization Methods

MBV were isolated from UBM-ECM by enzymatic digestion using collagenase or elastase, or incubation by a high salt solution. Prior studies have successfully isolated MBV by using

collagenase digestion of ECM before obtaining MBV by ultracentrifugation [41, 56]. The present study shows that MBV can be isolated after elastase as well as collagenase digestion of the ECM. Alternatively, high concentrations of NaCl can be used to solubilize the ECM and as an elution buffer to dissociate MBV from the fibrils. Herein, we show the size and morphology of MBV are consistent with previous reports [95] by TEM imaging (Figure 2A, C, E). NTA was performed on samples for particle concentration and distribution of particle size, which showed average vesicle size range of 120-190 nm in diameter (Figure 2B, D, F). BCA results showed higher protein concentrations for enzymatically digested samples compared to MBV isolated by NaCl solution (Figure 2G).

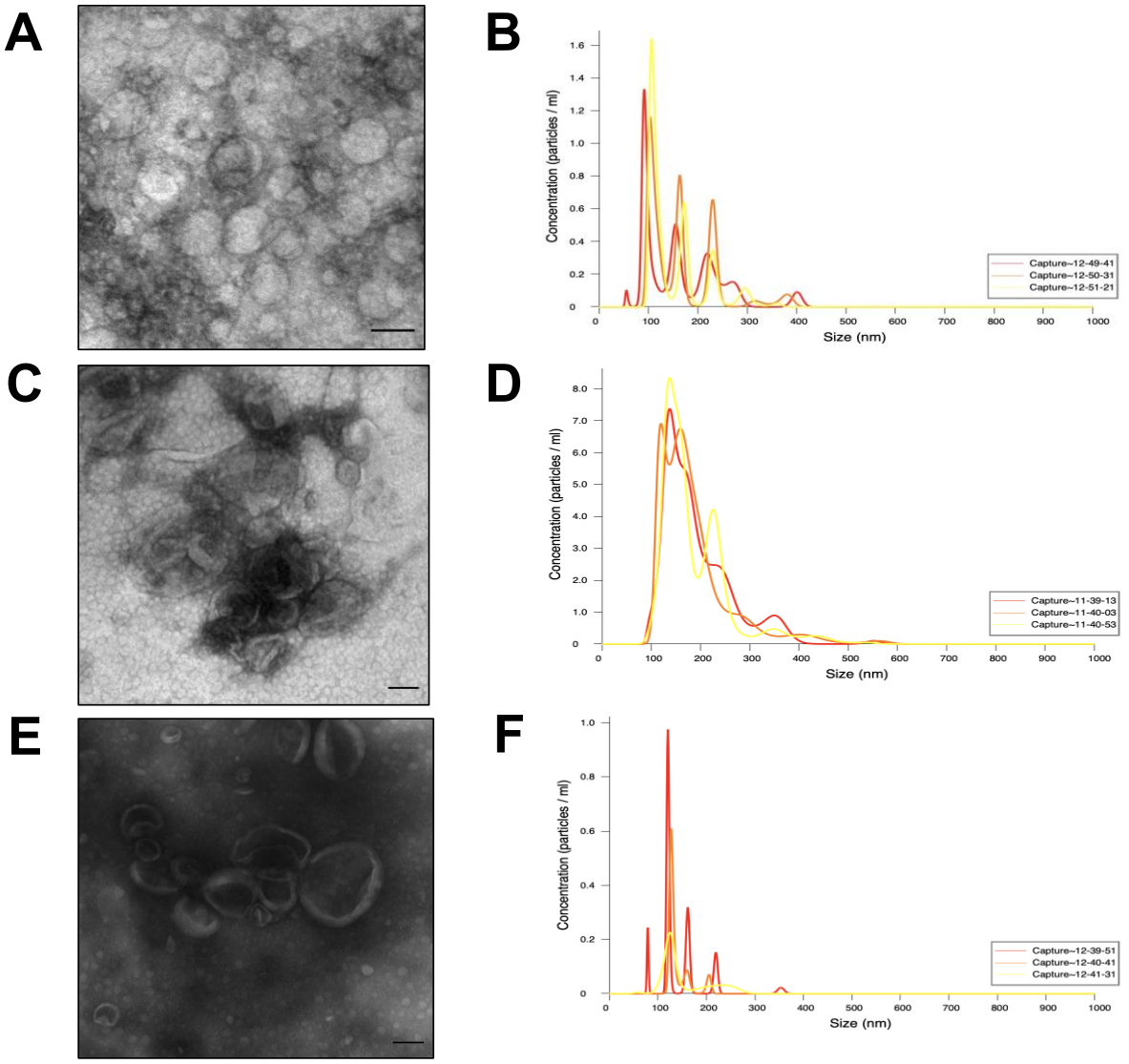


**G**

| Solubilization | Mean Total Protein Concentration (µg/mL) | Particle concentration (particles/mL) | MBV Particle per ug of Protein |
|---|---|---|---|
| Collagenase | 982.11 | 9.50E+10 | 9.67E+7 |
| Elastase | 809.23 | 4.01E+11 | 4.96E+8 |
| NaCl | 63.54 | 1.31E+11 | 2.06E+9 |

**Figure 2.** MBV can be isolated from UBM-ECM by enzymatic digestion using **(A, B)** collagenase or **(C,D)** elastase or using an elution buffer of **(E,F)** 0.5 M NaCl. The morphology and size of the vesicles were confirmed by TEM and NTA. **(G)** Protein concentrations of MBV vary among the samples isolated by different solubilization methods.

### 5.3.2 MBV-Associated LOX is Present in Pro-Peptide Form when Isolated with Elastase

MBV-associated LOX was identified in the 52 kDa pro-peptide form when isolated with elastase digestion. Western blot analyses show a degraded 32 kDa form of LOX when MBV were isolated with collagenase digestion (Figure 3A). To determine the effect of ECM solubilization methods upon MBV-associated LOX, ECM was digested with elastase, collagenase, or NaCl. MBV-associated LOX was present in the samples digested with elastase Neither collagenase nor NaCl isolation methods yielded significant amounts of MBV-associated LOX as determined by Western blot analyses (Figure 3B).

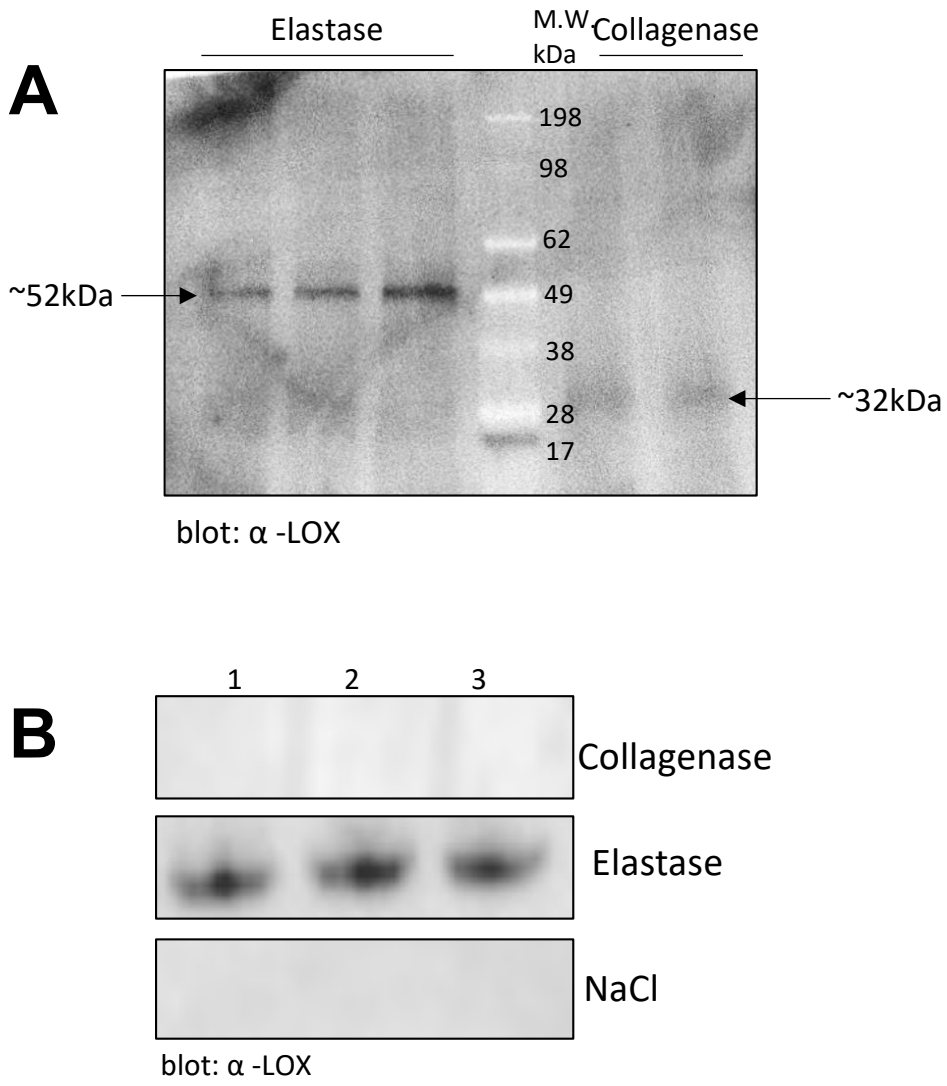


**Figure 3. LOX is associated with MBV isolated from elastase digestion. (A)** LOX is present in its pro-peptide form (52kDa) while **(B)** it is degraded or eluted with collagenase digestion or NaCl, respectively.

### 5.3.3 LOX is Associated on the Surface of MBV

Results from immunolabeling and immunoprecipitation studies show that LOX is associated on the surface of MBV. TEM images from immunolabeling experiments showed positive labeling of gold particles, which are associated to LOX, in samples isolated with elastase digestion (Figure 4A). Gold particles were present in samples isolated by NaCl solution, but are

likely free LOX eluted off from MBV, not MBV-associated LOX. MBV isolated by collagenase digestion and treated with proteinase K had no signs of gold particles. MBV were not lysed and intact, which confirms that the binding streptavidin gold particles to biotin-conjugated LOX is on the surface MBV.

Western blot analysis also confirm that MBV-associated LOX is on the surface. LOX was present in MBV isolated by the elastase digestion method and were absent in those treated with proteinase K (Figure 4B). Proteinase K acts as a broad spectrum protease and removes the surface proteins of MBV.

In addition, TEM images from immunoprecipitation (IP) studies revealed presence of vesicles in UBM-ECM and SIS-ECM samples. Similar to the immunolabelling studies, MBV were not lysed and intact before precipitation of LOX. Results confirm that LOX precipitated with MBV isolated from UBM-ECM and SIS-ECM while immunoglobulin G (IgG) control samples had no presence of vesicles (Figure 4C).

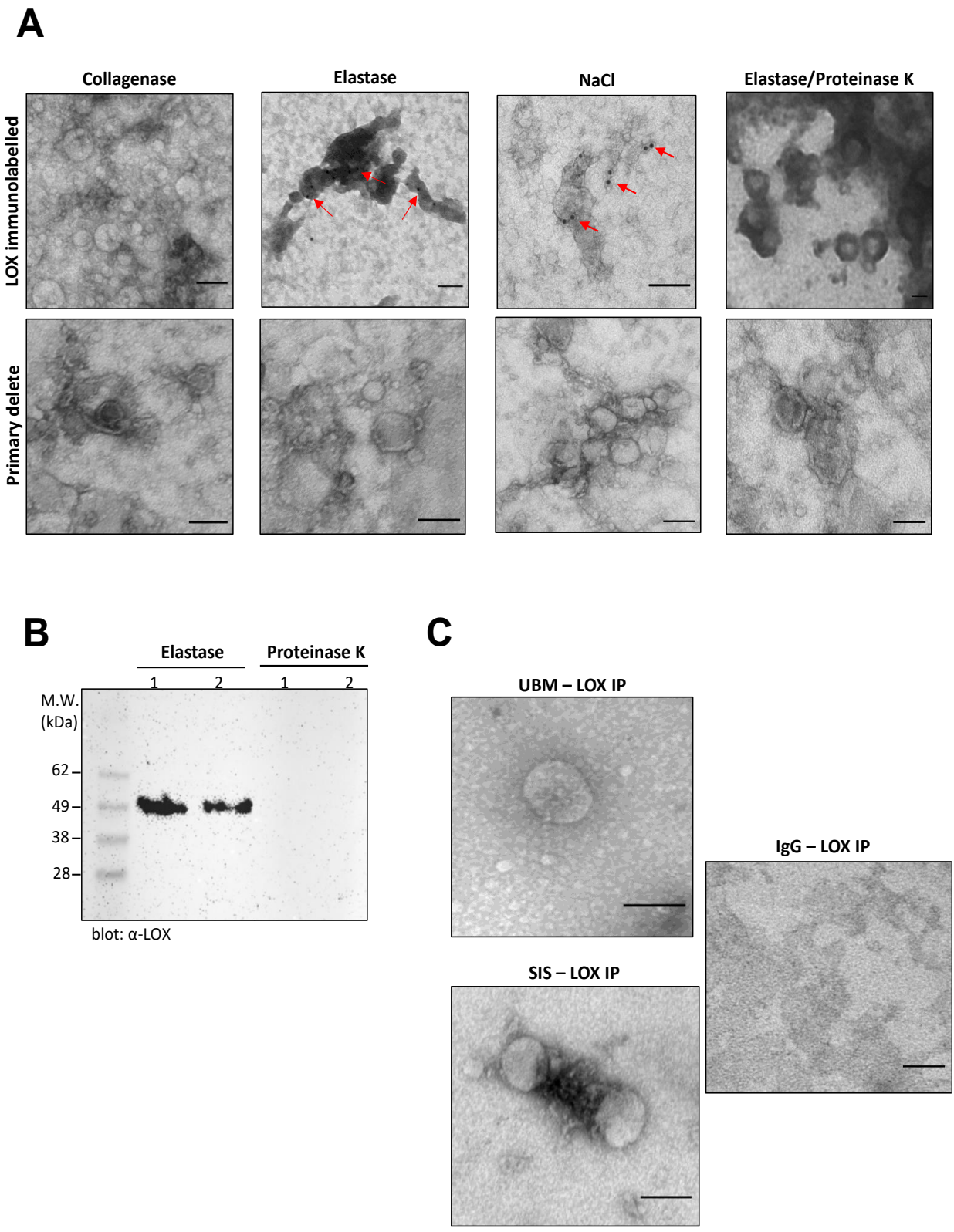
A
Collagenase
Elastase
NaCl
Elastase/Proteinase K
LOX immunolabelled
Primary delete
B
Elastase
Proteinase K
1
2
1
2
M.W.
(kDa)
62
49
38
28
blot: α-LOX
C
UBM – LOX IP
IgG – LOX IP
SIS – LOX IP

**Figure 4. (A)** Immunolabelling was performed with biotin conjugated LOX and streptavidin gold particles (10 nm in diameter) to be imaged by TEM. Positive labeling of gold particles (red arrows) were shown in MBV isolated from elastase and were completely absent in collagenase samples. Gold particles appeared in NaCl samples but are likely free LOX eluted off from MBV. Gold particles were also absent in samples isolated by elastase digestion and treated with proteinase K. **(B)** Western blot analyses showed that LOX was associated with MBV digested by elastase and was absent on proteinase K treated samples. **(C)** MBV-associated LOX was immunoprecipitated from MBV isolated from urinary bladder matrix (UBM) and small intestinal submucosa (SIS) by enzymatic digestion with elastase. All scale bars are 100 nm.

## 5.4 Discussion

The present study shows that MBV can be isolated from ECM by different solubilization methods. MBV have been reported to survive the various decellularization processes of ECM and were previously identified in several types of ECM bioscaffolds including urinary bladder matrix ECM (UBM-ECM), small intestinal submucosa ECM (SIS-ECM), and dermis ECM, along with their commercially available equivalent scaffolds [41]. Past studies involved the use of collagenase from *clostridium histolyticum* as an enzyme to disrupt the ECM prior to successive steps of centrifugation for isolation of MBV. In addition, enzymes such as pepsin and proteinase K were used to compare their effects on ECM bioscaffolds [41]. MBV were identified with unique signatures and miRNA cargo among the various ECM bioscaffolds, which may be, in part, due to the specific decellularization protocols and anatomic location of the source tissue. The present study investigates the effect of different solubilization methods on UBM-ECM for isolating MBV. Herein, MBV can be isolated by not only by enzymatic digestion of the ECM, but also by solubilization of ECM by solubilization in a high concentrated salt (NaCl) solution.

Herein, the presence of lysyl oxidase (LOX) as a surface protein was observed in MBV isolated with elastase digestion. We found the enzymatic activity and components of the collagenase enzyme had undesirable tryptic activity when digesting the ECM. The collagenase product is a mixture of enzymes secreted by *clostridium histolyticum* and contains trypsin-like proteases including clostripain, leucine aminopeptidase, and neutral proteases [96, 97]. It is plausible that the collagenase digestion method cleaves and removes the surface-bound proteins on MBV, which is undesirable for studying MBV-associated LOX. Using elastase from human sputum, which has been shown to function as a type of "collagenase" and cleave triple helical collagen [98], LOX was identified to be associated to the surface of MBV. However, the method of solubilization of ECM does influence the molecular weight of MBV-associated LOX. When elastase from human leucocytes is used to digest the ECM before MBV isolation, LOX is associated to the lipid membrane of MBV in its 52 kDa form. When collagenase is used to digest the ECM, LOX appears to be degraded and/or cleaved by various enzymatic products with tryptic activity. LOX is also eluted off MBV when solubilized in high concentration of NaCl solution. The expression of LOX is driven by hypoxia-inducible factors (HIFs) and gets glycosylated in the Golgi apparatus into its pro-peptide form [99, 100]. The identification of the pro-peptide LOX associated with MBV suggest that LOX may become associated to the surface of MBV during vesicle secretion into the extracellular space. LOX on the surface of MBV must be bound and interacting with another protein(s), which we have yet to identify. Further studies will be performed to identify MBV-associated LOX binding partners.

Although the history of the LOX genome can be traced back to the pre-metazoan times [101], there is a limited amount of information about the enzymatic mechanism of LOX and the variability of the protein across tissues and different species [102, 103]. In addition, there are

significant challenges associated with the isolation and purification of LOX. LOX is highly insoluble in aqueous buffers and it has been difficult to obtain large quantities of the enzymatically active recombinant protein [58]. Prior studies have used lengthy dialysis procedures that require multiple buffers and refolding of the protein and extraction using high concentration of urea [104-106]. More recently, solubility tags have been incorporated in buffers to purify enzymatically active LOX, but have resulted in a decreased yield of protein [58]. Results reported herein represent the first identification of MBV-associated LOX and offer insights into the mechanisms by which LOX is incorporated into the extracellular space.

## 5.5 Conclusions

Results from the present study show that MBV can be isolated by various digestion and solubilization methods of ECM. Specifically, ECM can be enzymatically digested by collagenase and elastase, along with solubilization by high concentration of salt solution. Results identified that LOX is associated to the surface of MBV by elastase digestion, whereas it is degraded or eluted off the surface of MBV by the other methods. Such implications provide insights into how LOX is associated to extracellular vesicles such as MBV and incorporated in the extracellular milieu, which is not fully understood and requires further investigation.

## 5.6 Acknowledgements

This study is in progress and acknowledges the contributions of Jordan Birkhimer and Dr. Stephen F. Badylak. Jonathan Franks, Ming Sun, and Mara Sullivan at the Center for Biologic Imaging (CBI) at the University of Pittsburgh are greatly appreciated for their support.

# 6.0 Matrix-Bound Nanovesicles in Native Porcine Tissues

## 6.1 Introduction

Matrix-bound nanovesicles (MBV) are relatively a new discovery in the field of extracellular vesicles. MBV have been described as bioactive components of the matrix, where they can recapitulate the biologic effects of the parent ECM, including differentiation of neural stem cells and modulation of macrophage phenotype [41, 56].

Studies have successfully isolated MBV from decellularized ECM from various tissue sources. Although MBV were discovered to be retained embedded in the matrix after the decellularization process, it is possible that the quality of the vesicles and their surface proteins may be affected or subjected to degradation. Herein, it is hypothesized that the specific decellularization process on tissues may affect the presence of LOX associated to the surface of MBV. The present study shows that MBV can be isolated from native porcine tissues without processing by decellularization. Results show that MBV are present in a variety of tested source tissue. The concentration of MBV and total protein content varied from tissue to tissue. Because MBV were isolated from native tissues, these results cannot be attributed to tissue-specific decellularization processes, but rather, tissue-specific biological composition and function. Isolating MBV directly from native tissues provide insights for future studies investigating MBV-associated surface proteins that may be subjected to degradation by the decellularization process.

## 6.2 Materials and Methods

### 6.2.1 Isolation of MBV from Native Porcine Tissues

To determine if the decellularization process affects the quality and enzymatic activity of MBV-associated LOX, MBV were isolated from a variety of native porcine tissues. MBV were isolated from non-decellularized porcine tissues, including brain, bladder, heart, skeletal muscle, ovary, pancreas, small intestine, and Achilles tendon. For all tissue types, 2 g of wet weight samples were finely minced and rinsed with PBS before enzymatically digested by 4 μg/ml elastase in buffer [20 mM Tris (pH = 7.5), 150 mM NaCl] for 20 hours at 37°C on an orbital rocker. Samples were sequentially centrifuged at 500 xg for 5 minutes, 2,500 xg for 20 minutes, and 10,000 xg for 30 minutes (3 times) at 4°C to remove cells and large debris. Samples were then passed through a 0.2 μm filter and ultracentrifuged at 100,000 xg for 70 minutes at 4°C. MBV pellets were resuspended in PBS. Particle size and concentration were determined using Nanoparticle Tracking Analyses (NTA) [54] and bicinchoninic acid (BCA) assays. Samples were evaluated in biological triplicates.

### 6.2.2 Transmission Electron Microscopy (TEM)

MBV samples were imaged by TEM as previously described. Briefly, re-suspended MBV were placed on formvar-coated grids with 1% uranyl acetate for negative staining. Grids were imaged at 80 kV with a JEOL 1400 transmission electron microscope (JEOL Peabody, MA) with a side mount AMT 2k digital camera (Advanced Microscopy Techniques, Danvers, MA). Size of MBV was determined from representative images using JEOL TEM software.

### 6.2.3 Western Blot Analysis

1 x $10^9$ particles/ml of MBV isolated from each tissue were resuspended in Laemmli buffer containing 5% β-mercaptoethanol (Sigma-Aldrich). Samples were resolved by sodium dodecyl sulfate polyacrylamide gel electrophoresis (SDS-PAGE) in a 4-20% Mini-PROTEAN® TGX™ Stain-Free polyacrylamide gel (Bio-Rad) at 150 V in running buffer (25 mM Tris, 190 mM glycine, 0.1% SDS) and transferred on to a PVDF membrane for 3 hours at 150 mA in transfer buffer (25 mM Tris, 190 mM glycine, 20% methanol). Membranes were analyzed by Western blot using 1:1000 dilution of LOX antibody (LS-Bio, LS-C141072) in blocking buffer (5% non-fat milk in TBS) overnight at 4°C. Membranes were washed thoroughly in 0.1% Tween-20 in TBS and incubated with 1:2000 dilution of horseradish peroxidase secondary antibody (Dako) in blocking buffer for 1 hour at room temperature. Bio-Rad Western ECL solution (Bio-Rad, Hercules, MA) was applied to each membrane for 5 minutes before imaging.

## 6.3 Results

### 6.3.1 MBV Isolated from Native Porcine Tissues Contain MBV-associated LOX

In order to compare MBV isolated from different porcine tissues without any effects from the decellularization process, MBV were isolated from whole porcine tissues that did not undergo processing by decellularization protocols. Porcine tissues varying in anatomical location (i.e., bladder, brain, heart, muscle, ovary, pancreas, small intestine, and tendon) were enzymatically digested by elastase before isolation of MBV. TEM imaging confirmed the presence of rounded

structures that are similar in size and shape of previously reported MBV [41] (Figure 5). Results from NTA showed similar particle concentrations across all tissue samples except brain tissue. Brain tissue is likely to have more remnant lipids and other proteins in the sample. BCA analyses showed total protein concentrations vary between the tissue samples. These results are shown in Table 2 and displayed in Figure 6 below. Our results show not only the heterogeneity of MBV that can be isolated from specific tissues, but that the isolation of MBV is not limited to decellularized ECM.

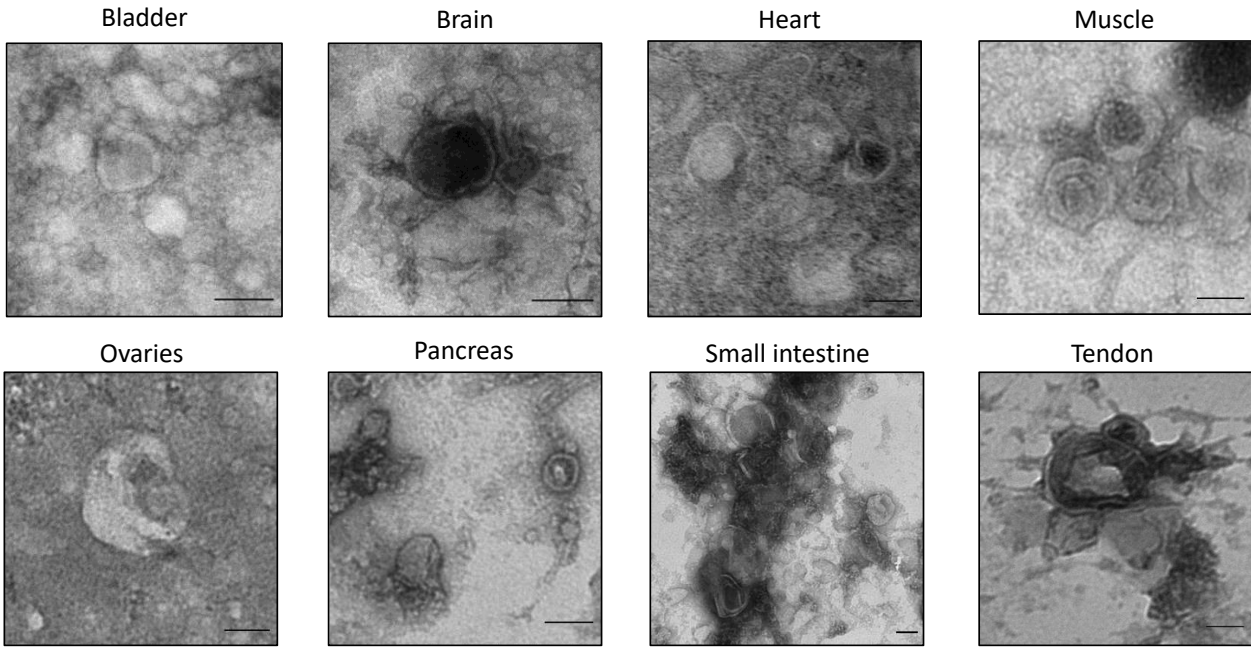


**Figure 5. MBV isolated from various native porcine tissues.** Transmission electron microscopy (TEM) images confirm the presence of MBV in all porcine tissue samples (scale bars = 100 nm).

**Table 3. Quantification of protein and particle concentrations of MBV isolated from native porcine tissues**

| Sample | Mean Total Protein Concentration (µg/ml) | Particle concentration (particles/mL) | MBV Particle per µg of Protein |
|---|---|---|---|
| Bladder | 3671.57 | 5.09E+12 | 1.39E+09 |
| Brain | 756.35 | 5.57E+11 | 7.37E+08 |
| Heart | 903.00 | 3.41E+11 | 3.78E+08 |
| Skeletal muscle | 1142.50 | 3.60E+11 | 3.15E+08 |
| Ovary | 484.81 | 2.76E+11 | 5.70E+08 |
| Pancreas | 500.15 | 6.45E+11 | 1.29E+09 |
| Small intestine | 1621.78 | 8.14E+11 | 5.02E+08 |
| Tendon | 279.00 | 7.95E+10 | 2.85E+08 |

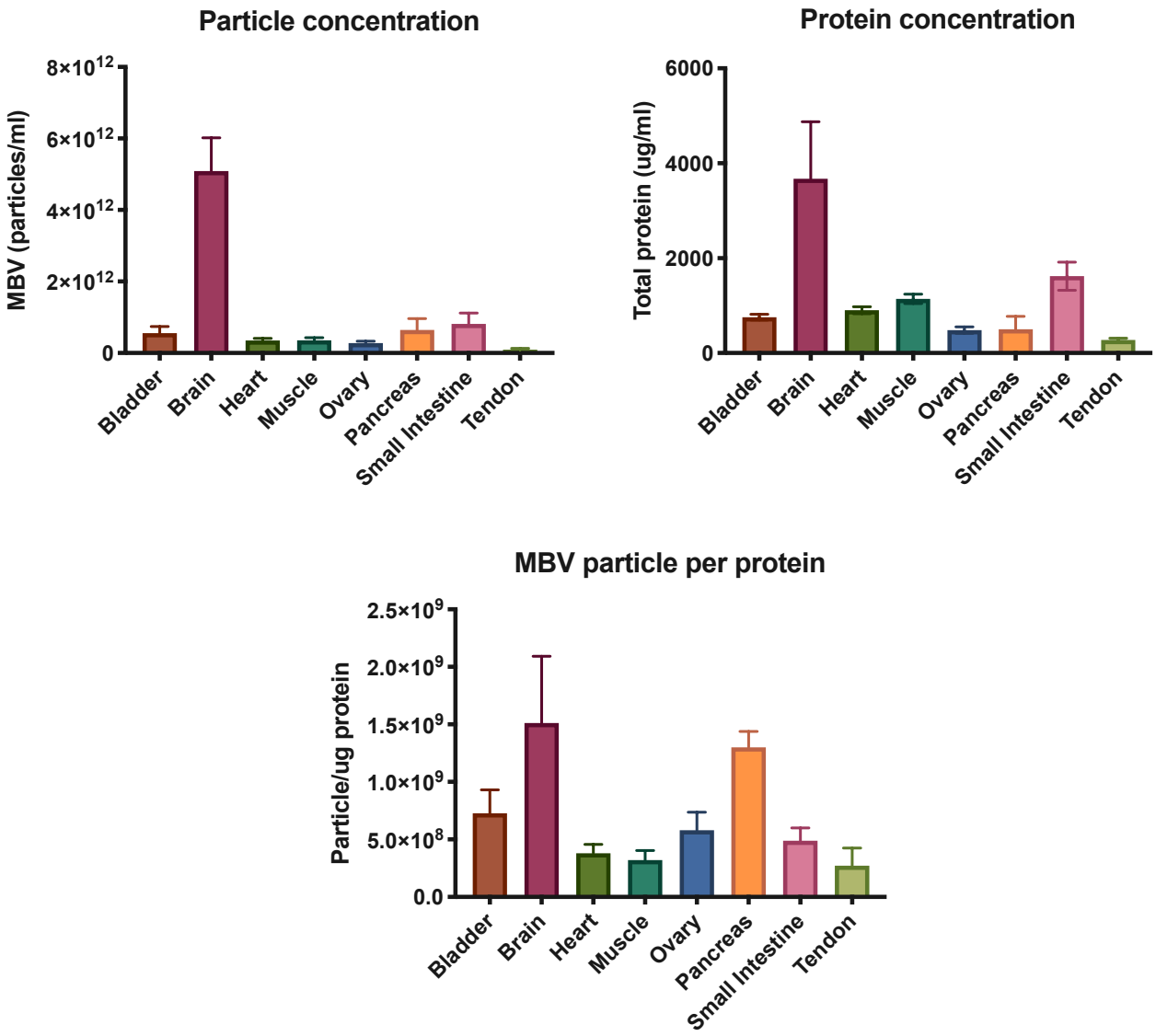


**Figure 6. Quantification of particle and total protein quantification of MBV isolated from native porcine tissues.**

### 6.3.2 MBV-Associated LOX is Present in a Variety of Tested Source Tissue

The presence of MBV-associated LOX in native porcine tissues was investigated. Results from Western blots showed differential products of LOX in varying molecular weights and abundance (Figure 7). The presence of multiple bands may be differential products or degradation

of LOX [107], or non-specific binding of the antibody. Further experiments are required to validate the results and optimize the experiment using different LOX antibodies.

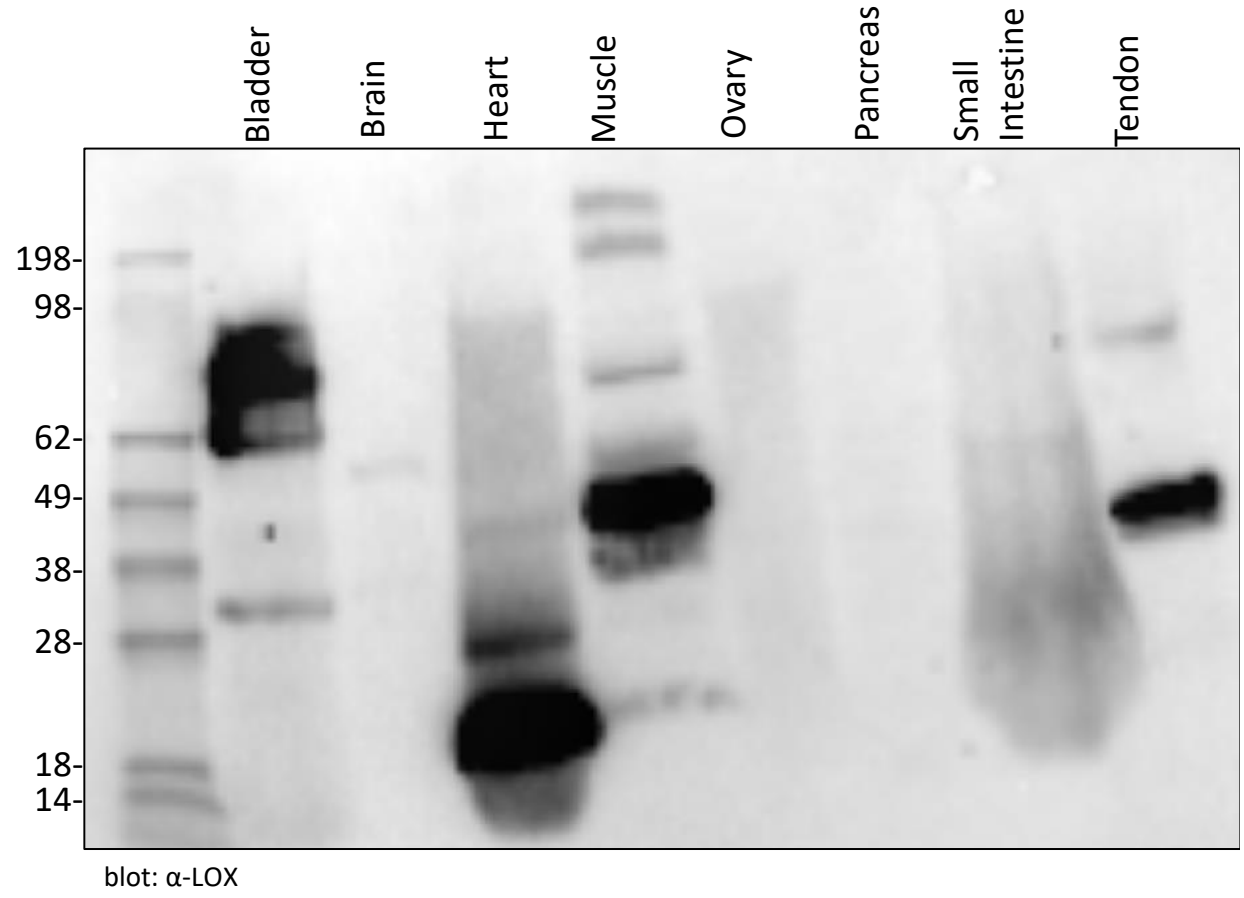


**Figure 7. Presence of MBV-associated LOX in native porcine tissues.**

The present study investigates MBV isolated from native porcine tissues, of which they were not decellularized previously. The preparation of ECM bioscaffolds requires intensive processing steps, where the decellularization process includes physical, chemical, mechanical methods of processing and manufacturing. A list of various decellularization processes are summarized in Table 3. Porcine tissues are harvested and subjected to mechanical removal of

excess tissue and various chemicals and detergents. Then, the samples are frozen and lyophilized into a dry state to allow mechanical comminution into a powder.

**Table 4. Decellularization processes for various tissues**

| Tissue Source | Decellularization Process | Reference |
|---|---|---|
| Urinary bladder | Mechanical removal of muscular layers; 0.1% peracetic acid and water washes | [108] |
| Small intestine | Mechanical removal of muscular layers; 0.1% peracetic acid and water washes | [94] |
| Dermis | Mechanical removal of fat, connective tissue, and epidermis; washes with 0.25% trypsin, 70% ethanol, 3% H2O2, 1% Triton X-100, 0.26% EDTA/0.69% Tris, 0.1% peracetic acid/0.4% ethanol, water, and PBS | [109] |
| Skeletal muscle | Mechanical removal of fat and connective tissue; washes with 2:1 v/v chloroform/methanol, graded series of ethanol, 0.2% trypsin/0.2% EDTA, 2% sodium deoxycholate, 1% Triton X-100, 0.1% peracetic acid/4% ethanol, water and PBS | [110] |
| Brain | Mechanical removal of dura matter; washes with 0.02% trypsin/0.05% EDTA, 3% Triton X-100, 1 M sucrose, 4% deoxycholate, 0.1% peracetic acid, and water | [110] |
| Esophagus | Mechanical removal of muscularis layer; washes with 1% trypsin/0.05% EDTA, 1 M sucrose, 3% Triton X-100, 10% deoxycholate, 0.1% peracetic acid, 4% ethanol, 100 U/ml DNAse, water, and PBS | [111] |

The effects of decellularization on the resulting biologic scaffold and the associated host remodeling response have been reported [112, 113]. Decellularization of ECM bioscaffolds is in fact critical for avoiding inflammatory responses that can mitigate or completely inhibit

constructive remodeling events. For example, macrophages are key players in the host response and are activated in the presence of tissue damage, inflammation, and infection. Macrophages subsequently release a variety of cytokines and chemokines [114] that also influence the tissue repair and remodeling process, particularly in the presence of biologic scaffolds [40, 115]. The presence of allogeneic or xenogeneic cells within a biologic scaffold has been associated to pro-inflammatory cytokines, increased M1-like macrophage polarization, and poor remodeling outcomes [116]. Although the importance of decellularization in ECM biologic scaffolds is clear, it is not known if decellularization of tissues is required for isolation of MBV for therapeutic applications. MBV are secreted by tissue-resident cells and integrated into the fibrillar matrix, from which they can be isolated by enzymatic digestion. It is plausible that decellularization of tissues is not required prior to isolation of MBV.

The present study presents MBV isolated from native porcine tissues including bladder, brain, heart, skeletal muscle, ovary, pancreas, small intestine, and Achilles tendon. Although the number of MBV particles were similar across tissue sources, total protein concentrations varied. When MBV-associated LOX was investigated by Western blot analyses, LOX was found to be present in varying amounts and differential forms or degraded products. Because the MBV samples were isolated directly from native tissue, the variable of the effects induced by the decellularization process can be omitted. The presence of MBV-associated LOX is likely due to the source tissue's biological composition and function. For example, brain tissue, which is made of primarily fat with very little matrix, has hardly any LOX, whereas the heart, which is a tissue that has an extensive ECM and experiences constant mechanical force, has higher amounts and differential products of LOX. This indicates that MBV contain different cargo along with its membrane-bound surface proteins for tissue-specific functions.

## 6.4 Conclusions

Results of the present study show, for the first time, MBV isolated from native porcine tissues that were not decellularized. Removing the decellularization step prior to isolating MBV allows investigation of MBV that were not subjected to tissue-specific decellularization protocols. MBV were found to vary in total protein concentrations anatomically different source tissues, including bladder, brain, heart, skeletal muscle, ovary, pancreas, small intestine, and Achilles tendon. Further, MBV-associated LOX appeared in different amounts and molecular weights between the tissue samples. The findings reported show the heterologous nature of MBV in and associated LOX among the diverse tissue sources.

## 6.5 Acknowledgements

This study is in progress and acknowledges the contributions of Jordan Birkhimer, Dr. George Hussey, and Dr. Stephen F. Badylak. Jonathan Franks, Ming Sun, and Mara Sullivan at the Center for Biologic Imaging (CBI) at the University of Pittsburgh are greatly appreciated for their support.

# 7.0 Isolation f MBV-Associated LOS from ECM Bioscaffolds

## 7.1 Introduction

Lysyl oxidase (LOX) is a copper dependent enzyme that catalyzes the cross-linking of the molecular units of collagen and elastin, which is an essential post-translational modification that occurs in the biogenesis of collagenous connective tissues [18]. LOX causes the oxidative deamination of peptidyl-lysine and hydroxylysine to peptidyl-α-aminoadipic-δ-semialdehyde, which is the precursor to various cross-links in collagen and elastin [117]. The LOX family of proteins exist in 5 different isoforms in mammalians, LOX and LOX-like isoforms 1-4 (LOXL1-4) [118]. Full characterization and understanding of the enzyme's catalytic activity remain unknown due to its highly insoluble properties and difficulties in obtaining large quantities of LOX [58]. Isolation of LOX procedures from tissue involve high concentrations of urea and extensive buffer exchanges [59, 60]. Nevertheless, it is widely reported that LOX is essential for proper ECM development and stabilization of tissues [8, 61, 62].

LOX has been identified in several proteomic analyses studies of ECM including Matrigel [70], ECM-produced by synovium-derived stem cells [71], and ovine forestomach matrix [72]. Biologic scaffolds composed of ECM have been used as surgical meshes and inductive templates for tissue remodeling in multiple anatomic sites, including rotator cuff, Achilles tendon, tibialis posterior, patellar tendons, and hernia, among others [119-122]. ECM scaffolds promote constructive tissue remodeling and at least partial restoration of function. The present study reports, for the first time to the best of our knowledge, an extracellular source of LOX associated to the ECM, specifically matrix-bound nanovesicles (MBV), which are lipid-bound extracellular vesicles

described as an integral component of the ECM. Recent studies attribute certain aspects of the constructive remodeling events to MBV have been shown to modulate cell behavior as a function of their internal cargo of biologically active signaling molecules (e.g. microRNAs) [41]. MBV influence neuron differentiation and promote a pro-remodeling macrophage phenotype [41, 55-57]. MBV are secreted by tissue-resident cells and integrated in the ECM, which make them distinctly different from extracellular vesicles existing in fluid (i.e., exosomes) [53]. The integration of MBV in the fibrillar matrix may be due to the surface proteins and constituent phospholipids, which may differ as a function of anatomic location from which the MBV are harvested. Such differences are important factors when considering potential therapeutic applications of MBV to deliver internal cargo or surface proteins to promote ECM remodeling and functional restoration. The goal of the present study was to identify MBV-associated LOX in various biologic scaffolds and compare the abundance of associated LOX proteins.

## 7.2 Methods

### 7.2.1 Preparation of ECM Bioscaffolds

*Urinary bladder matrix ECM (UBM-ECM)* – UBM-ECM was prepared as previously described [91]. The specific procedure of preparing UBM-ECM is detailed previously in section 5.2.2.

*Small intestinal submucosa ECM (SIS-ECM)* – SIS-ECM was prepared as previously described [92, 93]. Briefly, the superficial layers of the tunica mucosa, the tunica serosa, and tunica muscularis externa were mechanically removed. The remaining tissue was decellularized and

disinfected by washing in 0.1% peracetic acid with 4% ethanol for 2 hours at 300 rpm. The tissue was then extensively rinsed with PBS and sterile $H_2O$. SIS-ECM was then lyophilized and milled into particulate using a Wiley Mill with a #60 mesh screen.

*Dermis ECM (dECM)* – dECM was prepared as previously described [109]. Briefly, the epidermis, connective tissue, and subcutaneous fat were removed by mechanical delamination. The remaining tissue was decellularized by washing in 0.25% trypsin for 6 hours, 70% ethanol for 10 hours, 3% $H_2O_2$ for 15 minutes, 1% Triton X-100 in 0.26% EDTA/0.69% tris for 6 hours with a solution change for an additional 16 hours, and 0.1% peracetic acid/4% ethanol for 2 hours. All chemical exposures were conducted at 300 rpm in an orbital shaker. dECM was extensively washed with sterile $H_2O$ and PBS between chemical exposures. dECM was then lyophilized and milled into particulate using a Wiley Mill with a #60 mesh screen.

*Tendon ECM (tECM)* – tEM was prepared by a vacuum-assisted method [123]. Briefly, muscle, fat, synovial sheath, and para-tenon were aseptically dissected from Achilles tendons. Decellularization was performed in a container capable of withstanding negative pressure/vacuum (e.g. desiccator) attached to a Welch 8925 DirecTorr Vacuum Pump (Gardner Denver Thomas, Inc. a division of Ingersoll Rand, Mt. Prospect, IL) fitted with a pressure gauge (Nagano Keiki Co. Ltd., Japan), controlled by a custom LabView (National Instruments, Austin, TX) program. A vacuum was created to approximately 100 kPa (~30" Hg). The prepared tendons were placed in a beaker with 300 mL of 12.5% NaCl. The vacuum parameters were 480 cycles, 120 seconds per cycle with 75% duty load. Tissues were then washed in H2O on an orbital shaker for 1 hour at room temperature. Tissues were placed in 12.5% NaCl in the vacuum for 180 cycles 3 more times with $H_2O$ washes in between.

All prepared scaffolds met stringent requirements for sufficient decellularization; specifically, no visible intact nuclei by DAPI and hematoxylin and eosin (H&E) staining, remnant DNA concentration <50 ng/mg total scaffold dry weight, and DNA fragment length <200 base pairs [124].

### 7.2.2 Isolation of MBV

MBV were isolated from decellularized porcine ECM bioscaffolds and some of their commercially available equivalents by enzymatic digestion as previously described with minor modifications [41]. Briefly, 400 mg of lyophilized powdered ECM was enzymatically digested with 4 μg/ml elastase (Elastin Products Company, SE563) in buffer (20 mM Tris pH 7.5, 150 mM NaCl) for 20 hours at 37°C on an orbital rocker. Samples were sequentially centrifuged at 500 xg for 5 minutes, 2,500 xg for 20 minutes, and 10,000 xg for 30 minutes (3 times) at 4°C. Samples were then passed through a 0.2 μm filter and ultracentrifuged at 100,000 xg for 70 minutes at 4°C. MBV pellets were resuspended in PBS. Particle size and concentration were determined using Nanoparticle Tracking Analyses (NTA) [54] and bicinchoninic acid (BCA) assays. Samples were evaluated in triplicate.

### 7.2.3 Transmission Electron Microscopy (TEM)

MBV samples were imaged by TEM as previously described. Briefly, re-suspended MBV were placed on formvar-coated grids with 1% uranyl acetate for negative staining. Grids were imaged at 80 kV with a JEOL 1400 transmission electron microscope (JEOL Peabody, MA) with

a side mount AMT 2k digital camera (Advanced Microscopy Techniques, Danvers, MA). Size of MBV was determined from representative images using JEOL TEM software.

### 7.2.4 SDS-PAGE and Silver Stain

1 x $10^9$ particles/ml of MBV isolated from each tissue were resuspended in Laemmli buffer containing 5% β-mercaptoethanol (Sigma-Aldrich). Samples were resolved by sodium dodecyl sulfate polyacrylamide gel electrophoresis (SDS-PAGE) in a 4-20% Mini-PROTEAN® TGX™ Stain-Free polyacrylamide gel (Bio-Rad) at 150 V in running buffer (25 mM Tris, 190 mM glycine, 0.1% SDS). For silver stain, gels were stored in fixing buffer overnight and then stained with a Pierce Silver Stain for Mass Spectrometry Kit (Life Technologies) following the manufacturer's instructions. For Western blot analyses, gels were transferred on to a PVDF membrane for 3 hours at 150 mA in transfer buffer (25 mM Tris, 190 mM glycine, 20% methanol). Membranes were analyzed by Western blot using 1:1000 dilution of LOX antibody (LS-Bio, LS-C141072), 1 μg/ml LOXL1 antibody (LS-Bio, LS-C110889), 1:1000 dilution of LOXL2 antibody (LS-Bio, LS-C369938), 1 μg/ml LOXL3 antibody (LS-Bio, LS-C135755), or 1:400 dilution of LOXL4 antibody (LS-Bio, LS-C295249) in blocking buffer (5% non-fat milk in TBS) overnight at 4°C. Membranes were washed thoroughly in 0.1% Tween-20 in TBS and incubated with 1:2000 dilution of horseradish peroxidase secondary antibody (Dako) in blocking buffer for 1 hour at room temperature. Bio-Rad Western ECL solution (Bio-Rad, Hercules, MA) was applied to each membrane for 5 minutes before imaging.

### 7.2.5 Enzyme-Linked Immunosorbent Assay (ELISA)

Enzyme-linked immunosorbent assay (ELISA) was used to determine the concentrations of MBV-associated LOX in UBM, SIS, dECM, and tECM. After isolation, resuspended MBV were used to perform ELISAs following specific manufacturing instructions (LS-Bio, LS-F53541). Samples were evaluated in quadruplicate.

## 7.3 Results

### 7.3.1 MBV Isolated from Various ECM Bioscaffolds

MBV were isolated and the presence of vesicles were confirmed by TEM (Figure 8A). Images showed that proteinase K does not disrupt the integrity or morphology of vesicles. Particle concentration of each samples were quantified by NTA and vesicles were an average size 90 – 200 nm in diameter (Figure 8B). Samples were evaluated in biologic triplicates.

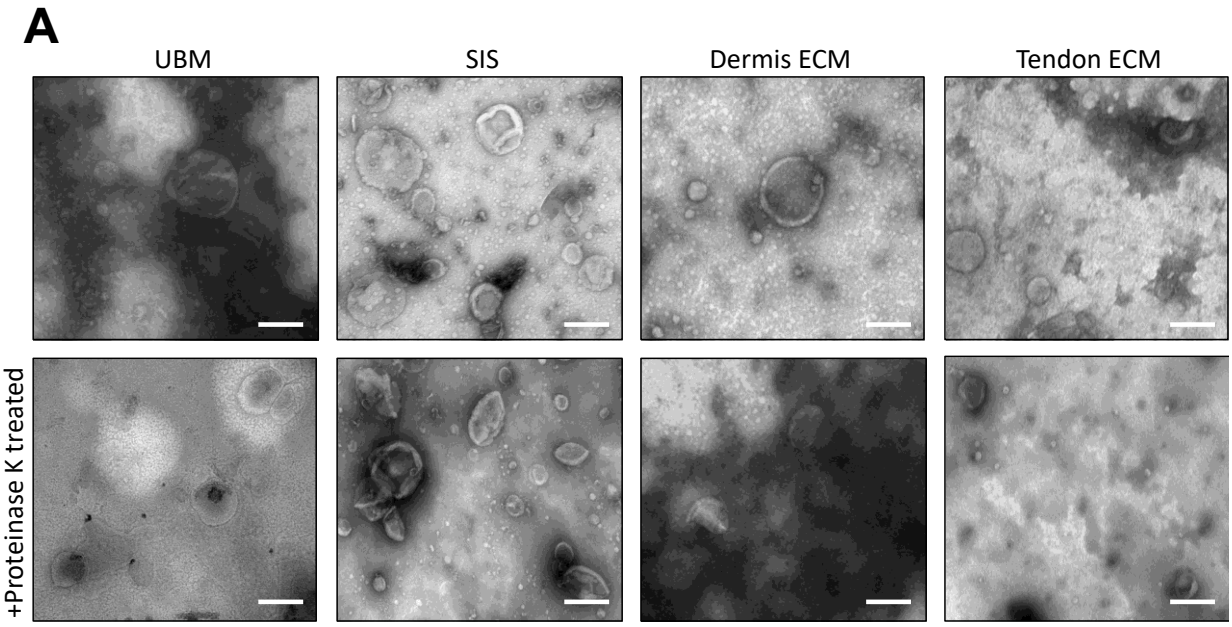
A
UBM
SIS
Dermis ECM
Tendon ECM
+Proteinase K treated

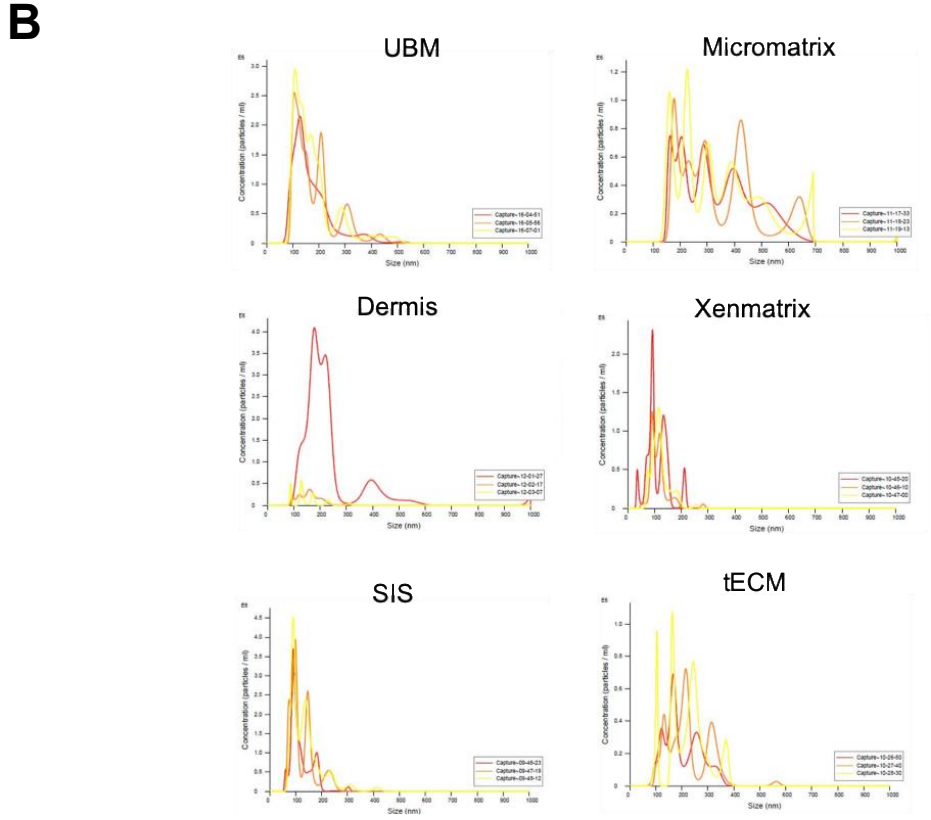
B
UBM
Micromatrix
Dermis
Xenmatrix
SIS
tECM

**Figure 8. MBV isolated from ECM bioscaffolds. (A)** TEM images of MBV confirmed presence of vesicles in all samples, including those treated with proteinase K (scale bars = 100 nm) **(B)** NTA of MBV isolated from various ECM and their commercially available equivalents.

### 7.3.2 Presence of LOX Isoforms in ECM Bioscaffolds

Results from Western blot analyses showed the presence or absence of LOX isoforms. Specifically, LOX was found associated to MBV isolated from UBM and its commercially available equivalent Micromatrix®, SIS, and tECM at the 52 kDa pro-peptide form (Figure 9). The other LOX isoforms were not present as determined by Western blots. Results from ELISA showed that MBV-associated LOX was the most abundant in UBM compared to the other ECM samples (Figure 10). Data is shown with mean ± SD.

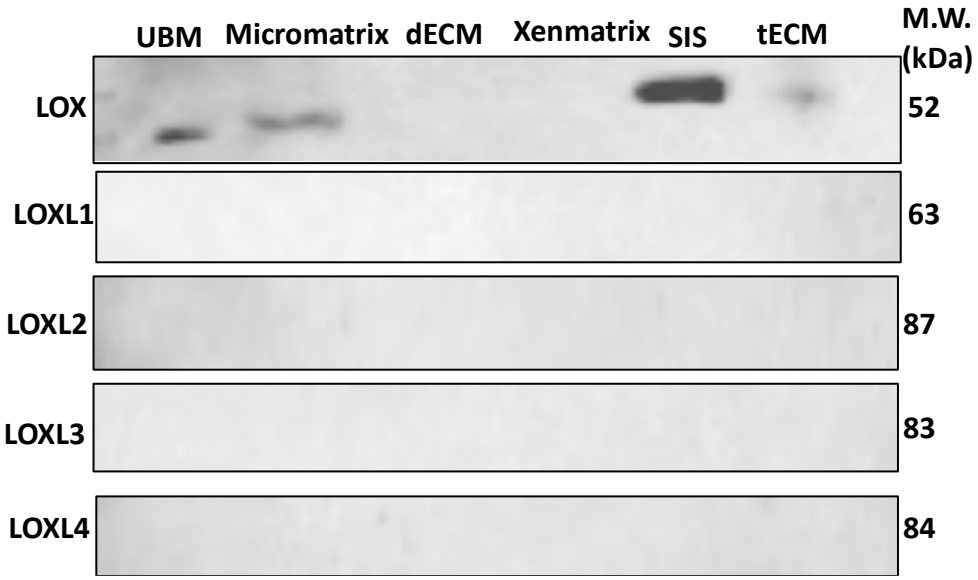


**Figure 9. Presence of LOX isoforms in ECM bioscaffolds.**

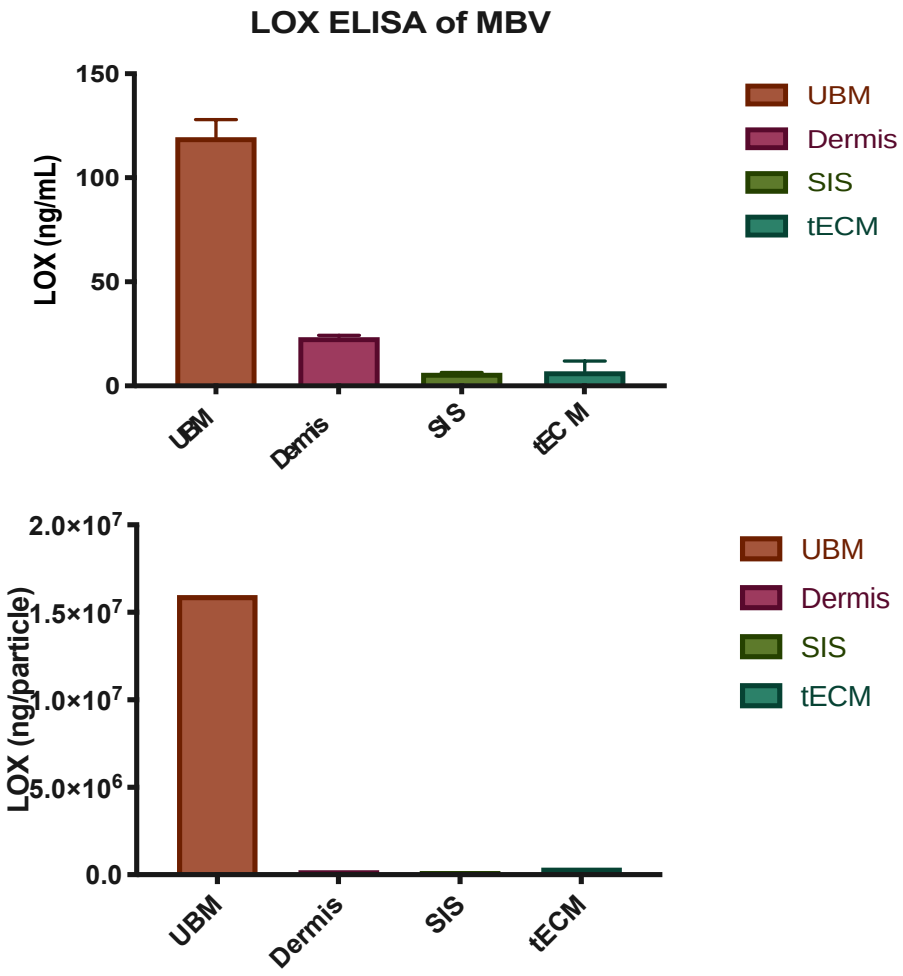


**Figure 10. Quantification of MBV-associated LOX by ELISA.**

### 7.3.3 Identification of Binding Partners of MBV-Associated LOX

A preliminary experiment was performed to identify the binding partners of MBV-associated LOX by SDS-PAGE and silver stain (Figure 11). MBV samples have clear bands in above 49kDa, which do not appear in samples treated with proteinase k. Degradation products of proteinase k are shown below 20 kDa.

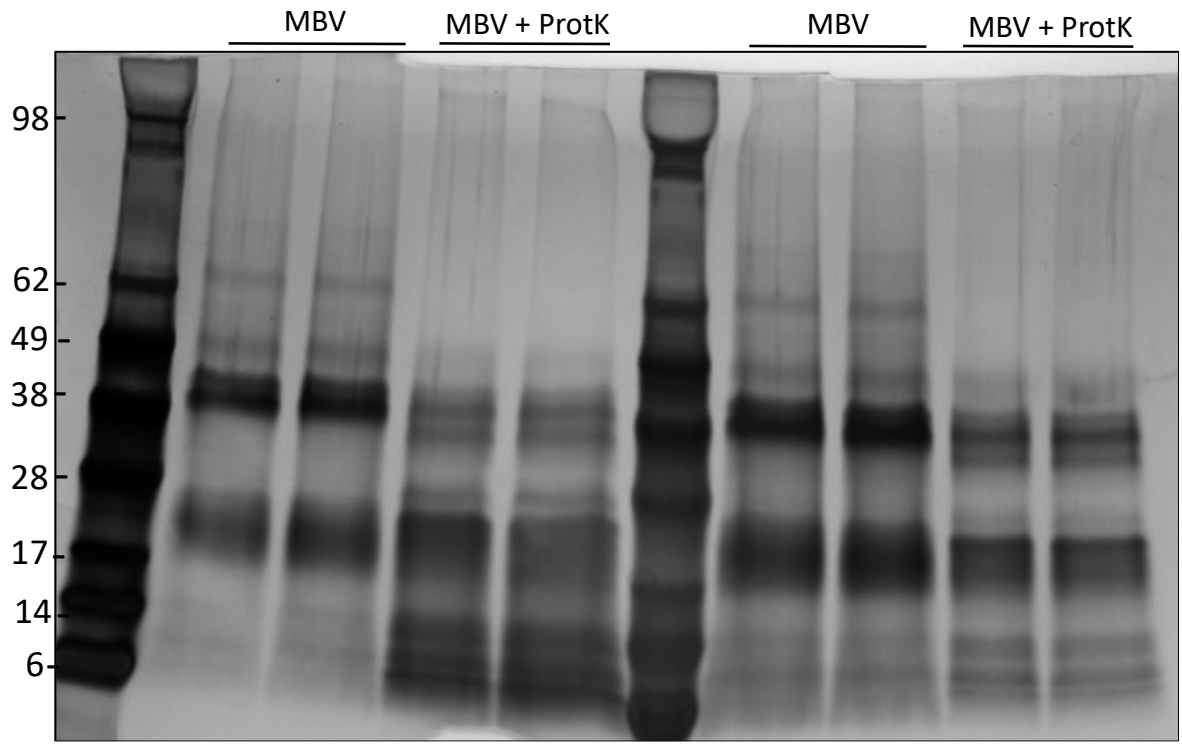


**Figure 11. SDS-PAGE and silver stain of MBV-associated LOX.** MBV samples have clear bands in above 49kDa, which do not appear in samples treated with proteinase k (ProtK). Degradation products of proteinase K are shown below 20 kDa.

### 7.4 Discussion

The role of LOX in the cross-linking of collagen and elastin has been studied in multiple tissues including skin, lung, and cardiovascular tissues [125-127]; and is essential for stabilization of the ECM [78, 128-130]. Studies have been limited in fully characterizing LOX and its mechanism due to its highly insoluble properties [58]. In fact, the 3-dimensional model of LOX was only recently described, and has facilitated further studies of LOX, its protein interactions, and in the design of LOX inhibitors [102]. LOX has been purified and isolated from tissues, such

as porcine aorta [59], or expressed through *in vitro* systems to investigate biological functions and mechanism of LOX [58, 131].

The challenges associated with the isolation and purification of LOX is widely known. LOX is highly insoluble in aqueous buffers and it has been difficult to obtain large quantities of the enzymatically active recombinant protein [58]. Prior studies have used lengthy dialysis procedures that require multiple buffers and refolding of the protein and extraction using high concentration of urea [104-106]. To the best of our knowledge, this is the first report describing a stable extracellular matrix-associated surface protein. The present study identifies the presence and abundance of LOX associated to MBV isolated from various ECM bioscaffolds. Herein, MBV-associated LOX is present in varying amounts in different ECM, which may be due to tissue specificity/function or the effects of the decellularization process to produce ECM.

MBVs are similar to exosomes in their nanometer size and containment of miRNA cargo but are different in which they lack common exosomal surface markers including CD63, CD81, CD9, and HSP70 [41]. The discovery MBV-associated LOX provides insights to the insoluble nature of LOX. It is plausible that, by association to the surface of MBV, the biological and functional role of LOX in cross-linking collagen is more controlled and tightly regulated to be shuttled directly to its specific matrix substrates.

There are many limitations to the present study. Full comparison to commercially available ECM, such as for SIS and tECM, would have furthered characterization of MBV-associated LOX. The experiments performed were biological replicates but future work including technical replicates is required to validate the data. In addition, the antibodies for the different LOX isoforms should be optimized for further Western blot analyses. Future work will identify and confirm the presence or absence of the other LOX isoforms associated to MBV. Last but not least, further

analyses of the silver stain data are required. Future will identify immunoprecipitated binding partners my downstream mass spectrometry analyses.

## 7.5 Conclusions

Results of the present study show that MBV-associated LOX is present in UBM, SIS, dECM, and tECM. Specifically, MBV isolated from UBM showed the most abundant amount of LOX in the 52 kDa pro-peptide form. MBV-associated LOX also shows distinctly different protein signatures compared to those treated with proteinase K. The findings of this study reports, for the first time, an extracellular source of LOX associated to the ECM. MBV provide a unique and attractive way to isolate LOX for possible therapeutic applications.

# 8.0 Enzymatically Active LOX Associated to Matrix-Bound Nanovesicles

## 8.1 Introduction

As iterated in previous chapters, lysyl oxidase (LOX) is an extracellular enzyme responsible for catalyzing the covalent cross-linking of collagen, which is an essential post-translational modification to the stabilization of tissues. The enzymatic role LOX plays in the extracellular space has long been studied but complete understanding of its biosynthesis, mechanism of action, co-factors, and substrate specificity is still necessary.

The synthesis and processing of LOX involves multiple processes that are commonly known with protein syntheses. LOX is synthesized in the cell cytoplasm and glycosylated before entering the Golgi apparatus, where it is processed to its inactive 52 kDa pro-peptide from [100]. This pro-peptide is secreted into the extracellular space, where it is cleaved and activated by pro-collagen C proteinases (e.g. BMP-1, TLL1, TLL2 [132]) to the 32 kDa enzymatically active form of LOX. BMP-1 has been most commonly reported to be involved in the proteolytic processing of the LOX precursor to [77, 79, 100]. However, recent studies have reported proteolysis of LOX occurs by alternative cleavage sites, specifically, downstream of the BMP-1 cleavage site [133]. This processing of LOX did not significantly affect the enzymatic activity, but rather modified the affinity towards collagen. In addition, and most interestingly, the LOX precursor was shown to be enzymatically active without the necessity of proteolysis.

The present study succeeds the findings of previous chapters reporting LOX associated to the surface of matrix-bound nanovesicles. Specifically, the enzymatic and functional activity of MBV-associated LOX, which was identified as the 52 kDa pro-peptide form, was investigated.

MBV-associated LOX was also determined for its effect upon collagen strength in an *in vitro* collagen construct model. The synthesis of collagen secretion from cells, and the subsequent assembly and cross-linking of fibers have been exhaustively studied. However, the mechanism by which extracellular fibrils self-assemble and form covalent cross-links in *vivo* is largely unknown. Herein, we identify the pro-peptide form of MBV-associated LOX is enzymatically active and has biologic effects on collagen construct development *in vitro*.

## 8.2 Methods

### 8.2.1 Preparation of Urinary Bladder Matrix (UBM)

Urinary bladder matrix (UBM) was prepared as previously described [91]. The specific procedure of preparing UBM-ECM is detailed previously in section 5.2.2.

### 8.2.2 Isolation of MBV-Associated LOX

MBV were isolated by enzymatic digestion using 4 μg/ml elastase (Elastin Products Company, SE563) in buffer (20 mM Tris pH 7.5, 150 mM NaCl) for 20 hours at 37°C on an orbital rocker. The digested ECM was then subjected to centrifugation at 10,000 xg for 30 minutes to remove insoluble ECM remnants, and the supernatant passed through a 0.22 μm filter (Millipore). For preparing negative control samples, MBV were treated with 0.1 mg/ml proteinase K in buffer (20 mM Tris pH 7.5, 150 mM NaCl) for 1 hour at 37°C on an orbital rocker, which removed MBV surface proteins. The clarified supernatant containing the liberated MBV was then centrifuged at

100,000 xg (Beckman Coulter Optima L-90K Ultracentrifuge) at 4°C for 70 minutes. The MBV pellet was then resuspended in 1X PBS and the total protein concentration determined using the bicinchoninic acid (BCA) assay quantification kit (Pierce Chemical). Particle size and concentration were determined using Nanoparticle Tracking Analyses (NTA) [54]. Samples were evaluated in triplicate.

### 8.2.3 Inhibition of LOX Activity

After resuspending in PBS, MBV-associated LOX samples were lysed in buffer containing 150 mM NaCl, 1% Triton, and 50 mM Tris (pH = 8) using a sonic dismembrator (Fisherbrand™). Samples were centrifuged at 13,000 xg at 4°C for 5 minutes. The supernatant was collected and kept on ice. Samples were treated with 0, 5, 10, 20, 50, 100, 250, or 500 μM of irreversible LOX inhibitor β-aminopropionitrile (BAPN) at 37°C overnight. Samples were assessed for enzymatic activity of LOX using the Lysyl Oxidase Activity Assay Kit (Abcam, ab112139) per manufacturer's instructions. All samples were evaluated in triplicate.

### 8.2.4 Isolation of Primary Tenocytes

Primary tenocytes were isolated from rat tendons as previously described with slight modifications [134]. Rat tails were obtained from Sprague-Dawley rats that were euthanized for reasons unrelated to the present study, and the tendons were separated from their outer sheaths into a dish containing 1X PBS + 1% antibiotic-antimycotic (ThermoFisher Scientific) to remove unwanted debris and contaminants (Figure 12A). After rinsing in PBS, tendons were digested in 3 mg/mL collagenase from *clostridium histolyticum* (Sigma-Aldrich, C0130) in buffer containing

20 mM Tris (pH = 7.5), 150 mM NaCl, and 5 mM $CaCl_2$ in high glucose DMEM (ThermoFisher Scientific) on an orbital rotator at 37°C for 4 hours. The digested tendons were passed through a 70 μm cell strainer (ThermoFisher Scientific) and centrifuged at 1.4 xg for 5 minutes. The cell pellet was resuspended in media consisting of DMEM, 20% fetal bovine serum (FBS) (Invitrogen), and 1% antibiotic-antimycotic, and counted using a hemocytometer. Cells were plated at 1 x $10^6$ cells in T25 culture flasks and maintained at 37°C and 5% $CO_2$ with complete medium change every 2 days for 4 days.

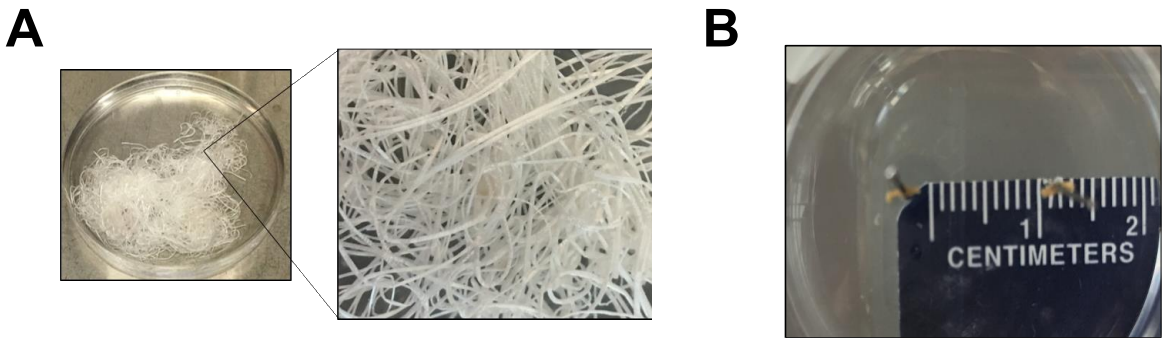


**Figure 12. Isolation of tenocytes. (A)** Primary tenocytes were isolated from rat tail tendons digested in collagenase. **(B)** Cells were used for producing in vitro tendon constructs in 6-well plates coated with Sylgard, with 2 silk sutures pinned 1 cm apart.

### 8.2.5 *In Vitro* Collagen Fibril Formation

When primary tenocytes were confluent, tenocytes were disassociated by trypsin and used for the self-organizing collagen construct system [7, 135]. A 6-well culture plate was coated with 1.5 mL of SYLGARD®184 (Sigma-Aldrich, 761036) and allowed to set at 37°C for 48 hours. Two silk sutures, separated by 1.0 cm, were pinned to the coated plates (Figure 12B). The plates were washed in 70% ethanol for 45 minutes, exposed to UV for 1 hour, and washed with sterile PBS.

Primary tenocytes were suspended in culture medium containing 50 mg of human fibrinogen, 10 μg/ml aprotinin, and 1 unit of human thrombin (all from Sigma Aldrich) and allowed to set in culture for 30 minutes at 37°C. Media was added to the surface of cell-fibrinogen culture as needed to prevent drying. Media was changed every other day, with the addition of 0.33 mM L-ascorbic acid 2-phosphate 33.3 μM L-proline (both from Sigma Aldrich). 1 x $10^9$ particles/ml UBM-ECM MBV isolated from UBM-ECM were added during media changes after the cell-fibrinogen cultures were plated.

### 8.2.6 Histology

Collagen constructs were harvested and fixed in 10% neutral buffered formalin (NBF) for at least 7 days. Samples were then embedded in paraffin, cut into 5 μm longitudinal sections, and mounted onto glass slides for Masson's trichrome staining.

### 8.2.7 Quantification of Soluble Collagen

Soluble collagen content was determined in 7 day collagen constructs using Sircol™ Soluble Collagen Assay kit (Biocolor). Samples were treated with 1 x $10^9$ particles/ml MBV, MBV treated with 500 μM BAPN, MBV treated with 0.1 mg/ml proteinase K, or media as controls. Constructs were harvested from the plates and rinsed in 1X PBS and stored at -20°C prior to experiments.

### 8.2.8 Statistical Analysis

Student's unpaired t-test was performed to compare MBV-associated LOX activity between MBV and those treated either BAPN or proteinase K. Values are expressed as mean ± standard deviation (SD) because one technical replicate was performed for each biological sample (n = 3).

## 8.3 Results

### 8.3.1 BAPN Inhibits MBV-Associated LOX Activity

β-aminopropionitrile (BAPN) is an irreversible LOX inhibitor [136]. When MBV are treated with increasing concentrations of BAPN, the enzymatic activity of MBV-associated LOX decreased as measured by colorimetric absorbance (O.D.) (Figure 13A). Significant differences are shown beginning from 10 μM of BAPN. In a separate experiment, MBV treated with 50 μM of BAPN showed significantly decreased LOX activity measured by fluorescence (RFU) (Figure 13B). MBV-associated LOX activity is 2-fold greater compared to samples treated with BAPN. MBV-associated LOX activity is detectable by both colorimetric (O.D.) and fluorescence (RFU). Results in the present study confirm that BAPN inhibits MBV-associated LOX.

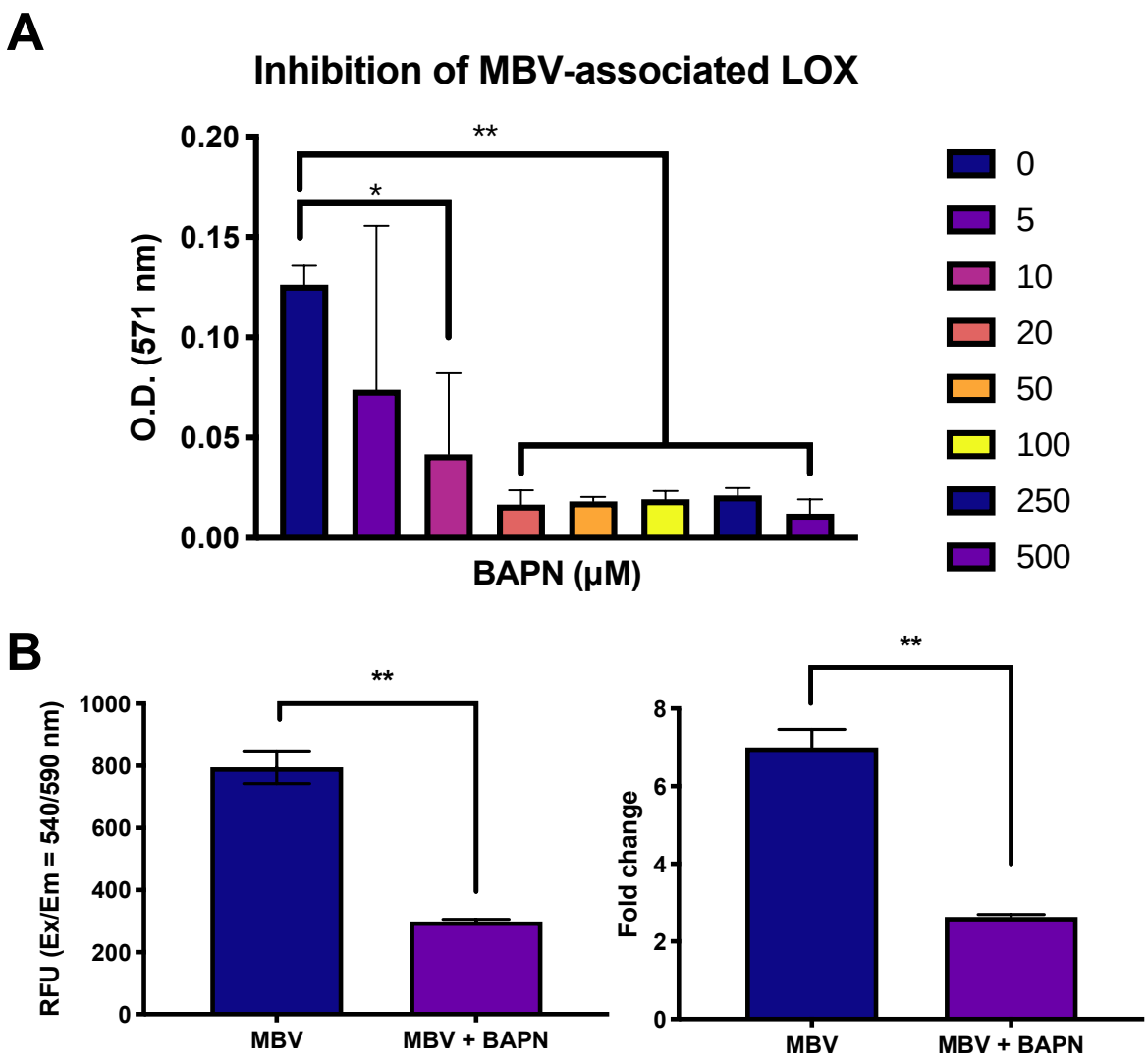


**Figure 13. Inhibition of MBV-associated LOX. (A)** MBV-associated LOX activity is significaintly inhibited with increasing concentrations of LOX inhibitor β-aminopropionitrile (BAPN). **(B)** MBV were treated with 50 μM of BAPN and show significant decrease (more than 2-fold) in LOX activity.

### 8.3.2 MBV-Associated LOX is Enzymatically Active

The enzymatic activity of MBV-associated LOX determined. Results showed a significant decrease in MBV-associated LOX activity when samples were treated with proteinase K, which removes MBV surface proteins, as measured by absorbance (O.D.) (Figure 14). Results suggest

that MBV samples treated with proteinase K may not contain as much enzymatic LOX compared to those non-treated. MBV-associated LOX is enzymatically active.

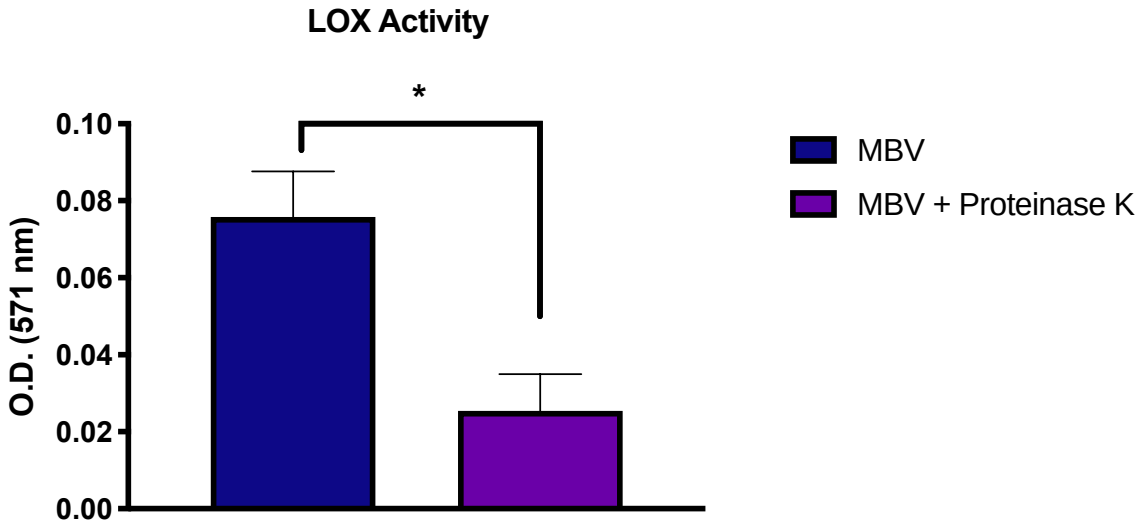


**Figure 14. MBV-associated LOX is enzymatically active.** Enzymatic activity of MBV-associated LOX is significantly decreased when treated with proteinase K.

*In vitro* studies demonstrated the effect of MBV-associated LOX on grown collagen constructs. By day 3 after plating, samples with MBV treatment showed constructs that were more contracted compared to those left untreated (Figure 15A). The collagen constructs were a linear construct. Further morphologic differences were observed at 7 days, where the MBV treated samples were defined and compact (opaquer in the middle), whereas the constructs not treated were loosely developed (Figure 15B). This suggests MBV-associated LOX has functional activity on collagen constructs during development *in vitro*. In addition, soluble collagen was quantified, and those constructs treated with MBV contain the least amount of soluble collagen, suggesting those non-treated are less developed (Figure 15C). Histomorphological stain by Masson's Trichrome showed presence of organized collagen (in blue) beginning to develop on the periphery of a 10 day collagen construct (Figure 15D). The fibrinogen used in plating the cells has likely

converted to fibrin, which stains in red by Masson's Trichrome. The presence of collagen in the constructs suggests primary tenocytes may be active in remodeling during construct development and synthesizing proteins to produce their own ECM.

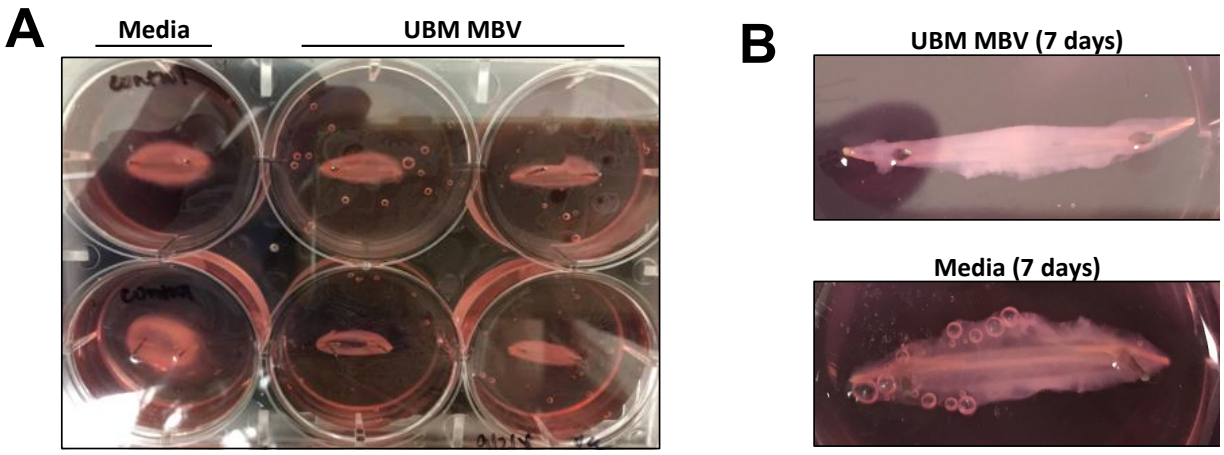
A
Media
UBM MBV
B
UBM MBV (7 days)
Media (7 days)

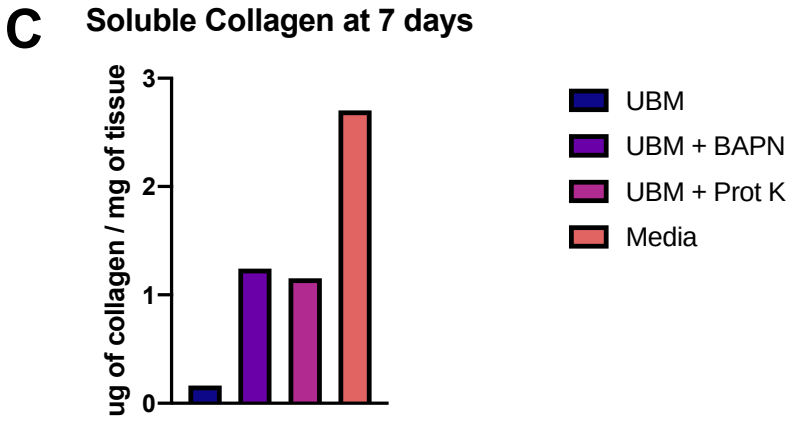
C
Soluble Collagen at 7 days
ug of collagen / mg of tissue
0
1
2
3
UBM
UBM + BAPN
UBM + Prot K
Media

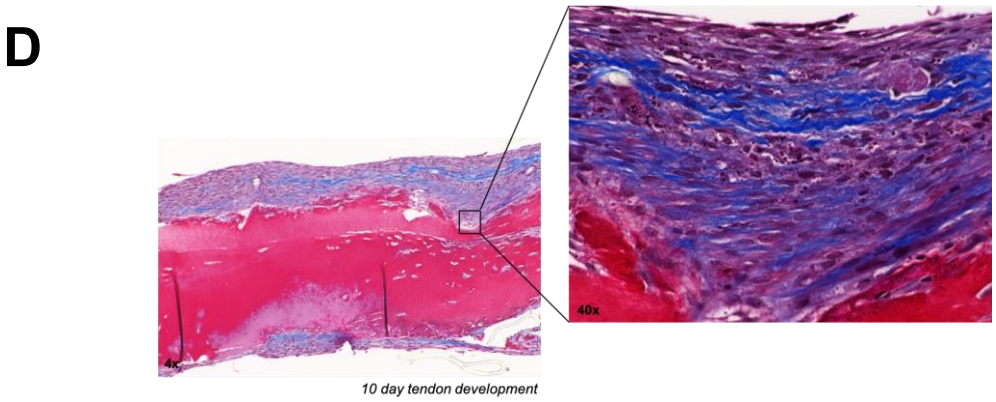
D
4x
40x
10 day tendon development

**Figure 15. (A)** MBV-associated LOX influenced the contraction of tendon constructs at day 3 of culture. **(B)** At 7 days, morphological difference between samples were clear. MBV treated samples were defined and compact whereas the tendons not treated were loosely developed. This suggests MBV-associated LOX has functional activity on in vitro collagen constructs during development. **(C)** Quantification of soluble collagen in collagen constructs. Soluble collagen was quantified where those treated with MBV contain the least amount of soluble collagen, suggesting those non-treated are less developed. **(D)** Histology of constructs composed of tenocytes and fibrinogen (red) and the development of organized collagen (in blue) as stained by Masson's Trichrome.

## 8.4 Discussion

The present study investigates the enzymatic activity of MBV-associated LOX. The role of LOX in the cross-linking of collagen and elastin has been studied in multiple tissues including skin, lung, and cardiovascular tissues [125-127] and LOX is essential for stabilization of the ECM [78, 128-130]. Studies have been limited in fully characterizing LOX and its mechanism due to its highly insoluble properties [58]. LOX activity is essential in the formation of covalent bonds between collagen molecules and overall stabilization of tissues. Herein, we show that MBV-associated LOX is enzymatically active and present on the surface of MBV in its pro-peptide form when isolated by enzymatic digestion using elastase.

LOX is synthesized in the cell cytoplasm and glycosylated before entering the Golgi apparatus, where it is processed to its inactive 52 kDa pro-peptide from [100]. This pro-peptide is secreted in to the extracellular space, where it is cleaved and activated by pro-collagen C proteinases (e.g. BMP-1, TLL1, TLL2 [132]) to the 32 kDa enzymatically active form of LOX. BMP-1 has been most commonly reported to be involved in the proteolytic processing of the LOX precursor to [77, 79, 100]. Although the post-translational processing of LOX was known to be

required for enzymatic activity, recent studies reveal otherwise. Specifically, Rosell-Garcia *et al*. reported that the 52 kDa pro-peptide from of LOX is fully capable of cross-linking collagen [133]. The authors also show that cleavage of LOX by BMP-1 or ADAMTS into a "mature" 32 kDa form does not increase LOX enzymatic activity, but rather, increases the ability of LOX to bind to collagen. In other words, LOX does not need to be cleaved in order to be enzymatically active and the proteolytic processing allows for increased binding to different specific substrates. Results presented in the present study confirm that the pro-peptide form of LOX is, in fact, enzymatically active.

Numerous studies have shown effective ECM-mediated repair and reconstruction of a variety of tissue types, including skeletal muscle, esophagus, dura mater, rotator cuff, and tendon, among others. The present study identified the presence of enzymatically active LOX associated with MBV, which provides new insights to procedures for isolating LOX. The present study also demonstrates MBV-associated LOX activity that affects the growth of collagen constructs *in vitro*. MBV-associated LOX may provide a feasible method to administer LOX as a therapy to enhance and strengthen tissues during overuse injuries and diseases such as tendinopathy. Although innate healing does occur during tendinopathy alongside degeneration, it results in a mechanically weaker tendon formed by scar tissue and collagen fibers with inferior integrity [137]. Therefore, there is a significant need for a treatment approach to tendinopathy that can be enacted before complete rupture to provide a mechanically strengthened and remodeled tissue. In addition to tendinopathy, MBV-associated LOX has therapeutic potential in cases where the tissue strength and integrity is weakened, such as large skin grafts, cutaneous wounds, cartilage and ligament repair, and pelvic organ prolapse to name a few [12]. MBV-associated LOX may be useful in administering

enzymatically active LOX that could support the crosslinking of collagen and enhance the strength of tissues.

The enzymatic activity of MBV-associated LOX was measured and demonstrated in an *in vitro* system for development of collagen constructs. The results show increased formation of constructs when treated with MBV. The constructs are made up of primary tenocytes and fibrinogen when they are plated. The evidence of collagen in more developed constructs (10 days) suggest that the primary tenocytes may be producing their own ECM during development. Further studies will determine the mechanical strength of the grown collagen constructs.

There are many limitations to this study. Although the presence of LOX is valid in our results, the use of recombinant LOX as a positive control is still required. The enzymatic of MBV-associated must be determined in samples isolated by the various solubilization methods as described in Chapter 5. In addition, because tenocytes respond to mechanostimulation and are sensitive to changes in the mechanical environment, the lack of mechanical stimulation in the *in vitro* system is a limitation. Collagen constructs need further investigation such as quantification of insoluble collagen, which suggests more cross-linking, and measurement of mechanical strength between the treated and non-treated groups. Future studies will be aimed at further facilitating the constructs developed by MBV-associated LOX *in vivo* for effective site-specific applications of tissue strengthening.

## 8.5 Conclusions

Results of the present study show that the 52 kDa form of LOX present on MBV is enzymatically active. The findings of this study are consistent with recent reports concerning the

proteolytic processing of LOX. Specifically, LOX does not require proteolytic cleavage to be enzymatically active. The proteolytic processing ultimately allows for increased binding to different specific substrates, such as collagen and elastin in the extracellular space. MBV-associated LOX promotes the development of collagen constructs *in vitro*, suggesting faster development of mature collagen fibrils. Results from the present study convey MBV-associated LOX influences microstructural arrangement of fibers in the matrix by enhancing LOX-mediated collagen cross-linking. Implications of this study may guide future *in vivo* studies that would implement MBV as a therapy to strengthen overused and injured tissues.

## 8.6 Acknowledgements

This study is in progress and acknowledges the contributions of Jordan Birkhimer, Serena Fisher, and Dr. Stephen F. Badylak. Jonathan Franks, Ming Sun, and Mara Sullivan at the Center for Biologic Imaging (CBI) at the University of Pittsburgh are greatly appreciated for their support.

# 9.0 Tendinopathy and its Degenerative Process: Potential Therapeutic Opportunity for MBV-Associated LOX

## 9.1 Introduction

Tendinopathy is one of the most common musculoskeletal diseases that affect both general and athletic populations. In the U.S., 33 million patients are affected annually by musculoskeletal injuries, of which 50% involve tendons and ligaments [138]. Tendinopathy is an overuse injury associated with thickening of the tendon along with chronic pain, inflammation, and tendon degeneration [139, 140]. Some of the symptoms of tendinopathy include discomfort, swelling, crepitation, and local tenderness. However, tendinopathy can be asymptomatic for a long time until it is very advanced. Symptoms vary from patient to patient with inconsistent nature of mild to moderate symptoms that often worsen before tendinopathy is diagnosed. Although the affected tendon may heal naturally overtime with the natural turnover of collagen fibers, the healed tendon is often comprised of a proportion of scar tissue and has inferior mechanical strength compared to native, uninjured tendon tissue [141].

Within the past 50 years, clinical research has guided breakthroughs in orthopedic surgery that focus on joint replacements and soft tissue repairs. However, the treatment options available for diseases such as tendinopathies and tendon ruptures often leaves both doctor and patient with frustrations due to poor healing of the tendon. Surgical techniques and treatment options for damaged or diseased tendons are still plagued by complications such as adhesions, loss of strength, and possible formation of painful adhesions. Current treatment options for tendinopathy include rest, eccentric-concentric exercises, nonsteroidal anti-inflammatory drugs (NSAIDS), and platelet

rich plasma (PRP) therapy. However, there is no consensus on the preferred therapeutic option due to lack of proven data and insufficient understanding of tendon healing pathophysiology. In the case of complete tendon rupture, as in Achilles tendon rupture, surgical repair of the tendon is typically required, but it is associated with high morbidity and the possibility of re-rupture of the tendon ([13]). Spontaneous complete rupture of a tendon is always due to chronic degenerative changes that have started long before the injury. **Therefore, there is a significant need for a treatment approach to tendinopathy that can be enacted before complete rupture to provide a mechanically strengthened and remodeled tissue.** The current gold standard for tendon reconstruction is tendon suturing, but there is a limit to the amount of tissue that can be harvested before compromising the donor site. An ideal graft for tendon engineering and repair would avoid donor site morbidity, promote functional constructive remodeling, and have positive histological and mechanical results after implantation; all of which have been achieved by utilizing decellularized ECM as a biologic scaffold. ECM bioscaffolds facilitate constructive tissue remodeling, a process by which the scaffold material degrades with an associated infiltration of cells from surrounding tissues and release of bioactive components including matrix-bound nanovesicles (MBV).

The present study utilizes a rat model of collagenase-induced Achilles tendinopathy for further determination of the effects of MBV-associated LOX on the tendon healing process. The purpose of this study was to assess whether intra-tendon delivery of an ECM-derived hydrogel or MBV would improve the quality and timing of healing in Achilles tendon repair using a rat collagenase-induced tendinopathy model. Understanding the degenerative process of tendinopathy allows for optimization of timing when MBV-associated LOX can be utilized for cross-linking collagen and enhancing the strength of the healed neotendon. Once a tendinopathy model was

established and confirmed, a preliminary study was performed for treating tendinopathy using hydrogels and MBV derived from ECM.

## 9.2 Materials and Methods

### 9.2.1 Experimental Design Overview

The goals of this study were to 1) establish and confirm a rat Achilles tendinopathy model and 2) investigate the use of ECM-derived hydrogels and MBV as a non-invasive approach to treat tendinopathy. The study design is shown in Figure 1. Forty-eight Sprague Dawley rats received collagenase injections in the Achilles tendon to induce tendinopathy. The degenerative process of the tendon was observed at 3, 7, 10, 14, 28, 56, 84, and 112 days and rats were divided for histomorphological assessment (n = 4 at each timepoint) and uniaxial mechanical testing (n = 2 at each timepoint) (Fig. 16, blue arrows). An additional study was performed where ECM hydrogels and MBV were used as treatments 14 days after the collagenase injection (Fig. 16, orange arrows). For this study, the effect of treatments was observed at 1 week and 6 weeks after treatments. Animals were divided for histomorphological assessment (n = 3 at each timepoint) and uniaxial mechanical testing (n = 3 at each timepoint).

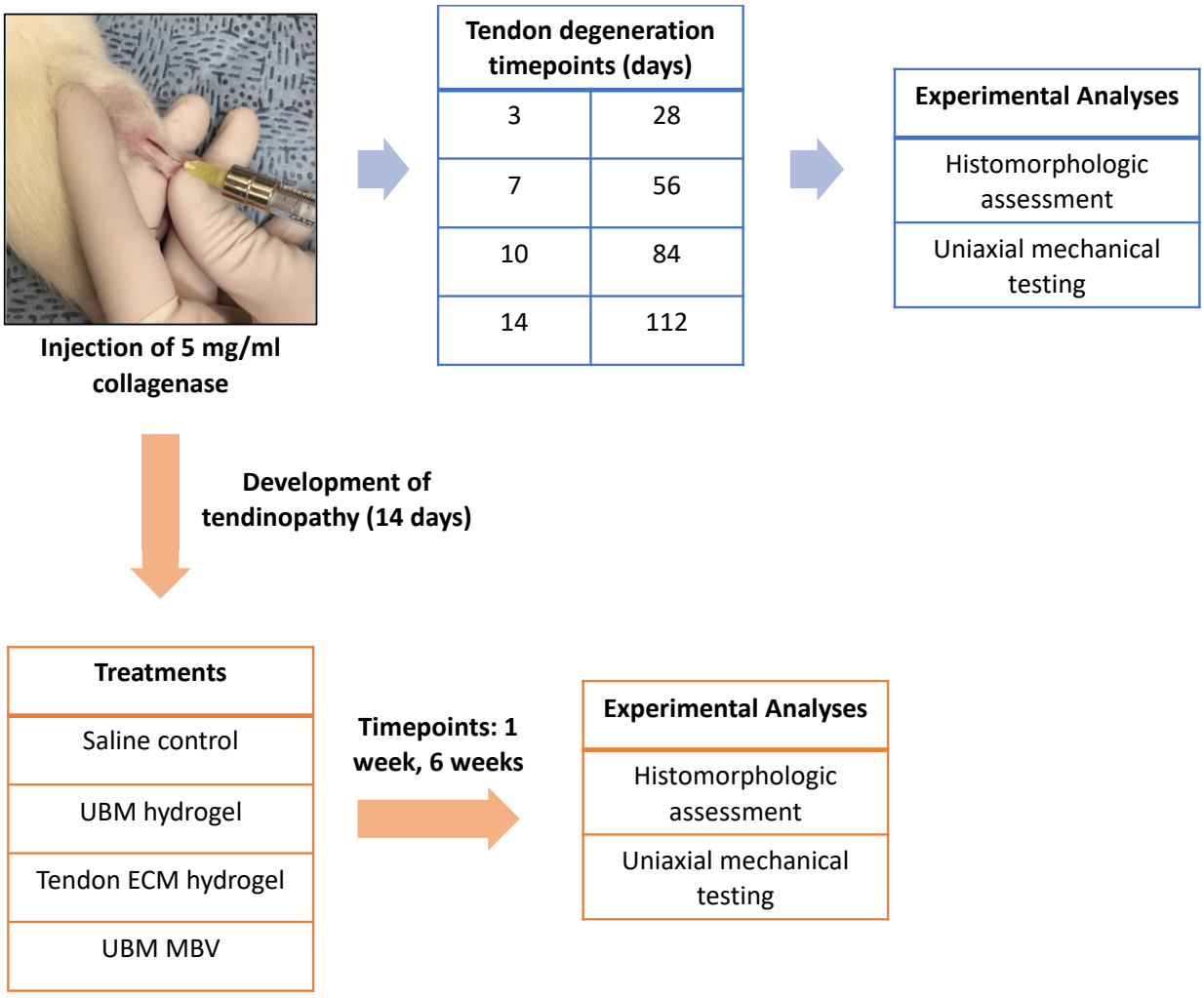


**Figure 16. Experimental Design Overview.** Tendinopathy is induced by injection of collagenase. The degeneration process of the tendon was observed at 3, 7, 10, 14, 28, 56, 84, and 112 days followed by histomophological assessment and uniaxial mechanical testing **(blue arrows)**. In another study, tendionpathy was treated using ECM-derived hydrogels and MBV after 14 days of collagenase injection **(orange arrows)**. Experimental analyses included histomopholic assessment and uniaxial mechanical testing at 1 week and 6 weeks post treatments.

### 9.2.2 Achilles Tendinopathy Rat Model

To induce tendinopathy, a single incision was made in the superficial tissues overlying the right Achilles tendon to expose the tendon tissue (Figure 17A) and 60 µl of 5 mg/ml collagenase

from *clostridium histolyticum* (Sigma, C0130) was injected (Figure 17B). The contralateral left tendons were left untreated to serve as controls. Tendon degeneration was observed for 3, 7, 10, 14, 28, 56, 84, and 112 days. Analyses included histomorphological assessment and uniaxial tensile mechanical testing of tendons.

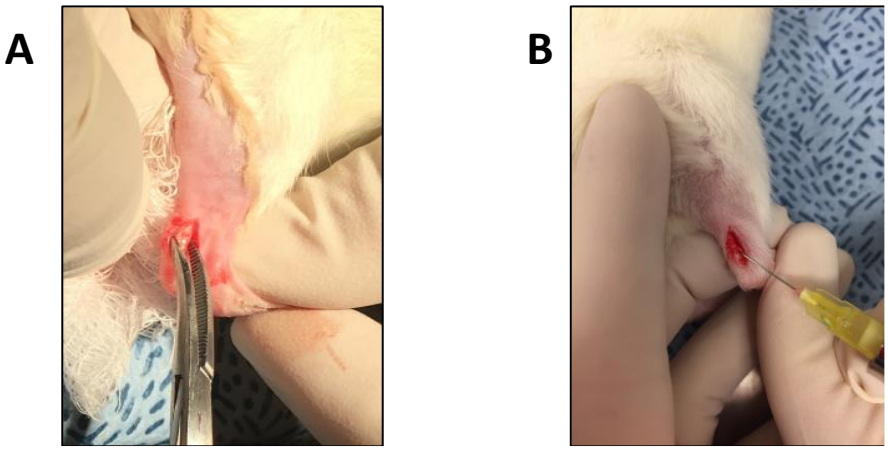


**Figure 17. Achilles tendinopathy rat model. (A)** A single incision is made to expose the tendon, grasped with curved hemostat in the figure. **(B)** 60 µl of 5 mg/mL of collagenase from *clostridium histolyticum* is injected into the tendon to induce tendinopathy

### 9.2.3 Preparation of Tendon ECM (tECM)

Achilles tendons were harvested from domestic pics (50-54 kg) and the tendon sheath and paratenon were removed. Tendons were cut into 1x1 cm pieces and pounded into approximately 2 mm thickness with a heavy mallet. The tissues were subjected to 5 freeze-thaw cycles in deionized water by using liquid nitrogen. Subsequently, tissues were washed 3 times in 4% Triton X-100 (Sigma Aldrich, St. Louis, MO) on an orbital shaker for 20 minutes at room temperature, and incubated in deionized water overnight at 37°C on an orbital shaker at 300 rpm. After the incubation, tendons were washed in PBS (Fisher Scientific) for 30 minutes 4 times, 0.1% peracetic acid (Rochester Midland Corp., Rochester, NY) in 4% ethanol for 2 hours, PBS for 15 minutes,

Type I H2O for 15 minutes 2 times, and a final PBS wash for 15 minutes. All washes were performed at room temperature with agitation on an orbital shaker at 300 rpm unless otherwise stated. Finally, tissues were frozen and lyophilized for future experiments. Tendon ECM (tECM) met stringent requirements for sufficient decellularization; specifically, no visible intact nuclei by DAPI and hematoxylin and eosin (H&E) staining, remnant DNA concentration less than 50 ng/mg total dry weight of ECM, and DNA fragment length less than 300 base pairs.

### 9.2.4 Preparation of ECM Hydrogels

Urinary bladder matrix (UBM) [108] and tendon ECM (tECM) were prepared as described previously. ECM hydrogels were then prepared using lyophilized and powdered UBM and tECM as described previously [142]. Briefly, powdered ECM (10 mg/ml) was digested with pepsin in 0.01 M HCl at room temperature with a constant stir for 48 hours, and stored at -20°C. Hydrogels were thawed right before use as treatments, and neutralized (pH = 7.4) with 0.1 M NaOH and diluted to the final concentration of 8 mg/ml.

### 9.2.5 Isolation of MBV

Matrix-bound nanovesicles (MBV) were isolated from UBM as described previously [41]. Briefly, lyophilized and powdered UBM ECM (10 mg dry weight) was enzymatically digested by collagenase (0.1 mg/ml) in buffer [50 mM Tris (pH = 8), 5 mM $CaCl_2$, 200 mM NaCl] for 24 hours at room temperature. Enzymatically digested ECM was then subjected to successive centrifugation at 10,000 xg for 30 min and the supernatant was passed through a a 0.22 μm filter (Millipore). The clarified supernatant was then centrifuged at 100,000 xg (Beckman Coulter Optima L-90K

Ultracentrifuge) at 4°C for 70 min. The MBV pellet was then resuspended in 100 μl of 1X sterile PBS.

### 9.2.6 Treatment of Achilles Tendinopathy

Fourteen days post-injection of collagenase, tendons were treated with either UBM hydrogel, tECM hydrogel, MBV isolated from UBM, or saline as a control. Neutralized hydrogels and MBV were kept on ice. 50 μl of each respective treatment was then injected directly into the injured tendon.

### 9.2.7 Necropsy

Animals were sacrificed by $CO_2$ inhalation and cervical dislocation at their pre-determined timepoint for both studies. Samples that were harvested which included the calcaneus, Achilles tendon, and gastrocnemius muscle tissues. Samples for histology were fixed in 10% neutral buffered formalin (NBF) while samples for mechanical testing were wrapped in gauze soaked in PBS and kept on ice. Uniaxial tensile mechanical testing was performed immediately after tissue harvest.

Samples for histology were fixed in NBF for at least 7 days. Samples were then embedded in paraffin, cut into 5 μm longitudinal sections, and mounted onto glass slides for H&E staining.

### 9.2.8 Uniaxial Tensile Mechanical Testing

Immediately after tissue harvest, uniaxial tensile mechanical testing was performed using the Instron 3340 series mechanical testing systems (MTS® Eden Prairie, MN). Harvested tendons were clamped at proximal and distal ends with serrated-jaw metal grips (Figure 18). Sandpaper was placed between the tissue and grips to prevent slippage. The resulting load was measured using a 100 N load cell. A uniaxial tensile ramp-to-failure was applied at a strain rate of 0.1%/s and the resultant load was recorded. Samples were tested to failure, which was indicated by complete tear of tendons. The stress-strain curve was analyzed to determine ultimate peak stress.

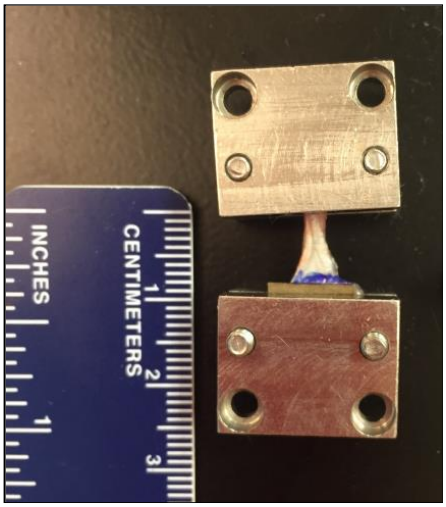


**Figure 18. Harvested tendons were held at proximal and distal ends 1 cm apart by serrated-jaw metal grips. Sandpaper was placed between the tissue and grips to prevent slippage.**

### 9.2.9 Scanning Electron Microscopy (SEM)

Native porcine Achilles tendons were processed for SEM. Briefly, samples were harvested and rinsed in 1X PBS before fixing in 2.5% glutaraldehyde in 0.1 M PBS (pH = 7.4) for 10 minutes.

The tissues were cut into small blocks (8 $mm^3$) and were washed thoroughly in three changes of 0.1 M PBS for 15 minutes each. Samples were dehydrated in a graded serious of ethanol in PBS including 30%, 50%, 70%, 90% for 15 minutes each. Samples were than dehydrated in 100% for 15 minutes three times. Samples were mounted on sputter coated with 3.5 nm of gold/palladium alloy.

### 9.2.10 Statistical Analysis

A two-way ANOVA and Fisher's least significant difference (LSD) post-hoc analysis was used to compare the independent variables treatment and timepoints. For statistical analysis, significance was set at $p < 0.05$. Error bars represent standard deviation.

## 9.3 Results

### 9.3.1 Histological Assessment of Degenerating Tendons

Achilles tendons were evaluated by histomorphological assessment. Representative images are shown of tendon tissue sections stained with H&E at each timepoint (Figure 19A). At 3 days, robust inflammatory cellular infiltration is present, with a mixture of neutrophils and mononuclear cells. At 7 days, there is more dense cellular infiltration compared to 2 days, with large nuclear bundles and areas of degeneration. At 10 days, there is a decrease in mononuclear cells and regression of vascularity. At 14 days, there are a mix of aligned and not aligned fibroblast cells with almost no inflammatory cells present. At 28 days, there are areas of regenerating tendon with

increased cellularity. There appears to be new matrix production and proliferation of fibroblasts. At 56 days, there are similar histologic findings with signs of a healing tendon and aligned fibroblasts indicating maturation. At 84 days, there were signs of chondrogenesis without the presence of inflammatory cells. Finally, at 112 days, there are highly aligned mature collagen fibers but a lack of uniform cell alignment. Gross morphology of the tendons is shown in Figure 19B, where tendons with collagenase-induced degeneration show relative thickening and irregularity over the course of the disease process.

**A**

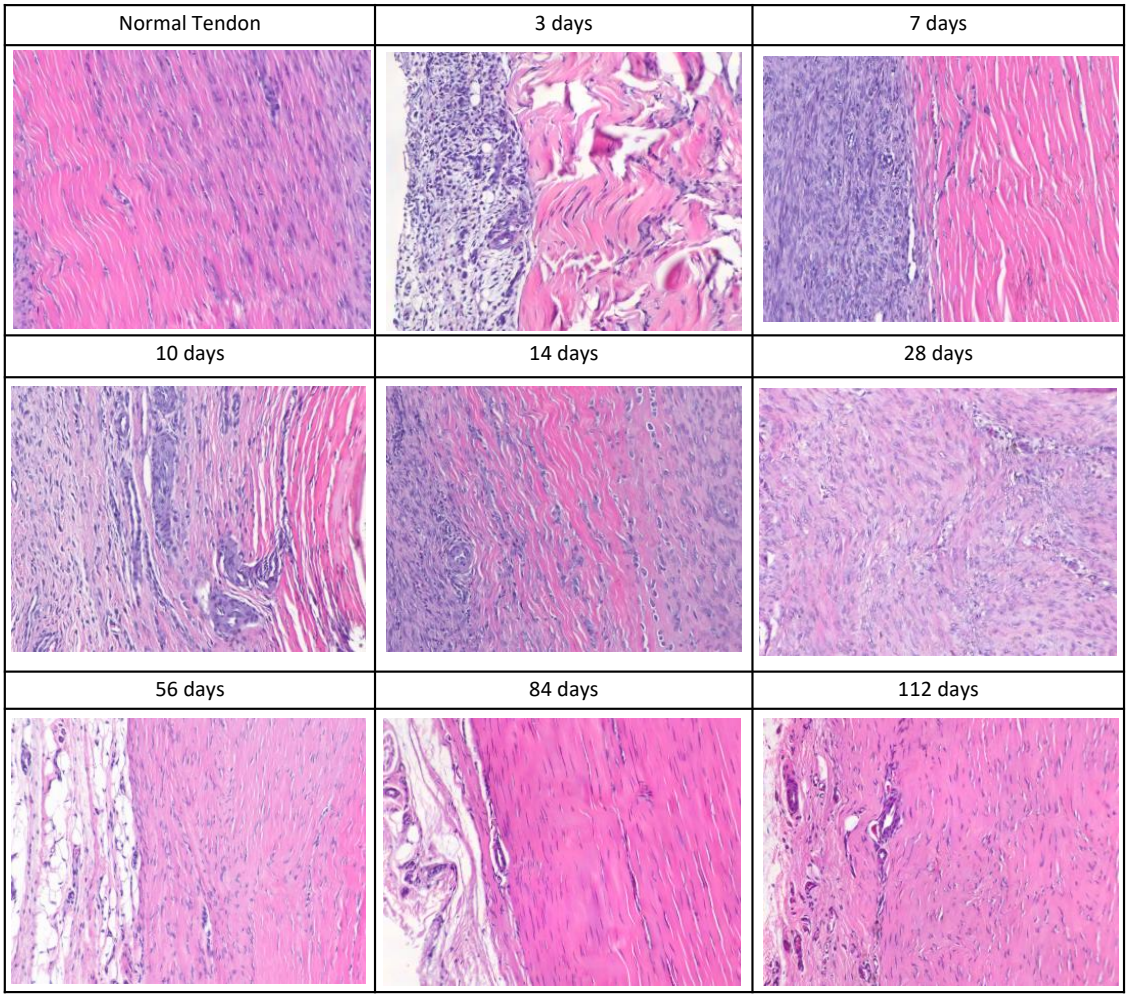
Normal Tendon
3 days
7 days
10 days
14 days
28 days
56 days
84 days
112 days

**B**

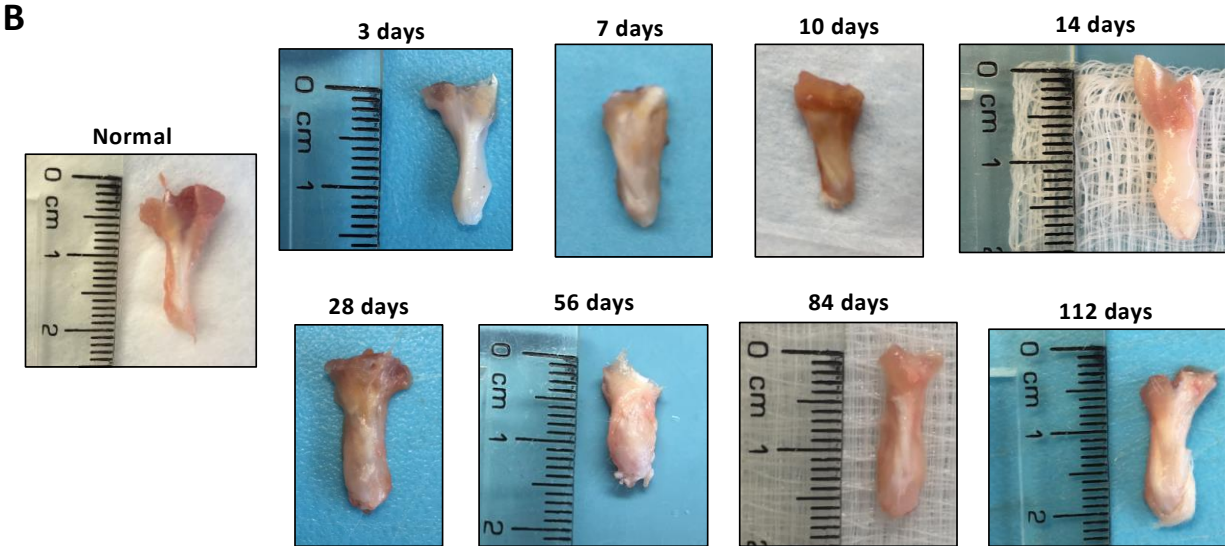
Normal
3 days
7 days
10 days
14 days
28 days
56 days
84 days
112 days

**Figure 19. Histomorphological assessment and gross images of tendons.**

### 9.3.2 Uniaxial Tensile Strength of Degenerating Tendons

The mechanical strength of tendons injected with collagenase were not statistically significant compared to normal tendons. Although few tendons exhibit high values of peak stress until ultimate failure, the individual datapoints were not reproducible for statistical significance (Figure 20). Tendons harvested at 56 days had experimental errors of tissue slippage from the metal grips, resulting in damage to the tissues that prevented further data collection on these samples.

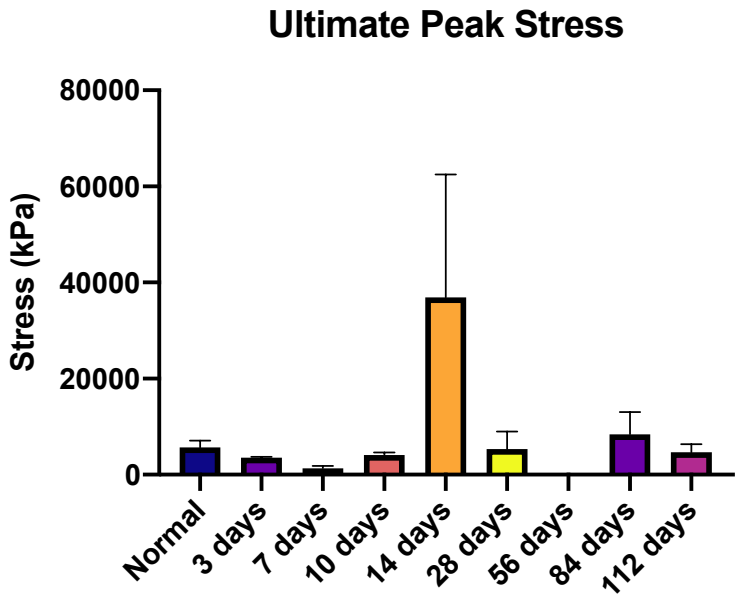


**Figure 20. Uniaxial tensile mechanical testing of tendons from collagenase-induced tendinopathy.**

### 9.3.3 Achilles tendinopathy is Induced at 14 Days Post-Collagenase Injection

Collagenase was injected to induce tendinopathy in rat Achilles tendons. Histological assessment verified an inducible tendinopathy model that compares favorably to tendinopathy in humans, which is characterized by cellular infiltration and inflammation in the tendon tissue (Figure 21).

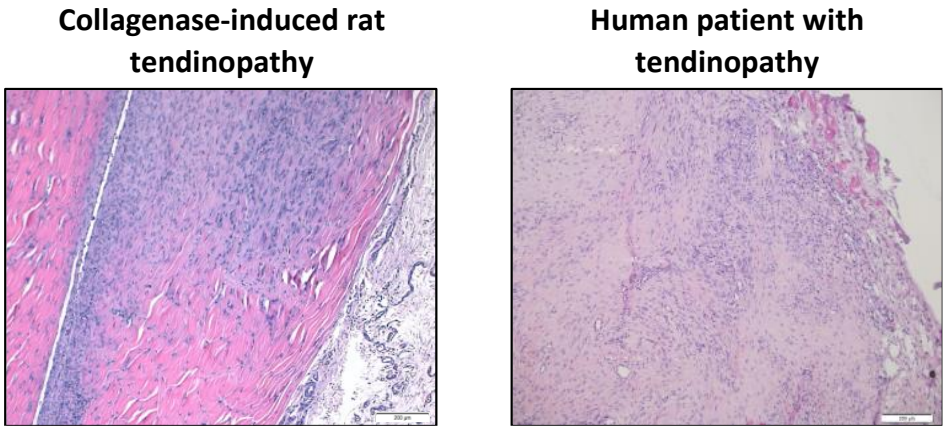


**Figure 21. Tendinopathy induced in rat model.** At 14 days, histology verified an inducible tendinopathy model that compares favorably to tendinopathy in humans that is characterized by cellular infiltration and inflammation in the tendon.

### 9.3.4 ECM Hydrogels and MBV Affect Achilles Tendinopathy

Treatments including UBM hydrogel, tECM hydrogel, MBV, and saline (control) were applied to injured tendons after 14 days of induced tendinopathy. At the 1 week timepoint, histomorphological assessment by H&E staining showed cellular infiltration and neovascularization at the level expected for healing response in normally poorly vascularized tissues such as the tendon [143]. Cellular response was greater at the 1 week timepoint compared to 6 weeks (Figure 22). At the 6 week time point, the relative healing response of the tendon is

most notable in the ECM hydrogel and MBV treatment groups compared to the saline (control) group.

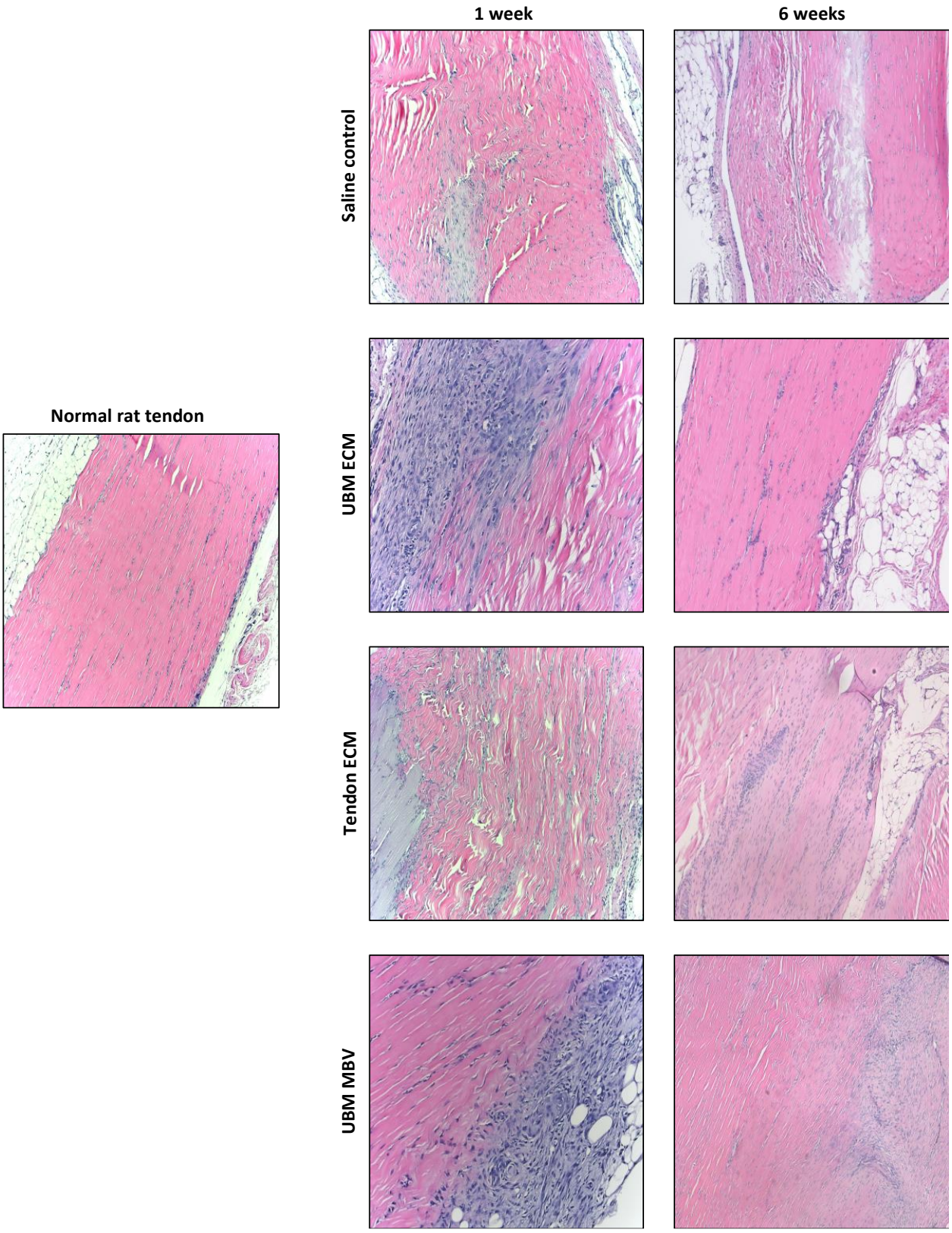
1 week
6 weeks
Saline control
UBM ECM
Tendon ECM
UBM MBV
Normal rat tendon

**Figure 22. Tendons were harvested and processed for histology by hematoxylin and eosin (H&E) staining.** Evidence of cellular infiltration and neovascularization corresponds to the healing response in normally poorly vascularized tissues such as the tendon. At the 1 week time point, there is a more robust cellular response than at 6 weeks. At the 6 week time point, the relative healing response is most notable in the ECM treatment and MBV groups compared to the saline (control) group.

Results from uniaxial mechanical tensile testing on treated tendons showed promising trends between the treatment groups (Figure 23). Although the data was not statistically significant, peak stress values between the treatment groups suggest there was an effect on the tendon remodeling process.

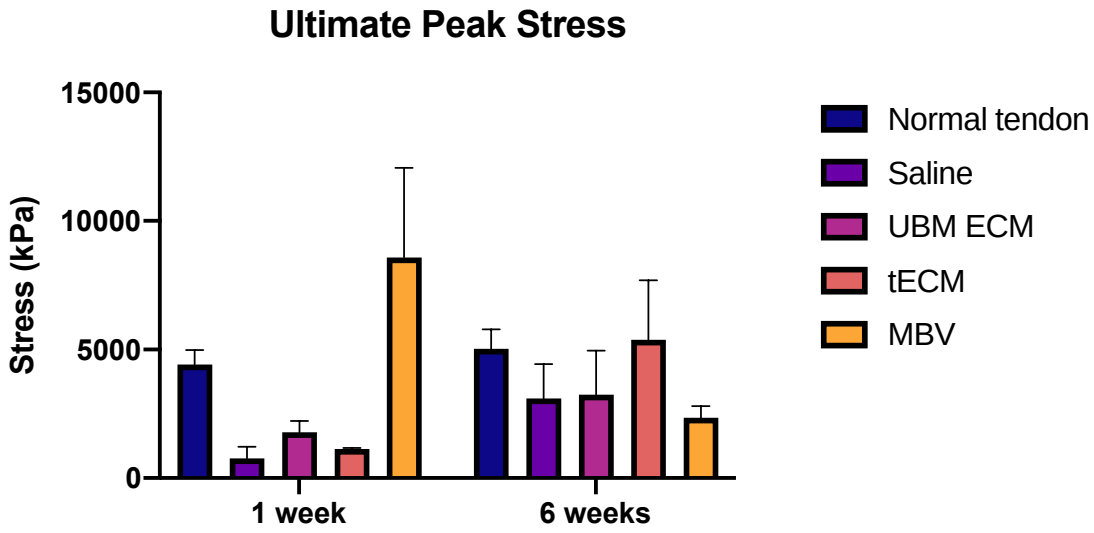


**Figure 23. Comparison of mean peak stress values of rat tendons at 1 week and 6 weeks with standard error.** Though results are not statistically significant, there are promising trends between the treatment groups with respect to the peak stress values as the tendon was remodeling.

## 9.4 Discussion

The term “tendinopathy” is used as an umbrella term to describe a painful condition of the tendon [141]. Although “tendinopathy” can describe any diseased or disordered tendon tissue, it includes complex processes that involve changes in biological structure, composition, and mechanics. In tendinopathic tissues , there are degenerative changes in the extracellular matrix (ECM) [144]. In the presence of tendinopathy, the healing response is defective due to accumulated micro-injuries from overuse and the tendon tissue is unable to repair effectively. The present study investigates the effect of ECM-derived hydrogels and matrix-bound nanovesicles (MBV) as treatments in a rat Achilles tendinopathy model. These treatments provide a novel, non-invasive regenerative medicine-based approach to treat an acute Achilles tendon injury by using an injectable ECM-based material. Hydrogels have been gaining popularity as a delivery vehicle of cells, growth factors, and other bioactive molecules [145]. In addition, MBV have been described as bioactive components of ECM and have been shown to recapitulate the biologic effects of the parent ECM [41].

Although the Achilles tendon is the largest and strongest tendinous tissue in the body, it is subjected to substantial loads of that frequently cause microtears and overuse injuries. Overuse injuries have been a perpetual orthopedic problem and the recurrence of these injuries begins during exertion as the tendon is subjected to repetitive tissue microtrauma [146]. Repetitive microtrauma results in microscopic injuries that are notoriously known to not be diagnosed until the injuries have worsened. Repetitive use and activity may eventually lead to cumulative microtrauma that weakens collagen cross-linking, non-collagenous matrix, and vascular elements of the tendon tissue [147]. Tendon pathology is often the result of overuse and strain that causes

an accumulation of the aforementioned tendon microtears without sufficient time for complete healing and matrix turnover [139, 148].

The field of orthopaedic surgery has experienced incredible advancements since its inception from historical wartimes to progressive developments in the last 50 years. Clinical research has guided significant breakthroughs in orthopedic surgeries that focus on joint replacements and soft tissue repairs [149, 150]. However, the treatment options available for diseases such as tendinopathies and tendon ruptures still require invasive surgeries that often result in patient discomfort and restricted foot movement. Despite advancements in orthopedic surgical techniques and technologies, the incomplete knowledge and understanding of the mechanisms steering tendinopathy prevents the development of better therapies. One of treatment strategies for musculoskeletal injuries has been the administration of platelet rich plasma (PRP) to stimulate regeneration of the injured tissue [151-153]. Despite published studies reporting success with PRP treatment, the data is not sufficient to consider it as the treatment of choice. PRP treatment also has batch-to-batch variability and concentration variation. Additionally, it requires blood from the patient, which could ideally be avoided with alternate therapies. Furhter, the potential of PRP depends on the donor, so obtaining blood from older patients for use as PRP is questionable. Ultimately, the current available treatment options have the disadvantage of providing insufficient repair of the injured tendon. Even with PRP and/or stem cells, the enhancement of healing is not sufficient, and the field of orthopedic surgery needs more effective treatment options. Thus, there is a need for a non-invasive approach for treating tendinopathy that promotes the regenerative process of the injured tendon. An ECM-based material such as bioscaffold or MBV would be a great treatment option.

Acellular ECM biologic scaffolds have been used to provide a compatible and instructive template for endogenous cell infiltration and differentiation that provide a supportive microenvironment that promotes a constructive remodeling response. In addition, hydrogels derived from components of the ECM (e.g., collagen, hyaluronic acid, and elastin) have been implemented in numerous studies and clinical applications. Herein, the use of hydrogels derived from decellularized mammalian tissue is investigated to implement the advantages of using ECM as a bioscaffold in regenerative medicine. ECM hydrogels have the advantage of retaining the full biochemical complexity of native tissue as compared to hydrogels composed of only individual ECM components. Hydrogels derived from UBM, which contain the milieu of bioactive ECM components, have been shown to retain the inherent bioactivity of the native matrix with the ability to promote constructive remodeling in heterologous tissue applications [142, 154, 155].

By augmenting the natural healing process of an injured tissue, ECM-derived materials such as hydrogels and MBV provide an inductive template that recapitulate the appropriate microenvironmental niche for host cell infiltration and differentiation. Although the results from the present study do not reach statistical significance, they provide important insights into the therapeutic potential of ECM to reinforce the regenerative process of the injured tendons as they heal.

## 9.5 Conclusions and Limitations

Herein, the therapeutic effect of ECM-derived hydrogels and MBV isolated from ECM were studied in an *in vivo* rat Achilles tendinopathy model. The results of this study show that treatment of a collagenase-induced tendinopathy with ECM hydrogel and MBV in a rat model

induces a robust healing response, including cellular infiltration and neovascularization, when compared treated with saline alone. The ECM hydrogel and MBV treatments provide a potential non-invasive method promoting restoration of tendon mechanical strength and collagen cross-linking. Future work will include isolated PRP as an experimental group in a head-to-head trial with currently available treatment options.

There were multiple limitations to the study. The uniaxial mechanical tensile testing of rat Achilles tendons included challenges with tissue mounting and reliable fixation to the metal grips at each end of the tendon tissue. Tendons often slipped from the grips, which ultimately impacted the quality of the tissues being tested. In addition, MBV were isolated by enzymatic digestion of collagenase. While the isolation process of MBV aims to eliminate all collagenase used the digesting the ECM, any contamination of MBV with residual collagenase could impact and potentially negate the positive impacts of MBV on tendon healing and strengthening. Future work will include MBV isolated by elastase digestion, where lysyl oxidase (LOX) would remain associated to the surface of MBV to regulate cross-linking of collagen in the tissue. The therapeutic potential of applying MBV-associated LOX is overall an attractive tool for enhancing the biomechanical properties of injured tissue.

## 9.6 Acknowledgements

This study acknowledges the contributions by Dr. Urszula Zdanowicz, Scott Johnson, and Dr. Stephen F. Badylak. In addition, the assistance of Lori Walton in preparing the histological sections is gratefully acknowledged.

# 10.0 Dissertation Summary and Future Perspectives

The work presented in this dissertation identified and investigated an extracellular source of lysyl oxidase (LOX), specifically associated to matrix-bound nanovesicles (MBV). The central hypothesis addressed in this work is that MBV are an extracellular source of LOX and can be used to implement the enzymatic function of LOX in regulation of collagen and the ECM. Major findings for each specific aim are summarized below.

**Specific Aim 1:** Identification and characterization of LOX isoforms in MBV isolated from ECM bioscaffolds

Summary of major findings: MBV-associated LOX was isolated from urinary bladder matrix ECM (UBM-ECM), small intestinal submucosa ECM (SIS-ECM), dermal ECM (dECM), and tendon ECM (tECM). For this work, the process of tECM preparation was developed and optimized. The effect of different ECM solubilization methods prior to isolating MBV by ultracentrifugation was investigated. These solubilization methods included enzymatic digestion with elastase and collagenase or incubation in a high salt (NaCl) solution. MBV-associated LOX was identified to be present on the surface of MBV when elastase was used to enzymatically digest ECM. These results persisted in vesicles that were isolated from native porcine tissues that were not processed by decellularization. When solubilization was carried out with collagenase or NaCl solution, MBV-associated LOX was degraded or eluted off the vesicles. These results suggest that MBV-associated LOX is bound to other lipid-membrane proteins, which were either disrupted by the non-specific activity of collagenase or dissociated by the high NaCl solution.

In our previous studies, enzymatic digestion of ECM by collagenase was utilized to digest the ECM before isolating MBV by ultracentrifugation [41, 56]. The findings of Specific Aim 1 provide insights on how MBV are firmly embedded in the ECM and how different solubilization methods of ECM can affect the presence MBV surface proteins like LOX.

Future perspectives: LOX plays an integral role in ECM remodeling and ultimately determines the extent of intermolecular cross-linking between collagens and elastin. The presence of LOX associated to the surface of MBV reveals more information about how MBV are integrated within the matrix and how they function differently than extracellular vesicles found in biological fluids. The challenges associated with isolation and purification of LOX have limited studies investigating LOX and its specific mechanisms in normal physiology, fibrosis, and cancer metastasis. The discovery of LOX as a surface protein of MBV provides new insights to a possible alternative pathway LOX is secreted into the extracellular space.

The varying amount of MBV-associated LOX identified in various ECM sources in varying amounts suggests the functional role LOX plays in specific tissues. In addition, successful isolation of MBV directly from native porcine tissues is evidence that decellularization of tissues is not required prior to the isolation of MBV. Although the decellularization process for ECM biologic scaffolds is important to avoid detrimental immune responses, it is plausible that decellularization of source tissues may not be required prior to isolation of MBV that is ultimately intended for therapeutic purposes. This would greatly streamline the process of isolating MBV, potentially improving the time and cost associated with implementing MBV-associated LOX in clinical applications. Future work should determine if MBV isolated from native tissues has the same biologic effect compared to MBV isolated from decellularized ECM.

For additional future work, the effects of other solubilization and isolation methods to isolate MBV-associated LOX should be investigated. For example, solubilization of ECM with pepsin and isolation of MBV-associated LOX size-exclusion chromatography (SEC) have not been explored. Pepsin has been utilized to solubilize ECM for preparation of hydrogels [156], and has been shown to partially digest the ECM compared to proteinase K [41]. This would offer a more specific or gentle method of solubilization, potentially resulting in the retention of more MBV-associated LOX or other MBV surface proteins. The use of SEC to isolate MBV may also provide higher yield and purity of vesicles compared to those isolated by ultracentrifugation [157]. These isolation methods may affect the presence of other LOX isoforms associated to MBV, which could be explored by Western blot analysis or furthered by liquid chromatography-tandem mass spectrometry (LC/MS) for global proteomics.

**Specific Aim 2:** Determine the biologic activity of MBV-associated LOX

Summary of major findings: MBV-associated LOX was identified in its 52 kDa pro-peptide form when isolated by using elastase digestion before ultracentrifugation. Although LOX is previously known to require extracellular processing by pro-collagen proteinases for enzymatic activity, MBV-associated LOX is enzymatically active. The enzymatic activity of MBV-associated LOX is inhibited by treatment with BAPN. In addition, MBV-associated LOX activity significantly decreases when treated with proteinase K. The mechanism of LOX's association to the MBV surface was suggested by the distinctly different protein signatures of MBV-associated LOX with and without treatment of proteinase K. Specifically, the absence of LOX on the surface of MBV following proteinase K treatment suggests a possible membrane-bound protein partner.

However, more work is needed to confirm that proteinase K did not simply disrupt LOX that was interacting directly with the MBV lipid membrane.

Future perspectives: Of the LOX isoforms, LOX and LOXL1 have similar pro-domains that require cleavage for their activation. However, recent studies have reported that the proteolytic processing of LOX allows for substrate specificity and binding for cross-linking [133]. This information may be relevant to MBV-associated LOX, which in the present dissertation was determined to be enzymatically active. The presence of LOX bound to the surface of MBV suggests an alternative pathway of LOX secretion, where the pro-peptide LOX piggybacks along with MBV into the extracellular space. Then, proteolytic processing may occur by pro-collagen proteinases to cleave MBV-associated LOX for proteolytic processing and specific substrate binding.

There is evidence in literature identifying ECM proteins interacting with LOX that may be important in the extracellular proteolytic processing of the pro-peptide LOX. Fogelgren *et al.* reported cellular fibronectin, as well as tropoelastin and collagen, interacting with LOX in glutathione S-transferase pull-down and solid phase binding assays [78]. Maruhashi *et al.* reported the interaction of periostin with BMP-1, which enhanced the deposition of BMP-1 in the ECM, and resulted in proteolytic cleavage of LOX [79]. Sasaki *et al.* reported that the proteolytic processing of LOX is decreased in fibulin-4 deficient osteoblasts and rescued when recombinant fibulin-4 was added, suggesting the importance of fibulin-4 for LOX's enzymatic role to cross-link collagen and elastin [158]. Thrombospondin-1 has also been identified to bind to collagen and inhibit the processing of LOX by BMP-1 [159]. The evidence of LOX's interaction with various substrates maybe applicable to MBV-associated LOX and its biological role in the matrix. It is plausible that there are even subpopulations of MBV that do not have LOX associated to its surface.

LOX that is associated to MBV may represent a directed mechanism in which the cell releases MBV-associated LOX for cross-linking of specific substrates in the extracellular space.

Although studies provide insight to extracellular proteins interacting with LOX, the lipid-membrane associated partners of LOX bound to the surface of MBV remains unknown. MBV remain structurally intact even after the decellularization process and isolation from ECM [41]. Thus, the identified LOX protein with MBV is clearly associated to the outer surface rather than the lumen of MBV. The findings of Specific Aim 2 may provide better understanding to MBV's constituent phospholipid profiles, which has been shown to be distinctly different to extracellular vesicles in biologic fluids (i.e., exosomes) [53]. This has important implications for the use of MBV as a therapeutic similar to the use of exosomes for diagnostic purposes [160].

Future experiments should determine the enzymatic activity of MBV-associated LOX in MBV isolated by various solubilization methods as described in Chapter 5. Determining if the proteolytically processed MBV-associated LOX is enzymatically active would provide further insight into the enzymatic mechanism of LOX. In addition, the effect of specific substrates binding with MBV-associated LOX should be investigated. It is plausible that the enzymatic activity of MBV-associated LOX is increased when bound to fibronectin. Alternatively, a bound substrate may serve to protect the pro-peptide of LOX and decreases its activity. Future work is needed to further investigate the biologic role of MBV-associated LOX.

**Specific Aim 3:** Determine the effect of MBV isolated ECM on the mechanical properties of a grown collagen construct *in vitro* by measurement of mechanical strength

Summary of major findings: MBV-associated LOX isolated from UBM showed biological and functional activity on collagen constructs during development i*n vitro*. The isolation of

primary tenocytes from rat tails and the collagen construct *in vitro* system were optimized for the study. Constructs that were treated with MBV showed clear morphological differences compared to those left untreated. Specifically, MBV treated constructs were defined and compact whereas those not treated were loosely developed. In addition, the development of constructs was enhanced by the treatment of MBV and constructs contracted more quickly in a linear form. Histologically, treated constructs grown out to 10 days showed the development of collagen in the periphery of the constructs. This suggests MBV-associated LOX has functional activity on *in vitro* tendon mimics during development.

Future perspectives: LOX has been identified to play important roles during tissue development and organogenesis [161, 162]. The ability of LOX to modulate the cross-linking of collagen and subsequent deposition of the ECM gives great potential for MBV-associated LOX to have such effects. MBV-associated LOX has biologic effects on the development of collagen constructs *in vitro,* suggesting its ability to modulate the main constituents of ECM. Biomaterials composed of ECM have successfully been used as surgical meshes, powders, and hydrogels in a variety of surgical applications for tissue engineering and regeneration. Many types of ECM are also FDA-approved and can be preserved to be used as an "off-the-self" product [163, 164].

UBM-ECM is commercially available (MicroMatrix®, ACell) and one of the main ECM types that was used to investigate MBV-associated LOX in the present dissertation. With further testing and investigation, MBV-associated LOX has great potential to become a readily available commercialized product to strengthen tissues. Future experiments would include additional *in vitro* studies that would be used for further analyses. Such analyses would include MBV treated with LOX inhibitor BAPN, MBV isolated from various ECM bioscaffolds, and MBV isolated by various methods of solubilizing ECM. Further understanding of the development of collagen

constructs can be investigated by the use of qRT-PCR characterization of the expression of genes that are associated with the ECM (e.g., collagen, elastin, fibrin, MMPs). In addition, testing the mechanical strength of the grown tendon constructs would be performed.

An ideal collagen construct would have an increased mechanical strength and collagen fibril organization when MBV-associated LOX is administered. Further, the deposition of collagen present in the construct should be enhanced in the presence of MBV-associated LOX. These characteristics of an ideal construct may be better achieved *in vitro* if grown in an environment where constant or intermittent mechanical stimulation is included. Studies have shown the importance of mechanical cues and mechanical loading during development of embryonic tendons [6, 165]. The addition of mechanical stimulation may enhance the functional properties of the developing construct that may be implemented alongside treatment with MBV-associated LOX.

The findings of Specific Aim 3 provide insight to the effects MBV-associated LOX on *in vitro* development of collagen constructs. In order to further understand the role of MBV-associated LOX, efforts should focus on how MBV-associated LOX influences cross-linking of collagen and how this cross-linking affects the strength and mechanical properties of ECM. The work in the present dissertation and future studies can together provide a functional application for MBV-associated LOX that can be implemented in tissue engineering design of biologics to regulate cross-linking of collagen.

## Bibliography


[1] H. Lodish, A. Berk, C.A. Kaiser, M. Krieger, M.P. Scott, A. Bretscher, H. Ploegh, P. Matsudaira, Molecular cell biology, Macmillan2008.

[2] D.F. Holmes, Y. Lu, T. Starborg, K.E. Kadler, Collagen fibril assembly and function, Current topics in developmental biology, Elsevier2018, pp. 107-142.

[3] D.E. Birk, P. Brückner, Collagens, Suprastructures, and Collagen Fibril Assembly, in: R.P. Mecham (Ed.), The Extracellular Matrix: an Overview, Springer Berlin Heidelberg, Berlin, Heidelberg, 2011, pp. 77-115.

[4] D. Hulmes, Collagen diversity, synthesis and assembly, Collagen, Springer2008, pp. 15-47.

[5] C. Bonnans, J. Chou, Z. Werb, Remodelling the extracellular matrix in development and disease, Nature reviews Molecular cell biology 15(12) (2014) 786-801.

[6] J.E. Marturano, J.D. Arena, Z.A. Schiller, I. Georgakoudi, C.K. Kuo, Characterization of mechanical and biochemical properties of developing embryonic tendon, Proceedings of the National Academy of Sciences 110(16) (2013) 6370-6375.

[7] A. Herchenhan, F. Uhlenbrock, P. Eliasson, M. Weis, D.R. Eyre, K.E. Kadler, S.P. Magnusson, M. Kjaer, Lysyl Oxidase Activity Is Required for Ordered Collagen Fibrillogenesis by Tendon Cells, 290(26) (2015) 16440-16450.

[8] S.B. Liu, N. Ikenaga, Z.-W. Peng, D.Y. Sverdlov, A. Greenstein, V. Smith, D. Schuppan, Y. Popov, Lysyl oxidase activity contributes to collagen stabilization during liver fibrosis progression and limits spontaneous fibrosis reversal in mice, The FASEB Journal 30(4) (2016) 1599-1609.

[9] M.K. Jansen, K. Csiszar, Intracellular localization of the matrix enzyme lysyl oxidase in polarized epithelial cells, Matrix biology 26(2) (2007) 136-139.

[10] F.A. Saad, M. Torres, H. Wang, L. Graham, Intracellular lysyl oxidase: effect of a specific inhibitor on nuclear mass in proliferating cells, Biochemical and biophysical research communications 396(4) (2010) 944-949.

[11] J.M. Mäki, Lysyl oxidases in mammalian development and certain pathological conditions, Histology and histopathology (2009).

[12] L. Cai, X. Xiong, X. Kong, J. Xie, The Role of the Lysyl Oxidases in Tissue Repair and Remodeling: A Concise Review, Tissue Engineering and Regenerative Medicine 14(1) (2017) 15-30.

[13] P.C. Trackman, Lysyl Oxidase Isoforms and Potential Therapeutic Opportunities for Fibrosis and Cancer, Expert Opinion on Therapeutic Targets 20(8) (2016) 935-945.

[14] S. Ricard-Blum, G. Baffet, N. Théret, Molecular and tissue alterations of collagens in fibrosis, Matrix Biology 68 (2018) 122-149.

[15] L. Perryman, J.T. Erler, Lysyl oxidase in cancer research, Future oncology 10(9) (2014) 1709-1717.

[16] L. Wu, Y. Zhu, The function and mechanisms of action of LOXL2 in cancer, International journal of molecular medicine 36(5) (2015) 1200-1204.

[17] T.R. Cox, D. Bird, A.M. Baker, H.E. Barker, M.W.Y. Ho, G. Lang, J.T. Erler, LOX-Mediated Collagen Crosslinking Is Responsible for Fibrosis-Enhanced Metastasis, Cancer Research 73(6) (2013) 1721-1732.

[18] L.I. Smith-Mungo, H.M. Kagan, Lysyl oxidase: properties, regulation and multiple functions in biology, Matrix biology 16(7) (1998) 387-398.

[19] T.R. Cox, J.T. Erler, Remodeling and homeostasis of the extracellular matrix: implications for fibrotic diseases and cancer, Disease models & mechanisms 4(2) (2011) 165-178.

[20] M.V. Barrow, C.F. Simpson, E.J. Miller, Lathyrism: a review, The Quarterly review of biology 49(2) (1974) 101-128.

[21] C.F. Spurney, S. Knoblach, E.E. Pistilli, K. Nagaraju, G.R. Martin, E.P. Hoffman, Dystrophin-deficient cardiomyopathy in mouse: expression of Nox4 and Lox are associated with fibrosis and altered functional parameters in the heart, Neuromuscular Disorders 18(5) (2008) 371-381.

[22] H.-J. Moon, J. Finney, T. Ronnebaum, M. Mure, Human lysyl oxidase-like 2, Bioorganic chemistry 57 (2014) 231-241.

[23] P.C. Trackman, Functional importance of lysyl oxidase family propeptide regions, (2018) 1-9.

[24] T.R. Cox, J.T. Erler, Lysyl oxidase in colorectal cancer, American Journal of Physiology-Gastrointestinal and Liver Physiology 305(10) (2013) G659-G666.

[25] M.V. Panchenko, W.G. Stetler-Stevenson, O.V. Trubetskoy, S.N. Gacheru, H.M. Kagan, Metalloproteinase activity secreted by fibrogenic cells in the processing of prolysyl oxidase potential role of procollagen C-proteinase, Journal of Biological Chemistry 271(12) (1996) 7113-7119.

[26] L. Thomassin, C.C. Werneck, T.J. Broekelmann, C. Gleyzal, I.K. Hornstra, R.P. Mecham, P. Sommer, The Pro-regions of lysyl oxidase and lysyl oxidase-like 1 are required for deposition onto elastic fibers, Journal of Biological Chemistry 280(52) (2005) 42848-42855.

[27] V.G. Martínez, S.K. Moestrup, U. Holmskov, J. Mollenhauer, F. Lozano, The conserved scavenger receptor cysteine-rich superfamily in therapy and diagnosis, Pharmacological reviews 63(4) (2011) 967-1000.

[28] J.K. Mouw, G. Ou, V.M. Weaver, Extracellular matrix assembly: a multiscale deconstruction, Nature reviews Molecular cell biology 15(12) (2014) 771-785.

[29] M.J. Bissell, H.G. Hall, G. Parry, How does the extracellular matrix direct gene expression?, Journal of theoretical biology 99(1) (1982) 31-68.

[30] R. Xu, A. Boudreau, M.J. Bissell, Tissue architecture and function: dynamic reciprocity via extra-and intra-cellular matrices, Cancer and metastasis reviews 28(1-2) (2009) 167-176.

[31] S.F. Badylak, The extracellular matrix as a biologic scaffold material☆, Biomaterials 28(25) (2007) 3587-3593.

[32] W.E. Poel, Preparation of acellular homogenates from muscle samples, Science 108(2806) (1948) 390-391.

[33] Y. Zhang, B.P. Kropp, H.-K. Lin, R. Cowan, E.Y. Cheng, Bladder regeneration with cell-seeded small intestinal submucosa, Tissue engineering 10(1-2) (2004) 181-187.

[34] E. Alicuben, S. DeMeester, Onlay ventral hernia repairs using porcine non-cross-linked dermal biologic mesh, Hernia 18(5) (2014) 705-712.

[35] V.J. Mase, J.R. Hsu, S.E. Wolf, J.C. Wenke, D.G. Baer, J. Owens, S.F. Badylak, T.J. Walters, Clinical application of an acellular biologic scaffold for surgical repair of a large, traumatic quadriceps femoris muscle defect, Orthopedics 33(7) (2010).

[36] G.K. Bejjani, J. Zabramski, Safety and efficacy of the porcine small intestinal submucosa dural substitute: results of a prospective multicenter study and literature review, Journal of neurosurgery 106(6) (2007) 1028-1033.

[37] U.G. Longo, A. Lamberti, S. Petrillo, N. Maffulli, V. Denaro, Scaffolds in tendon tissue engineering, Stem cells international 2012 (2012).

[38] V. Agrawal, S. Tottey, S.A. Johnson, J.M. Freund, B.F. Siu, S.F. Badylak, Recruitment of progenitor cells by an extracellular matrix cryptic peptide in a mouse model of digit amputation, Tissue engineering Part A 17(19-20) (2011) 2435-2443.

[39] J.E. Reing, L. Zhang, J. Myers-Irvin, K.E. Cordero, D.O. Freytes, E. Heber-Katz, K. Bedelbaeva, D. McIntosh, A. Dewilde, S.J. Braunhut, Degradation products of extracellular matrix affect cell migration and proliferation, Tissue Engineering Part A 15(3) (2009) 605-614.

[40] J.E. Valentin, A.M. Stewart-Akers, T.W. Gilbert, S.F. Badylak, Macrophage participation in the degradation and remodeling of extracellular matrix scaffolds, Tissue Engineering Part A 15(7) (2009) 1687-1694.

[41] L. Huleihel, G.S. Hussey, J.D. Naranjo, L. Zhang, J.L. Dziki, N.J. Turner, D.B. Stolz, S.F. Badylak, Matrix-bound nanovesicles within ECM bioscaffolds, 2(6) (2016) e1600502-12.

[42] S.E. Andaloussi, I. Mäger, X.O. Breakefield, M.J. Wood, Extracellular vesicles: biology and emerging therapeutic opportunities, Nature reviews Drug discovery 12(5) (2013) 347-357.

[43] L.A. Hargett, N.N. Bauer, On the origin of microparticles: From "platelet dust" to mediators of intercellular communication, Pulmonary circulation 3(2) (2013) 329-340.

[44] Y. Ouyang, J.-F. Mouillet, C.B. Coyne, Y. Sadovsky, Placenta-specific microRNAs in exosomes–good things come in nano-packages, Placenta 35 (2014) S69-S73.

[45] B.L. Deatherage, B.T. Cookson, Membrane vesicle release in bacteria, eukaryotes, and archaea: a conserved yet underappreciated aspect of microbial life, Infection and immunity 80(6) (2012) 1948-1957.

[46] E. Van der Pol, A. Böing, E. Gool, R. Nieuwland, Recent developments in the nomenclature, presence, isolation, detection and clinical impact of extracellular vesicles, Journal of thrombosis and haemostasis 14(1) (2016) 48-56.

[47] V. Hyenne, S. Ghoroghi, M. Collot, C. Carapito, A.S. Klymchenko, J.G. Goetz, Studying the Fate of Tumor Extracellular Vesicles at High Spatiotemporal Resolution Using the Zebrafish Resource Studying the Fate of Tumor Extracellular Vesicles at High Spatiotemporal Resolution Using the Zebrafish Embryo, (2019).

[48] K.-H. Park, B.-J. Kim, J. Kang, T.-S. Nam, J.M. Lim, H.T. Kim, J.K. Park, Y.G. Kim, S.-W. Chae, U.-H. Kim, Ca2+ signaling tools acquired from prostasomes are required for progesterone-induced sperm motility, Science signaling 4(173) (2011) ra31-ra31.

[49] A. Chairoungdua, D.L. Smith, P. Pochard, M. Hull, M.J. Caplan, Exosome release of β-catenin: a novel mechanism that antagonizes Wnt signaling, Journal of Cell Biology 190(6) (2010) 1079-1091.

[50] S. Elmore, Apoptosis: a review of programmed cell death, Toxicologic pathology 35(4) (2007) 495-516.

[51] E. Van der Pol, A.N. Böing, P. Harrison, A. Sturk, R. Nieuwland, Classification, functions, and clinical relevance of extracellular vesicles, Pharmacological reviews 64(3) (2012) 676-705.

[52] S.M. van Dommelen, P. Vader, S. Lakhal, S. Kooijmans, W.W. van Solinge, M.J. Wood, R.M. Schiffelers, Microvesicles and exosomes: opportunities for cell-derived membrane vesicles in drug delivery, Journal of Controlled Release 161(2) (2012) 635-644.

[53] G.S. Hussey, C. Pineda Molina, M.C. Cramer, Y.Y. Tyurina, V.A. Tyurin, Y.C. Lee, S.O. El-Mossier, M.H. Murdock, P.S. Timashev, V.E. Kagan, S.F. Badylak, Lipidomics and RNA sequencing reveal a novel subpopulation of nanovesicle within extracellular matrix biomaterials, Science Advances 6(12) (2020) eaay4361.

[54] M. Yáñez-Mó, P.R.-M. Siljander, Z. Andreu, A. Bedina Zavec, F.E. Borràs, E.I. Buzas, K. Buzas, E. Casal, F. Cappello, J. Carvalho, Biological properties of extracellular vesicles and their physiological functions, Journal of extracellular vesicles 4(1) (2015) 27066.

[55] Y. van der Merwe, A.E. Faust, E.T. Sakalli, C.C. Westrick, G. Hussey, K.C. Chan, I.P. Conner, V.L.N. Fu, S.F. Badylak, M.B. Steketee, Matrix-bound nanovesicles prevent ischemia-induced retinal ganglion cell axon degeneration and death and preserve visual function, Scientific Reports 9(1) (2019) 3482.

[56] L. Huleihel, J.G. Bartolacci, J.L. Dziki, T. Vorobyov, B. Arnold, M.E. Scarritt, C. Pineda Molina, S.T. LoPresti, B.N. Brown, J.D. Naranjo, Matrix-bound nanovesicles recapitulate extracellular matrix effects on macrophage phenotype, Tissue Engineering Part A 23(21-22) (2017) 1283-1294.

[57] G.S. Hussey, J.L. Dziki, Y.C. Lee, J.G. Bartolacci, M. Behun, H.R. Turnquist, S.F. Badylak, Matrix bound nanovesicle-associated IL-33 activates a pro-remodeling macrophage phenotype via a non-canonical, ST2-independent pathway, 3 (2019) 26-35.

[58] M.A. Smith, J. Gonzalez, A. Hussain, R.N. Oldfield, K.A. Johnston, K.M. Lopez, Overexpression of soluble recombinant human lysyl oxidase by using solubility tags: effects on activity and solubility, Enzyme research 2016 (2016).

[59] A. Borel, D. Eichenberger, J. Farjanel, E. Kessler, C. Gleyzal, D.J.S. Hulmes, P. Sommer, B. Font, Lysyl Oxidase-like Protein from Bovine Aorta, Journal of Biological Chemistry 276(52) (2001) 48944-48949.

[60] H.M. Kagan, K.A. Sullivan, T.A. Olsson III, A.L. Cronlund, Purification and properties of four species of lysyl oxidase from bovine aorta, Biochemical Journal 177(1) (1979) 203-214.

[61] E.A. Makris, D.J. Responte, N.K. Paschos, J.C. Hu, K.A. Athanasiou, Developing functional musculoskeletal tissues through hypoxia and lysyl oxidase-induced collagen cross-linking, Proceedings of the National Academy of Sciences 111(45) (2014) E4832-E4841.

[62] I.K. Hornstra, S. Birge, B. Starcher, A.J. Bailey, R.P. Mecham, S.D. Shapiro, Lysyl oxidase is required for vascular and diaphragmatic development in mice, Journal of Biological Chemistry 278(16) (2003) 14387-14393.

[63] J.M. Mäki, J. Räsänen, H. Tikkanen, R. Sormunen, K. Mäkikallio, K.I. Kivirikko, R. Soininen, Inactivation of the lysyl oxidase gene Lox leads to aortic aneurysms, cardiovascular dysfunction, and perinatal death in mice, Circulation 106(19) (2002) 2503-2509.

[64] R.J. Blaisdell, N. Giri, Mechanism of antifibrotic effect of taurine and niacin in the multidose bleomycin-hamster model of lung fibrosis: Inhibition of lysyl oxidase and collagenase, Journal of biochemical toxicology 10(4) (1995) 203-210.

[65] S.-S. Tang, P. Trackman, H. Kagan, Reaction of aortic lysyl oxidase with beta-aminopropionitrile, Journal of Biological Chemistry 258(7) (1983) 4331-4338.

[66] K.K. Kim, S. Abelman, N. Yano, J.R. Ribeiro, R.K. Singh, M. Tipping, R.G. Moore, Tetrathiomolybdate inhibits mitochondrial complex IV and mediates degradation of hypoxia-inducible factor-1α in cancer cells, Scientific reports 5 (2015) 14296.

[67] P. Kumar, A. Yadav, S.N. Patel, M. Islam, Q. Pan, S.D. Merajver, T.N. Teknos, Tetrathiomolybdate inhibits head and neck cancer metastasis by decreasing tumor cell motility, invasiveness and by promoting tumor cell anoikis, Molecular cancer 9(1) (2010) 206.

[68] K.K. Kim, S. Abelman, N. Yano, J.R. Ribeiro, R.K. Singh, M. Tipping, R.G. Moore, Tetrathiomolybdate inhibits mitochondrial complex IV and mediates degradation of hypoxia-inducible factor-1α in cancer cells, Scientific Reports 5(1) (2015) 14296.

[69] N. Kendall, P. Marsters, R. Scaramuzzi, B. Campbell, Expression of lysyl oxidase and effect of copper chloride and ammonium tetrathiomolybdate on bovine ovarian follicle granulosa cells cultured in serum-free media, REPRODUCTION-CAMBRIDGE- 125(5) (2003) 657-665.

[70] K.C. Hansen, L. Kiemele, O. Maller, J. O'Brien, A. Shankar, J. Fornetti, P. Schedin, An in-solution ultrasonication-assisted digestion method for improved extracellular matrix proteome coverage, Molecular & Cellular Proteomics 8(7) (2009) 1648-1657.

[71] J. Li, K.C. Hansen, Y. Zhang, C. Dong, C.Z. Dinu, M. Dzieciatkowska, M. Pei, Rejuvenation of chondrogenic potential in a young stem cell microenvironment, Biomaterials 35(2) (2014) 642-653.

[72] S.G. Dempsey, C.H. Miller, R.C. Hill, K.C. Hansen, B.C. May, Functional insights from the proteomic inventory of ovine forestomach matrix, Journal of proteome research 18(4) (2019) 1657-1668.

[73] J. Lin, J. Li, B. Huang, J. Liu, X. Chen, X.-M. Chen, Y.-M. Xu, L.-F. Huang, X.-Z. Wang, Exosomes: novel biomarkers for clinical diagnosis, The scientific world journal 2015 (2015).

[74] D.D. Taylor, C. Gercel-Taylor, MicroRNA signatures of tumor-derived exosomes as diagnostic biomarkers of ovarian cancer, Gynecologic oncology 110(1) (2008) 13-21.

[75] A. Thind, C. Wilson, Exosomal miRNAs as cancer biomarkers and therapeutic targets, Journal of extracellular vesicles 5(1) (2016) 31292.

[76] A. Mayorca-Guiliani, J.T. Erler, The potential for targeting extracellular LOX proteins in human malignancy, Onco Targets Ther 6 (2013) 1729-1735.

[77] M.I. Uzel, I.C. Scott, H. Babakhanlou-Chase, A.H. Palamakumbura, W.N. Pappano, H.-H. Hong, D.S. Greenspan, P.C. Trackman, Multiple Bone Morphogenetic Protein 1-related

Mammalian Metalloproteinases Process Pro-lysyl Oxidase at the Correct Physiological Site and Control Lysyl Oxidase Activation in Mouse Embryo Fibroblast Cultures, 276(25) (2001) 22537-22543.

[78] B. Fogelgren, N. Polgár, K.M. Szauter, Z. Újfaludi, R. Laczkó, K.S.K. Fong, K. Csiszar, Cellular Fibronectin Binds to Lysyl Oxidase with High Affinity and Is Critical for Its Proteolytic Activation, Journal of Biological Chemistry 280(26) (2005) 24690-24697.

[79] T. Maruhashi, I. Kii, M. Saito, A. Kudo, Interaction between Periostin and BMP-1 Promotes Proteolytic Activation of Lysyl Oxidase, 285(17) (2010) 13294-13303.

[80] S. Kalamajski, D. Bihan, A.M. Bonna, K. Rubin, R.W. Farndale, Fibromodulin Interacts with Collagen Cross-linking Sites and Activates Lysyl Oxidase, Journal of Biological Chemistry 291(15) (2016) 7951-7960.

[81] J. Ratajczak, M. Wysoczynski, F. Hayek, A. Janowska-Wieczorek, M. Ratajczak, Membrane-derived microvesicles: important and underappreciated mediators of cell-to-cell communication, Leukemia 20(9) (2006) 1487-1495.

[82] N.M. McKechnie, B.C. King, E. Fletcher, G. Braun, Fas-ligand is stored in secretory lysosomes of ocular barrier epithelia and released with microvesicles, Experimental eye research 83(2) (2006) 304-314.

[83] D. Virgintino, M. Rizzi, M. Errede, M. Strippoli, F. Girolamo, M. Bertossi, L. Roncali, Plasma membrane-derived microvesicles released from tip endothelial cells during vascular sprouting, Angiogenesis 15(4) (2012) 761-769.

[84] V. Luga, L. Zhang, A.M. Viloria-Petit, A.A. Ogunjimi, M.R. Inanlou, E. Chiu, M. Buchanan, A.N. Hosein, M. Basik, J.L. Wrana, Exosomes mediate stromal mobilization of autocrine Wnt-PCP signaling in breast cancer cell migration, Cell 151(7) (2012) 1542-1556.

[85] H. Peinado, M. Alečković, S. Lavotshkin, I. Matei, B. Costa-Silva, G. Moreno-Bueno, M. Hergueta-Redondo, C. Williams, G. García-Santos, C.M. Ghajar, Melanoma exosomes educate bone marrow progenitor cells toward a pro-metastatic phenotype through MET, Nature medicine 18(6) (2012) 883.

[86] H. Kalra, R.J. Simpson, H. Ji, E. Aikawa, P. Altevogt, P. Askenase, V.C. Bond, F.E. Borràs, X. Breakefield, V. Budnik, Vesiclepedia: a compendium for extracellular vesicles with continuous community annotation, PLoS Biol 10(12) (2012) e1001450.

[87] L. Balaj, R. Lessard, L. Dai, Y.-J. Cho, S.L. Pomeroy, X.O. Breakefield, J. Skog, Tumour microvesicles contain retrotransposon elements and amplified oncogene sequences, Nature communications 2(1) (2011) 1-9.

[88] B. Ashcroft, J. De Sonneville, Y. Yuana, S. Osanto, R. Bertina, M. Kuil, T. Oosterkamp, Determination of the size distribution of blood microparticles directly in plasma using atomic force microscopy and microfluidics, Biomedical microdevices 14(4) (2012) 641-649.

[89] T. Hata, K. Murakami, H. Nakatani, Y. Yamamoto, T. Matsuda, N. Aoki, Isolation of bovine milk-derived microvesicles carrying mRNAs and microRNAs, Biochemical and biophysical research communications 396(2) (2010) 528-533.

[90] M.A. Livshits, E. Khomyakova, E.G. Evtushenko, V.N. Lazarev, N.A. Kulemin, S.E. Semina, E.V. Generozov, V.M. Govorun, Isolation of exosomes by differential centrifugation: theoretical analysis of a commonly used protocol, Scientific reports 5 (2015) 17319.

[91] D.O. Freytes, R.S. Tullius, S.F. Badylak, Effect of storage upon material properties of lyophilized porcine extracellular matrix derived from the urinary bladder, Journal of Biomedical Materials Research Part A 78B(2) (2006) 327-333.

[92] S.F. Badylak, G.C. Lantz, A. Coffey, L.A. Geddes, Small intestinal submucosa as a large diameter vascular graft in the dog, Journal of Surgical Research 47(1) (1989) 74-80.

[93] S.F. Badylak, R. Tullius, K. Kokini, K.D. Shelbourne, T. Klootwyk, S.L. Voytik, M.R. Kraine, C. Simmons, The use of xenogeneic small intestinal submucosa as a biomaterial for Achille's tendon repair in a dog model, Journal of biomedical materials research 29(8) (1995) 977-985.

[94] S.F. Badylak, Small intestinal submucosa (SIS): a biomaterial conducive to smart tissue remodeling, Tissue engineering, Springer1993, pp. 179-189.

[95] R. Szatanek, M. Baj-Krzyworzeka, J. Zimoch, M. Lekka, M. Siedlar, J. Baran, The methods of choice for extracellular vesicles (EVs) characterization, International journal of molecular sciences 18(6) (2017) 1153.

[96] M. Zuccotti, U. Urch, R. Yanagimachi, Collagenase as an agent for dissolving the zona pellucida of hamster and mouse oocytes, Reproduction 93(2) (1991) 515-520.

[97] A. Breite, F. Dwulet, R. McCarthy, Tissue dissociation enzyme neutral protease assessment, Transplantation proceedings, Elsevier, 2010, pp. 2052-2054.

[98] J.E. Gadek, G.A. Fells, D.G. Wright, R.G. Crystal, Human neutrophil elastase functions as a type III collagen “collagenase”, Biochemical and biophysical research communications 95(4) (1980) 1815-1822.

[99] J.T. Erler, K.L. Bennewith, M. Nicolau, N. Dornhöfer, C. Kong, Q.-T. Le, J.-T.A. Chi, S.S. Jeffrey, A.J. Giaccia, Lysyl oxidase is essential for hypoxia-induced metastasis, Nature 440(7088) (2006) 1222-1226.

[100] P.C. Trackman, D. Bedell-Hogan, J. Tang, H. Kagan, Post-translational glycosylation and proteolytic processing of a lysyl oxidase precursor, Journal of Biological Chemistry 267(12) (1992) 8666-8671.

[101] X. Grau-Bové, I. Ruiz-Trillo, F. Rodriguez-Pascual, Origin and evolution of lysyl oxidases, (2015) 1-11.

[102] S.D. Vallet, M. Guéroult, N. Belloy, M. Dauchez, S. Ricard-Blum, A Three-Dimensional Model of Human Lysyl Oxidase, a Cross- Linking Enzyme, ACS Omega 4(5) (2019) 8495-8505.

[103] S.D. Vallet, A.E. Miele, U. Uciechowska-Kaczmarzyk, A. Liwo, B. Duclos, S.A. Samsonov, S. Ricard-Blum, Insights into the structure and dynamics of lysyl oxidase propeptide, a flexible protein with numerous partners, Scientific reports 8(1) (2018) 1-16.

[104] S.T. Jung, M.S. Kim, J.Y. Seo, H.C. Kim, Y. Kim, Purification of enzymatically active human lysyl oxidase and lysyl oxidase-like protein from Escherichia coli inclusion bodies, Protein expression and purification 31(2) (2003) 240-246.

[105] M. Ouzzine, A. Boyd, D. Hulmes, Expression of active, human lysyl oxidase in Escherichia coli, FEBS letters 399(3) (1996) 215-219.

[106] S.E. Herwald, F.T. Greenaway, K.M. Lopez, Purification of high yields of catalytically active lysyl oxidase directly from Escherichia coli cell culture, Protein expression and purification 74(1) (2010) 116-121.

[107] J. Xie, J. Jiang, Y. Zhang, C. Xu, L. Yin, C. Wang, P.C. Chen, K.P. Sung, Up-regulation expressions of lysyl oxidase family in anterior cruciate ligament and medial collateral ligament fibroblasts induced by transforming growth factor-beta 1, International orthopaedics 36(1) (2012) 207-213.

[108] D.O. Freytes, R.S. Tullius, S.F. Badylak, Effect of storage upon material properties of lyophilized porcine extracellular matrix derived from the urinary bladder, Journal of Biomedical Materials Research Part B: Applied Biomaterials: An Official Journal of The Society for Biomaterials, The Japanese Society for Biomaterials, and The Australian Society for Biomaterials and the Korean Society for Biomaterials 78(2) (2006) 327-333.

[109] J.E. Reing, B.N. Brown, K.A. Daly, J.M. Freund, T.W. Gilbert, S.X. Hsiong, A. Huber, K.E. Kullas, S. Tottey, M.T. Wolf, The effects of processing methods upon mechanical and biologic properties of porcine dermal extracellular matrix scaffolds, Biomaterials 31(33) (2010) 8626-8633.

[110] M.T. Wolf, K.A. Daly, J.E. Reing, S.F. Badylak, Biologic scaffold composed of skeletal muscle extracellular matrix, Biomaterials 33(10) (2012) 2916-2925.

[111] T.J. Keane, R. Londono, R.M. Carey, C.A. Carruthers, J.E. Reing, C.L. Dearth, A. D'Amore, C.J. Medberry, S.F. Badylak, Preparation and characterization of a biologic scaffold from esophageal mucosa, Biomaterials 34(28) (2013) 6729-6737.

[112] T.J. Keane, I.T. Swinehart, S.F. Badylak, Methods of tissue decellularization used for preparation of biologic scaffolds and in vivo relevance, Methods 84 (2015) 25-34.

[113] T.J. Keane, R. Londono, N.J. Turner, S.F. Badylak, Consequences of ineffective decellularization of biologic scaffolds on the host response, Biomaterials 33(6) (2012) 1771-1781.

[114] A. Mantovani, A. Sica, S. Sozzani, P. Allavena, A. Vecchi, M. Locati, The chemokine system in diverse forms of macrophage activation and polarization, Trends in immunology 25(12) (2004) 677-686.

[115] B.N. Brown, J.E. Valentin, A.M. Stewart-Akers, G.P. McCabe, S.F. Badylak, Macrophage phenotype and remodeling outcomes in response to biologic scaffolds with and without a cellular component, Biomaterials 30(8) (2009) 1482-1491.

[116] M. Sandor, H. Xu, J. Connor, J. Lombardi, J.R. Harper, R.P. Silverman, D.J. McQuillan, Host response to implanted porcine-derived biologic materials in a primate model of abdominal wall repair, Tissue Engineering Part A 14(12) (2008) 2021-2031.

[117] N. Nagan, H.M. Kagan, Modulation of lysyl oxidase activity toward peptidyl lysine by vicinal dicarboxylic amino acid residues. Implications for collagen cross-linking, Journal of Biological Chemistry 269(35) (1994) 22366-22371.

[118] J. Molnar, K. Fong, Q. He, K. Hayashi, Y. Kim, S. Fong, B. Fogelgren, K.M. Szauter, M. Mink, K. Csiszar, Structural and functional diversity of lysyl oxidase and the LOX-like proteins, Biochimica et biophysica acta (BBA)-proteins and proteomics 1647(1-2) (2003) 220-224.

[119] T. Thangarajah, C.J. Pendegrass, S. Shahbazi, S. Lambert, S. Alexander, G.W. Blunn, Augmentation of Rotator Cuff Repair With Soft Tissue Scaffolds, Orthop J Sports Med 3(6) (2015) 2325967115587495.

[120] S.F. Badylak, R. Tullius, K. Kokini, K.D. Shelbourne, T. Klootwyk, S.L. Voytik, M.R. Kraine, C. Simmons, The use of xenogeneic small intestinal submucosa as a biomaterial for Achille's tendon repair in a dog model, Journal of Biomedical Materials Research 29(8) (1995) 977-985.

[121] U.G. Longo, A. Lamberti, S. Petrillo, N. Maffulli, V. Denaro, Scaffolds in tendon tissue engineering, Stem Cells Int 2012 (2012) 517165.

[122] A. Ratcliffe, D.L. Butler, N.A. Dyment, P.J. Cagle, Jr., C.S. Proctor, S.S. Ratcliffe, E.L. Flatow, Scaffolds for tendon and ligament repair and regeneration, Ann Biomed Eng 43(3) (2015) 819-31.

[123] P. Lange, K. Greco, L. Partington, C. Carvalho, S. Oliani, M.A. Birchall, P.D. Sibbons, M.W. Lowdell, T. Ansari, Pilot study of a novel vacuum-assisted method for decellularization of tracheae for clinical tissue engineering applications, Journal of Tissue Engineering and Regenerative Medicine 11(3) (2015) 800-811.

[124] P.M. Crapo, T.W. Gilbert, S.F. Badylak, An overview of tissue and whole organ decellularization processes, Biomaterials 32(12) (2011) 3233-3243.

[125] Martínez-González, Varona, Cañes, Galán, Briones, Cachofeiro, Rodríguez, Emerging Roles of Lysyl Oxidases in the Cardiovascular System: New Concepts and Therapeutic Challenges, Biomolecules 9(10) (2019) 610-21.

[126] E. Noblesse, V. Cenizo, C. Bouez, A. Borel, C. Gleyzal, S. Peyrol, M.-P. Jacob, P. Sommer, O. Damour, Lysyl oxidase-like and lysyl oxidase are present in the dermis and epidermis of a skin equivalent and in human skin and are associated to elastic fibers, Journal of investigative dermatology 122(3) (2004) 621-630.

[127] J.S. Brody, H. Kagan, A. Manalo, Lung lysyl oxidase activity: relation to lung growth, American Review of Respiratory Disease 120(6) (1979) 1289-1295.

[128] M. Giampuzzi, G. Botti, M. Di Duca, L. Arata, G. Ghiggeri, R. Gusmano, R. Ravazzolo, A. Di Donato, Lysyl Oxidase Activates the Transcription Activity of Human Collagene III Promoter, 275(46) (2000) 36341-36349.

[129] H.M. Kagan, W. Li, Lysyl oxidase: Properties, specificity, and biological roles inside and outside of the cell, Journal of Cellular Biochemistry 88(4) (2003) 660-672.

[130] H. Kuivaniemi, Partial characterization of lysyl oxidase from several human tissues., Biochemical Journal 230(3) (1985) 639-643.

[131] K.M. Lopez, F.T. Greenaway, Identification of the copper-binding ligands of lysyl oxidase, Journal of neural transmission 118(7) (2011) 1101-1109.

[132] A.H. Palamakumbura, S. Jeay, Y. Guo, N. Pischon, P. Sommer, G.E. Sonenshein, P.C. Trackman, The propeptide domain of lysyl oxidase induces phenotypic reversion of ras-transformed cells, Journal of Biological Chemistry 279(39) (2004) 40593-40600.

[133] T. Rosell-García, A. Paradela, G. Bravo, L. Dupont, M. Bekhouche, A. Colige, F. Rodriguez-Pascual, Differential cleavage of lysyl oxidase by the metalloproteinases BMP1 and ADAMTS2/14 regulates collagen binding through a tyrosine sulfate domain, Journal of Biological Chemistry 294(29) (2019) 11087-11100.

[134] N. Mehrban, J. Bowen, E. Vorndran, U. Gbureck, L.M. Grover, Structural changes to resorbable calcium phosphate bioceramic aged in vitro, Colloids and Surfaces B: Biointerfaces 111 (2013) 469-478.

[135] L.M. Larkin, S. Calve, T.Y. Kostrominova, E.M. Arruda, Structure and functional evaluation of tendon–skeletal muscle constructs engineered in vitro, Tissue engineering 12(11) (2006) 3149-3158.

[136] I. Hajdú, J. Kardos, B. Major, G. Fabó, Z. Lőrincz, S. Cseh, G. Dormán, Inhibition of the LOX enzyme family members with old and new ligands. Selectivity analysis revisited, Bioorganic & Medicinal Chemistry Letters 28(18) (2018) 3113-3118.

[137] N. Maffulli, H.D. Moller, C.H. Evans, Tendon healing: can it be optimised?, Br J Sports Med 36(5) (2002) 315-6.

[138] F. Wu, M. Nerlich, D. Docheva, Tendon injuries: Basic science and new repair proposals, EFORT Open Rev 2(7) (2017) 332-342.

[139] Y. Xu, G.A.C. Murrell, The Basic Science of Tendinopathy, Clinical Orthopaedics and Related Research 466(7) (2008) 1528-1538.

[140] P. Renstrom, S.L.Y. Woo, Tendinopathy: a major medical problem in sport, Tendinopathy in athletes 2008 (2008) 1-9.

[141] R. Śmigielski, U. Zdanowicz, Achilles Tendon Pathology, Arthroscopy, Springer2016, pp. 1115-1124.

[142] D.O. Freytes, J. Martin, S.S. Velankar, A.S. Lee, S.F. Badylak, Preparation and rheological characterization of a gel form of the porcine urinary bladder matrix, Biomaterials 29(11) (2008) 1630-1637.

[143] P. Eliasson, T. Andersson, P. Aspenberg, Rat Achilles tendon healing: mechanical loading and gene expression, Journal of applied physiology 107(2) (2009) 399-407.

[144] J.D. Rees, N. Maffulli, J. Cook, Management of Tendinopathy, The American Journal of Sports Medicine 37(9) (2009) 1855-1867.

[145] J.L. Drury, D.J. Mooney, Hydrogels for tissue engineering: scaffold design variables and applications, Biomaterials 24(24) (2003) 4337-4351.

[146] P. Kannus, Etiology and pathophysiology of chronic tendon disorders in sports, Scand J Med Sci Sports 7(2) (1997) 78-85.

[147] M. Järvinen, L. Jozsa, P. Kannus, T. Järvinen, M. Kvist, W. Leadbetter, Histopathological findings in chronic tendon disorders, Scandinavian journal of medicine & science in sports 7(2) (1997) 86-95.

[148] D.T. Fung, V.M. Wang, N. Andarawis-Puri, J. Basta-Pljakic, Y. Li, D.M. Laudier, H.B. Sun, K.J. Jepsen, M.B. Schaffler, E.L. Flatow, Early response to tendon fatigue damage accumulation in a novel in vivo model, Journal of biomechanics 43(2) (2010) 274-279.

[149] K.G. Cornwell, A. Landsman, K.S. James, Extracellular matrix biomaterials for soft tissue repair, Clinics in podiatric medicine and surgery 26(4) (2009) 507-523.

[150] D.L. Butler, J.T. Shearn, N. Juncosa, M.R. Dressler, S.A. Hunter, Functional tissue engineering parameters toward designing repair and replacement strategies, Clinical Orthopaedics and Related Research® 427 (2004) S190-S199.

[151] R.J. De Vos, A. Weir, H.T. van Schie, S.M. Bierma-Zeinstra, J.A. Verhaar, H. Weinans, J.L. Tol, Platelet-rich plasma injection for chronic Achilles tendinopathy: a randomized controlled trial, Jama 303(2) (2010) 144-149.

[152] J.L. Dragoo, A.S. Wasterlain, H.J. Braun, K.T. Nead, Platelet-rich plasma as a treatment for patellar tendinopathy: a double-blind, randomized controlled trial, The American journal of sports medicine 42(3) (2014) 610-618.

[153] J.T. Finnoff, S.P. Fowler, J.K. Lai, P.J. Santrach, E.A. Willis, Y.A. Sayeed, J. Smith, Treatment of chronic tendinopathy with ultrasound-guided needle tenotomy and platelet-rich plasma injection, PM&R 3(10) (2011) 900-911.

[154] A.R. Massensini, H. Ghuman, L.T. Saldin, C.J. Medberry, T.J. Keane, F.J. Nicholls, S.S. Velankar, S.F. Badylak, M. Modo, Concentration-dependent rheological properties of ECM hydrogel for intracerebral delivery to a stroke cavity, Acta biomaterialia 27 (2015) 116-130.

[155] L. Zhang, F. Zhang, Z. Weng, B.N. Brown, H. Yan, X.M. Ma, P.S. Vosler, S.F. Badylak, C.E. Dixon, X.T. Cui, Effect of an inductive hydrogel composed of urinary bladder matrix upon functional recovery following traumatic brain injury, Tissue Engineering Part A 19(17-18) (2013) 1909-1918.

[156] M.T. Wolf, K.A. Daly, E.P. Brennan-Pierce, S.A. Johnson, C.A. Carruthers, A. D'Amore, S.P. Nagarkar, S.S. Velankar, S.F. Badylak, A hydrogel derived from decellularized dermal extracellular matrix, Biomaterials 33(29) (2012) 7028-7038.

[157] Y.Q. Koh, F.B. Almughlliq, K. Vaswani, H.N. Peiris, M.D. Mitchell, Exosome enrichment by ultracentrifugation and size exclusion chromatography, Frontiers in bioscience (Landmark edition) 23 (2018) 865-874.

[158] T. Sasaki, R. Stoop, T. Sakai, A. Hess, R. Deutzmann, U. Schloetzer-Schrehardt, M.-L. Chu, K. von der Mark, Loss of fibulin-4 results in abnormal collagen fibril assembly in bone, caused by impaired lysyl oxidase processing and collagen cross-linking, Matrix Biology 50 (2016) 53-66.

[159] S. Rosini, N. Pugh, A.M. Bonna, D.J. Hulmes, R.W. Farndale, J.C. Adams, Thrombospondin-1 promotes matrix homeostasis by interacting with collagen and lysyl oxidase precursors and collagen cross-linking sites, Science signaling 11(532) (2018) eaar2566.

[160] B. György, T.G. Szabó, M. Pásztói, Z. Pál, P. Misják, B. Aradi, V. László, E. Pállinger, E. Pap, A. Kittel, Membrane vesicles, current state-of-the-art: emerging role of extracellular vesicles, Cellular and molecular life sciences 68(16) (2011) 2667-2688.

[161] S. Wei, L. Gao, C. Wu, F. Qin, J. Yuan, Role of the lysyl oxidase family in organ development, Experimental and Therapeutic Medicine 20(1) (2020) 163-172.

[162] J.J. Ross, R.T. Tranquillo, ECM gene expression correlates with in vitro tissue growth and development in fibrin gel remodeled by neonatal smooth muscle cells, Matrix Biology 22(6) (2003) 477-490.

[163] M.J. Webber, O.F. Khan, S.A. Sydlik, B.C. Tang, R. Langer, A perspective on the clinical translation of scaffolds for tissue engineering, Annals of biomedical engineering 43(3) (2015) 641-656.

[164] B. Weber, P.E. Dijkman, J. Scherman, B. Sanders, M.Y. Emmert, J. Grünenfelder, R. Verbeek, M. Bracher, M. Black, T. Franz, Off-the-shelf human decellularized tissue-engineered heart valves in a non-human primate model, Biomaterials 34(30) (2013) 7269-7280.

[165] N.R. Schiele, J.E. Marturano, C.K. Kuo, Mechanical factors in embryonic tendon development: potential cues for stem cell tenogenesis, Current opinion in biotechnology 24(5) (2013) 834-840.